



II Conference

MTCKG

Modern Trends in Chemical  
Kinetics and Catalysis



# ABSTRACTS

## PART I

November 21-24  
1995

NOVOSIBIRSK  
RUSSIA

2027

SIBERIAN BRANCH OF THE RUSSIAN ACADEMY OF SCIENCES  
BORESKOV INSTITUTE OF CATALYSIS  
INSTITUTE OF CHEMICAL KINETICS AND COMBUSTION  
SCIENTIFIC COUNCIL ON CATALYSIS AND ITS INDUSTRIAL  
APPLICATION OF RAS AND MINISTRY OF SCIENCE OF THE RUSSIAN  
FEDERATION  
SCIENTIFIC BOARD ON CHEMICAL KINETICS AND STRUCTURE, RAS

The Second Conference  
"Modern trends in chemical kinetics and catalysis"

**ABSTRACTS**

PART I

Novosibirsk - 1995

УДК 66.097.3

542.97

541.124

*The Organizes express their gratitude to the sponsors  
for financial support:*

International Association for the Promotion of Cooperation with Scientists from  
the Independent States of the Former Soviet Union (INTAS)

Russian Foundation for Basic Research (RFBR)

Soros International Science Foundation (ISF)

## **PLENARY LECTURES**



**CATALYSIS BY MOLECULAR DESIGN****Kirill I. Zamaraev***Boriskov Institute of Catalysis, SB RAS, Novosibirsk, 630090, Russia*

The possibilities of molecular design in development of new catalysts and catalytic technologies will be discussed with the data obtained recently at the Borskov Institute of Catalysis as particular examples.

Examples from the following areas will be presented: homogeneous catalysis with metal complexes, heterogeneous catalysis with anchored metal complexes, heterogeneous catalysis with catalysts prepared via anchored metal complexes and organometallics, catalysis of olefin polymerization, catalysis by metals, catalysis by oxides, catalysis by zeolites, catalysis by heteropolyacids, catalysis with nontraditional oxidants and biomimetic catalysis.

The results presented in this lecture clearly show that studies at the molecular level play a rapidly increasing role in the development of new catalysts and processes.

With accumulation of information at the molecular level about the structure of catalysts and mechanisms of their action, the accents in the work on the development of new catalysts and catalytic reactions is expected to shift more and more from empirical search to intentional design.

## PHOTOCHEMISTRY OF 3D OPTICAL STORAGE MEMORY

A.S. Dvornikov, P.M. Rentzepis

Department of Chemistry, University of California, Irvine, CA 92717-2025

Advances in technology have improved computer processing and usage to very high levels making the memory capacity and I/O speed the limiting factors in performance (1). Therefore there is a mandatory need for a quantum jump improvement in information density storage and parallel access at high speed.

We believe that three dimensional storage devices may satisfy these needs(2,3). The memory device described here is based on the process presented in figure 1, which causes a molecule in the unwritten, ground state form, to be excited to a higher electronic state by the simultaneous absorption of two photons. The energy required to reach the excited state is greater than the energy of either photon alone therefore each beam propagates throughout the memory volume without being absorbed. However, when the sum of the energies of these photons is equal to or greater than the energy gap between ground and first electronic excited states of the molecule (see fig. 1), then at the point of beam intersection, the two photons may be absorbed simultaneously by molecule resulting in its excitation to a higher electronic state.

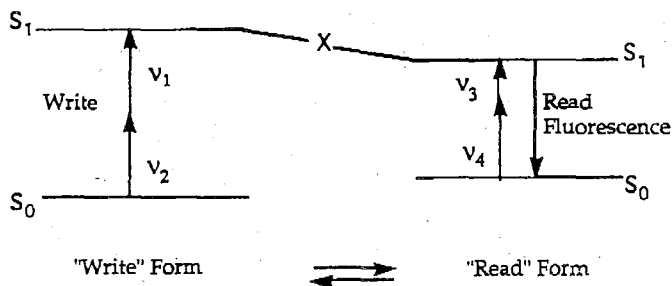


Figure 1. Energy level diagram for two-photon processes.

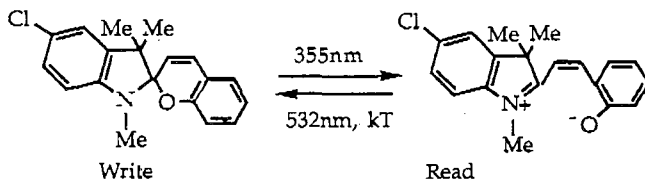
This excited state decays subsequently into a different molecular ground state which becomes the written form of the molecule. These written molecules have different structure, absorb at longer wavelength than the original molecules and are

read by the fluorescence induced by two photon absorption. It is possible to either store or access information by simply intersecting the two beams at any place within the 3D space, figure 2. The density of information which can be stored in volume  $V$  with wavelength  $\lambda$  is  $V/\lambda^3$ , i.e. for  $\lambda = 200$  nm the maximum density is  $10^{12}$  bit/cm<sup>3</sup>. An important property of this type of 3D device is the capability of writing and reading complete 2D pages (disks) with one flash and thus become truly amiable to parallel processing.

The experimental system used for writing and accessing 3D information is shown schematically in figure 2. It consists of picosecond Nd/YAG laser which is tuned by BBO crystals and a dye laser. This system allows for storing and accessing information of complete 2D planes, disks, at once inside the 3D volume, instead of the normal disk bit by bit process.

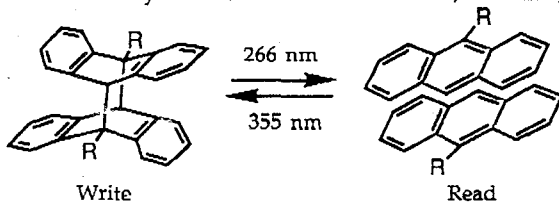
The class of materials which we have utilized for these 3D devices include spiropyran<sup>(4)</sup> or dimer<sup>(5)</sup> types of molecules.

Two forms of spiropyran molecules were used for writing and reading information. The closed, "write" form, absorbs below 400 nm and is transformed by light absorption to the open, "read" form, which has its absorption band maximum at 550nm.



Detection of the 600nm written form fluorescence provides the means for accessing stored information.

The dimer species, corresponding to "zero", absorb in the ultraviolet and upon excitation store information by transforming to the monomer, corresponding to "one". The information is accessed by the fluorescence of the written, monomer, form.

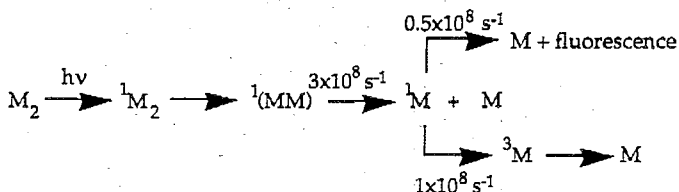


## PL-2

The monomer "read" form has its long wavelength absorption band at 300-400 nm, while the dimer, "write" form, has practically no absorption at wavelengths longer than 300 nm. The monomer 380-480 nm fluorescence quantum efficiency is approximately 30%, while the dimers do not fluorescence.

We will present the transient absorption spectra and ultra fast kinetics of the monomer/dimer process elsewhere.

Based on experimental data the mechanism for the monomer/dimer reaction is:



The rather fast rate of dimer dissociation,  $\sim 10^{-8}$  sec, and monomer fluorescence,  $\sim 10^{-8}$  sec, shows that the input and accessing of information is unusually fast compared to normal memories and quite advantageous if one considers that these rates corresponds to accessing a complete 2D plane, "disk" at this rate.

To store information patterns within the volume of the memory device, which consists of dimer molecules dispersed in a PMMA matrix, we used either two counter propagating 532 nm picosecond laser beams or two orthogally intersecting beams, see figure 2. When two 532 nm beams intersect the dimers, write form, in that area are excited by two photon absorption. The excited dimers photodissociate and form monomers, which are the written form, of the 3D memory.

To demonstrate the writing process we stored several 2D pages, megabit size disks, inside the volume of a  $1 \text{ cm}^3$  by intersecting, the 1064 nm information beam and the 532 nm, addressing beam. inside the memory cube, which made of photochromic material dispersed in poly(methyl methacrylate). The information store method is shown schematically in figure 2. The employment of special light modulators makes possible to store, within a  $1 \text{ cm}$  cube, several micron thick planes each containing gigabits of information. Accessing the stored information is achieved by the same optical system except that the wavelength of one or both beams is longer. In the case where the information of a entire page, disk, is to be accessed simultaneously, rather than in a single bit by bit mode, a single, low intensity 532 nm plane beam is used to illuminate the written 2D page and induce fluorescence by one photon process. The 532

nm beam has the dimensions of the 2D plane to read and intersects only this plane, see figure 2, without accessing any of the neighboring stored information.

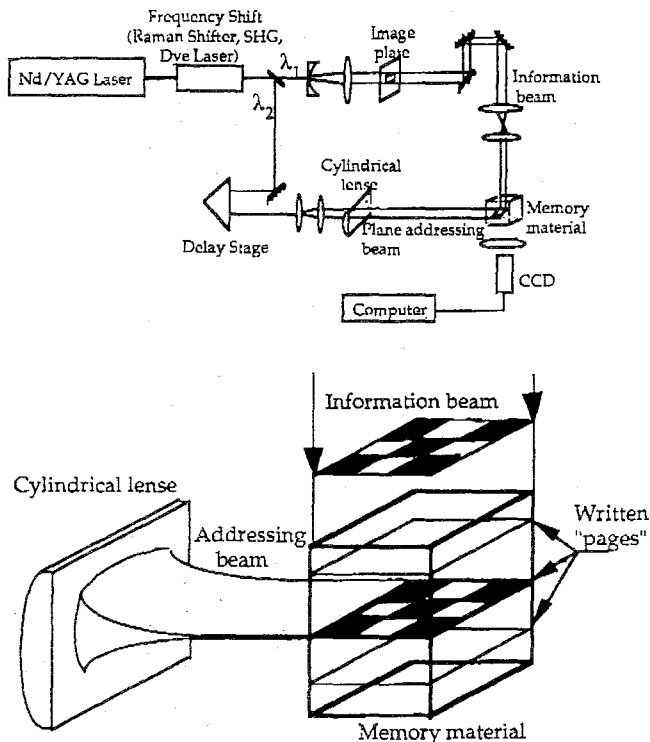


Figure 2. Experimental system used for storing and retrieving information in 3D.

The fluorescence is detected and recorded by a CCD which transmits the signal in digital form directly to the processor. The complete chessboard image was also written simultaneously by intersecting, inside the cube, the 1064 nm information carrying pulse, see fig. 2, and the 532 nm addressing beam shaped in the form of a thin,  $\sim 20 \mu\text{m}$ , plane. Accessing any 2D pattern within the memory volume is simply achieved by illuminating this area with a thin plane of light of the appropriate wavelength to induce fluorescence. Erasing the stored information in such 3D memory

## PL-2

devices may be achieved by irradiation of the written areas with the light of the wavelength required to excite the written form and induce.

The high density,  $\sim 10^{12}$  bit/cm<sup>3</sup>, their inherent suitability for parallel processing and absence of moving parts and low cost makes these 3D memory devices rather attractive for practical applications. Other molecular systems and operations are currently studied which may provide a large improvement over the materials and procedures used now.

### References

1. T.K. Gaylord, Opt. Spectra 6, 25 (1972).
2. A. S. Dvornikov, S. Esener and P. M. Rentzepis, in "Optical Computing Hardware", J. Jahns and S.H. Lee editors, Academic Press Inc., 1993, pp. 287-325.
3. A.S. Dvornikov, J. Malkin and P.M. Rentzepis, J. Phys. Chem., 98, 6746 (1994).
4. Bertelson R. C. , "Techniques of Chemistry: Photochromism" Vol. 3, p. 45, Brown G.M. , Ed., Wiley-Interscience, New York, 1971.
5. W.J. Tomlinson, E.A. Chandross, R.L. Fork, C.A. Pryde and A.A. Lamola, Applied Optics, 11, 533 (1972).

### Acknowledgment

This work was supported in part by the United States Air Force, Rome Laboratory under contract F-30602-93-0231.

## NON-TRADITIONAL MECHANISMS OF SOLID PHASE ASTROCHEMICAL REACTIONS

V. I. Goldanskii

*Semenov Institute of Chemical Physics RAS*

*Moscow, Russia*

Several new mechanisms of chemical reactions in solid phase found and investigated since early 70-s may have direct connections to the prebiotic evolution, in particular to the extraterrestrial scenario of such evolution.

Discovery of molecular tunneling by the example of radiation - induced polymerization of formaldehyde demonstrated the existence of non-vanishing chemical reactivity even near the absolute zero and allowed to put forward the hypothesis of cold prehistory of life. Crucial structural property of the biorganic world is its homochirality. Very cold solid environment hinders racemization and stabilizes optical activity under conditions typical for outer space.

Treatment of interstellar and cometary dust grains as hypothetical stages of prebiotic evolution includes the consideration of possible explosions of grains at overcritical concentrations of accumulated active centers. Totality of experimental data and theoretical approaches leads to the conclusion that such explosions can be of purely thermal rather than of thermal-wave (thermal-chain) nature.

The generation and recombination of free radicals in interstellar and interplanetary grains can result in the oscillations of radical concentrations and grain temperature. The origin of such oscillations as well as their properties are considered.

Peculiar new type of explosive processes - mechano-chemical explosions - was disclosed and explained. It is based on the positive feedback between the brittle fracture of irradiated vitreous and polycrystalline samples and the stimulation of chemical reactions at the surface of formed cracks. Initial fracture produces autowave propagation of the reaction front along the sample with a rate much above that of heat transfer but much below the sound velocity.

### PL-3

The revealing of many amino acids in meteorites and reports about non-racemity and enrichment by  $^{13}\text{C}$  of some of them attracted an interest to the question whether amino acids can be delivered intact to the Earth by a large impactor.

There are described the experiments which have demonstrated that shock waves with amplitudes as much as 500 kbar need not destroy amino acids but can instead initiate their condensation into oligopeptides.

## SPIN COHERENCE PHENOMENA IN RADICAL PAIRS RECOMBINATION

Yu.N.Molin, B.M.Tadjikov, V.M.Grigoryants, D.V.Stass and O.M.Usov

Institute of Chemical Kinetics and Combustion  
Novosibirsk 630090, Russia

**Introduction.** Radical pairs (RPs) produced in solution by light or ionizing radiation are formed in a spin correlated (singlet or triplet) state (see, e.g., [1,2]). This state is not an eigenstate of RP since magnetic interactions (hyperfine and Zeeman) usually exceed the exchange interactions between two radicals. Therefore, the initial state of spin-correlated RP is a coherent mixture of stationary states. If two stationary states are mixed, the probability to find a singlet-born RP in the singlet state behaves as:

$$P_S \sim |\exp(i\omega_1 t) + \exp(i\omega_2 t)|^2 \sim 1 + \cos[(\omega_1 - \omega_2)t],$$

where  $\omega_1$  and  $\omega_2$  are the frequencies of the states involved. For  $\omega_1 \neq \omega_2$  the S-T oscillations occur, hence the yield of recombination product of a given multiplicity should oscillate in time. In the magnetic field, where levels cross ( $\omega_1 = \omega_2$ ), the S-T transitions are frozen down. Therefore, sharp maximum for the singlet product yield could be observed in a steady state experiment.

**Experimental.** Singlet born radical ion pairs produced by ionizing radiation (X-rays or fast electrons from the  $^{90}\text{Sr}$  radioactive source) in hydrocarbon solvents were chosen to observe the spin coherence effects. The primary species -- solvent holes and free electrons -- were trapped by added aromatic acceptors. The singlet channel of recombination of secondary radical ion pairs yields fluorescence, thus making it possible to detect the singlet product yield. Recombination fluorescence was recorded using the single photon counting technique in time resolved experiments. In steady state experiments, the scanned magnetic field was modulated by a small alternating one (12.5 kHz) and the first derivatives of magnetic field effect curves were detected.

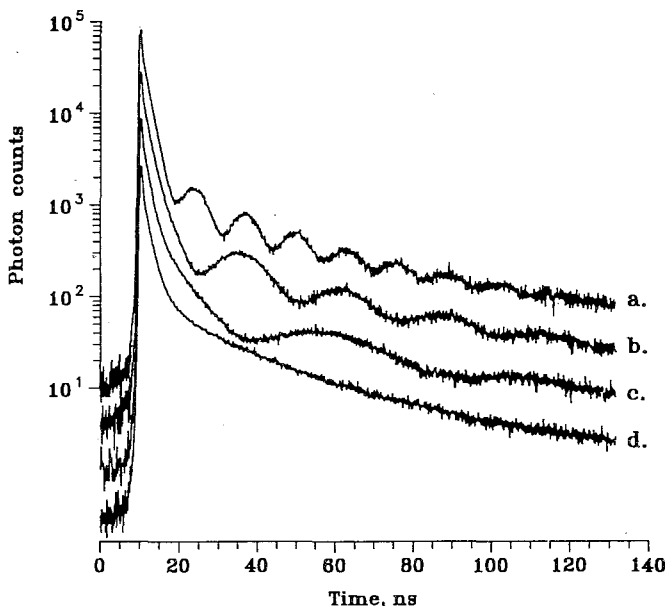


Fig.1. Recombination fluorescence decay curves of the  $10^{-3}\text{M}$  *p*-terphenyl- $\text{d}_{14}$  and  $3 \times 10^{-2}\text{M}$  diphenylsulfide- $\text{d}_{10}$  solution in isoctane at room temperature for magnetic fields: (a) 9600 G; (b) 4800 G; (c) 2400 G; (d) 170 G.

**Quantum oscillations.** In strong magnetic fields the oscillation frequencies coincide with the differences in the EPR spectrum frequencies of pair partners. Therefore, systems with simple EPR spectra are most suitable for observing oscillations. The S-T oscillations induced by hyperfine interactions were observed in the recombination of (tetramethylethylene) $^+/(p\text{-terphenyl-}d_{14})^-$  pairs [3], while those induced by *g*-factor difference were recorded (Fig.1) for the (diphenylsulfide- $\text{d}_{10}$ ) $^+/(p\text{-terphenyl-}d_{14})^-$  system [4,5]. For the latter system we have observed the phase shift of oscillations in various hydrocarbon solvents [5]. The shift is caused by the delay in (diphenylsulfide- $\text{d}_{10}$ ) $^+$  formation in reaction of solvent hole with a diphenylsulfide molecule. The rate constants for hole capture by diphenylsulfide molecules have been found to substantially exceed the diffusion controlled ones. The hopping mechanism of hole motion is supposed to be responsible for large values of rate constants. The life time of solvent holes has been estimated. The fraction of singlet-correlated pairs in the radiation track has been found from the oscillation amplitude to be 30 to 35%.

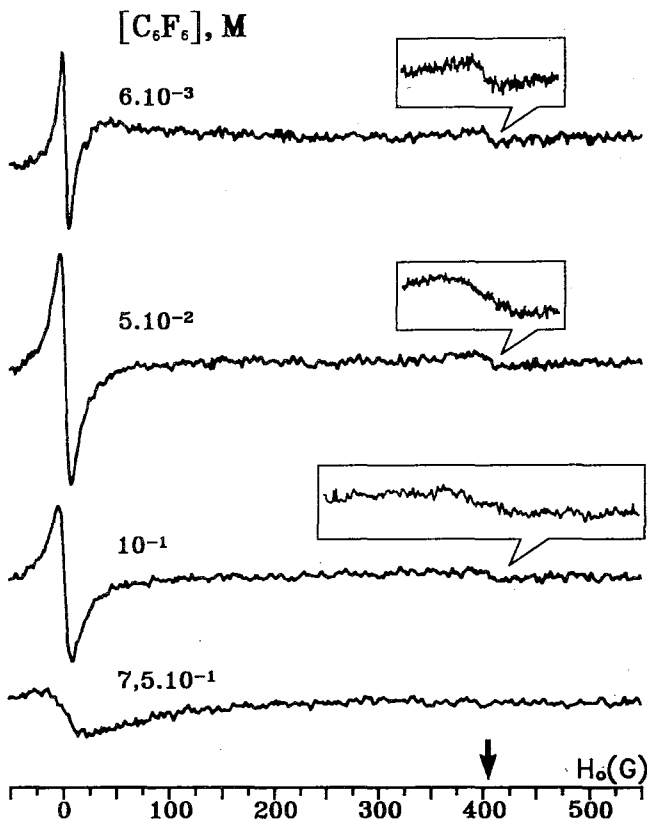


Fig.2. MARY-spectra of  $C_6F_6$  solutions in squalane for different  $C_6F_6$  concentrations (room temperature) taken as first derivatives. Inserts show magnified satellite line at  $H = 3a$ ,  $a = 135$  G being the hyperfine coupling constant for  $C_6F_6$  anion.

**Level crossing effects in MARY spectra.** The magnetic field dependence of radical reaction yield (MARY spectrum) is typically a smooth monotonous curve without any characteristic sharp features. Level crossing (or degeneracy) should however result in appearance of sharp extrema in MARY spectra for long lived spin-correlated pairs [6] as discussed above. We observed the local fluorescence maxima in zero field for arbitrary complex RPs provided the hyperfine couplings in one of the pair partner are negligibly small [7]. If only equivalent nuclei contribute to the hyperfine interactions, additional local maxima were observed in

characteristic "multiple" fields [8]. Breaking down of spin coherence in the course of ion-molecular charge transfer reaction leads to maxima broadening in both zero and multiple fields (Fig. 2). Relation between MARY line broadening and the rate of charge transfer is similar to that for EPR spectra. Rate constants of charge transfer reaction for hexafluorobenzene radical anion in squalane and *cis*-decalin radical cation in hexane have been extracted by simulation of MARY spectra [9].

**Conclusion.** Spin correlated radical ion pairs are the unique species where quantum coherence effects upon the reaction yield could be readily observed. The reason for this is a relatively long coherence life time of RP spin states on one hand and a small scale of magnetic interactions resulting in nanosecond time scale of quantum oscillations on another.

**Acknowledgment.** The work was supported by ISF, Grant #300, by INTAS, Grant #93-1626 and by the Russian Fund of Fundamental Research, Grant #93-03-5035.

### References

- [1] K.M.Salikhov, Yu.N.Molin, R.Z.Sagdeev and A.L.Buchachenko, Spin Polarization and Magnetic Effects in Radical Reactions (Elsevier, Amsterdam, 1984).
- [2] U.E.Steiner and T.Ulrich, *Chem. Rev.* **89** (1989) 51.
- [3] O.A.Anisimov, V.L.Bizyaev, N.N.Lukzen, V.M.Grigoryants and Yu.N.Molin, *Chem. Phys. Letters* **101** (1983) 131.
- [4] A.V.Veselov, V.I.Melekhov, O.A.Anisimov and Yu.N.Molin, *Chem. Phys. Letters* **136** (1987) 263.
- [5] V.M.Grigoryants, B.M.Tadjikov, O.M.Usov and Yu.N.Molin, *Chem. Phys. Letters* (submitted for publication).
- [6] O.A.Anisimov, V.M.Grigoryants, S.V.Kiyanov, K.M.Salikhov and Yu.N.Molin, *Teor. Eksper. Khim.* **18** (1982) 292 (in Russian).
- [7] D.V.Stass, N.N.Lukzen, B.M.Tadjikov and Yu.N.Molin, *Chem. Phys. Letters* **233** (1995) 444.
- [8] D.V.Stass, B.M.Tadjikov and Yu.N.Molin, *Chem. Phys. Letters* **235** (1995) 555.
- [9] D.V.Stass, N.N.Lukzen, B.M.Tadjikov, V.M.Grigoryants and Yu.N.Molin, *Chem. Phys. Letters* (submitted for publication)

## S P I N C A T A L Y S I S

Anatoly L. Buchachenko\* and Vitaly L. Berdinsky  
N.N. Semenov Institute of Chemical Physics,  
Russian Academy of Sciences,  
4 Kosygin str., Moscow 117977, Russia

Chemical reaction of spin carriers (radicals, paramagnetic ions, triplet molecules, etc) are selective, they are allowed to produce such products only whose total electron spin is identical to that of reagents. In particular, the triplet radical pair unables to recombine or disproportionate generating the diamagnetic molecules until its triplet state transforms into the singlet one.

Several factors may induce spin conversion, among them the magnetic interactions, Zeeman and Fermi, are the most significant. They result to the magnetic phenomena in chemical reactions, such as magnetic field effect, magnetic isotope effect, as well as chemically induced nuclear magnetic polarization<sup>1,2</sup>. Microwave pumping of the radical pairs stimulates also spin conversion and induces magnetic effects of the second generation - reaction yield detected magnetic resonance, stimulated nuclear polarization and radio induced magnetic isotope effect (for review see<sup>2,3</sup>).

Recently it has been experimentally discovered that in the radical triad one of the radical partners affects the chemical reactivity of the pair of others, inducing spin transformation of this pair. This phenomenon is shown to be caused by exchange interaction between the radical triad partners which stimulates

doublet-doublet spin evolution and produces the oscillating triplet-singlet spin conversion of the selected radical pair in radical triad under influence of the odd radical spin. In particular, for the starting triplet state of the selected radical pair its singlet state population  $\rho_{SS}^T(t)$  follows equation  $\rho_{SS}^T(t) = (\Delta J / 2\Omega)^2 \sin^2 \Omega t$  where  $\Delta J$  is the exchange energy difference between spin catalyzer and each of the partners of selected radical pair,  $2\Omega$  is the energy of doublet-doublet splitting in the spin triad.

Spin catalysis has been experimentally demonstrated for the molecular systems in which unambiguously exchange interaction operates only<sup>4,5</sup>. The recombination probability of the triplet RP (PhCHCH<sub>3</sub>CO CHCH<sub>3</sub>Ph) generated by photolysis of d,1-2,4-diphenyl-3-one was shown to increase three times in the presence of stable nitroxyl TEMPO when concentration of TEMPO, which is known to be the powerful radical scavenger, increases from 0 to 0.15 M. This result is a direct indication of the spin catalytic effect in radical reactions, it still demonstrates the predominance of the catalytic function of nitroxyls over their traditional function to be a radical acceptor<sup>4</sup>.

An other kinetic evidence of spin catalytic effect has been detected in the recombination of alkyl radicals with nitroxyl biradicals<sup>5</sup>. The rate constants of the first recombination of alkyl radical with one of the biradical termini was shown to exceed these of the second recombination with remaining monoradical terminus by 10-15%. The effect was attributed to the spin catalysis of the first recombination in the encounter pair of alkyl radical with one of the biradical termini by the second spin carrying terminus.

## References

- (1) Salikhov, K.M.; Molin, Yu.N.; Sagdeev, R.Z.; Buchachenko, A.L. *Spin Polarization and Magnetic Effects in Radical Reactions*; Elsevier: Amsterdam, 1984.
- (2) Buchachenko, A.L.; Frankevich, E.L. *Chemical Generation and Reception of Radio- and Microwaves*; VCH Publishers: New York, 1994.
- (3) Buchachenko, A.L. *Russ.Chem.Rev.* 1991, 62, 1073.
- (4) Step, E.N.; Buchachenko, A.L.; Turro, N.J. *J. Am. Chem. Soc.* 1994, 116, 5462.
- (5) Buchachenko, A.L.; Step, E.N.; Ruban, V.L.; Turro, N.J. *Chem. Phys. Lett.*, 1995, 233, 315.

## ESR Studies of Radical Kinetics in Solution and Zeolites

C. Blaettler and H. Paul

Physikalisch-Chemisches Institut, Universität Zuerich, Winterthurerstr. 190,  
CH-8057 Zuerich, Switzerland

During the past two decades, time-resolved ESR spectroscopy (TRESR) has established itself as a very suitable technique for accurate determinations of rate constants of radical reactions in solution, its main advantages being the unique radical specific resolution as well as the direct access to absolute radical concentrations [1,2]. Usually the experiment is performed by using a commercial ESR spectrometer with time-resolution of about 10  $\mu$ s, combined with photolytic radical generation by means of a cw UV lamp, the light of which is chopped by a rotating sector. With such an arrangement radical lifetimes of about  $\tau > 100 \mu$ s can be determined very accurately. For shorter lived species, kinetic investigations using TRESR are rare, despite the fact that lasers, delivering short and intense light pulses, and ESR detection systems with time-resolutions of 10-100 ns are standard equipments since several years. The difficulty lies in the evaluation of the time-dependent magnetization, measured in such experiments, which on the microsecond time scale is determined not only by the chemical kinetics but also by the spin dynamics. In addition, the spin system usually exhibits chemically induced electron polarization (CIDEP), i.e. it is not in thermal equilibrium. Thus, not only the number of parameters is increased, but also the direct access to the absolute radical concentration is lost.

Already for the simplest system, photolysis of a starting compound R-R into two identical radicals R which do nothing else but recombining, the dependence of the magnetization on time is determined by a variety of unknown parameters like the spectrometer sensitivity, the initial radical concentration, the spin polarization created in the geminate and in F-pairs, the rate constant of the radical termination, the spin-spin and spin-lattice relaxation times, and the amplitude of the microwave field in the ESR cavity. Nevertheless, it is possible to analyse the time-dependent magnetization rather accurately and to extract reliable kinetic parameters, even for more complicated reaction schemes. This will be demonstrated by an example, the TRESR determination of fast addition rate constants of *tert*-butyl radicals to a variety of substituted alkenes.

The method essentially works, because it determines a fast chemical radical kinetics of pseudo first order in competition to the decay of the geminate spin polarisation, due to spin-

lattice relaxation. Accordingly, its applicability is limited to radical decay times  $\tau$ , which are not too slow in comparison to spin relaxation, i. e. typically to the range  $\tau < 30 \mu\text{s}$ . As the successful analysis of the magnetization time-profiles requires some effort and also a rather careful design of the radical source, laser-flash photolysis with optical absorption measurement will be the preferable alternative for radical kinetics in this time-range in most cases. However, in cases of overlapping absorption bands or low optical absorptions, the here used TRESR method might well be the most suitable technique to get the desired kinetic information.

We will also briefly discuss some ESR experiments aiming at the detection of paramagnetic transients during and after UV-irradiation of ketones, absorbed in zeolites. In recent years, the photochemistry in zeolites has received increasing attention. However, experimental techniques to investigate reaction transients and their kinetics in these microcrystals have remained scarce, with optical diffuse reflectance spectroscopy having been the only more successful one in recent years [5].

It turns out that, using a suitable, optically transparent flow system, the sensitivity of time-resolved as well as steady-state ESR is sufficient to detect at least some of the transient radicals, and even spin correlated radical pairs, which are formed from photoexcited ketones in NaX-Zeolites. All gathered experimental evidence leads to the supposition, that the observed radicals are generated via a primary electron-transfer reaction from triplet excited ketone molecules to the zeolite lattice, followed by cleavage of the resulting cation. From the ESR spectra and their decay times it is concluded, that the radicals observed are strongly immobilized, sticking to the zeolites' cavity walls at different sites.

## References

- [1] H. Fischer and H. Paul, *Accounts Chem. Res.* **20** (1987) 200, and ref. cited therein.
- [2] A. Salikhov and H. Fischer, *Appl. Magn. Reson.* **5** (1993) 445, and ref. cited therein.
- [3] N. J. Turro and Z. Zhang in, "Photochemistry on Solid Surfaces". M. Anpo and T. Matsuura, Eds., Elsevier, Amsterdam, 1989.
- [4] V. Ramamurthy, D. F. Eaton, and J. V. Caspar, *Accounts Chem. Res.* **25** (1992) 299, and ref. cited therein.
- [5] F. L. Cozens, H. Garcia, and J. C. Scaiano, *J. Am. Chem. Soc.* **115** (1993) 11134, and ref. cited therein.

## ELECTRON TRANSFER PROCESSES IN COMPLEX ORGANIC REACTIONS STUDIED BY SPIN EFFECTS

T.V. Leshina

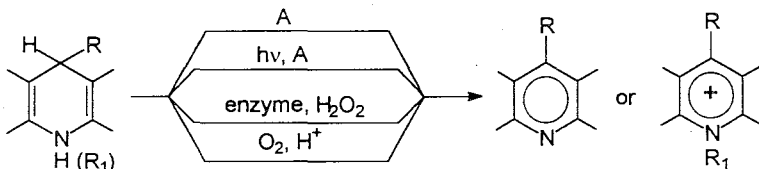
Institute of Chemical Kinetics and Combustion, Novosibirsk-90, 630090 Russia

Methods of spin chemistry (CIDNP and magnetic effects) now undoubtedly play a leading role in the investigations of elementary stages in complex organic reactions. Applications of these techniques allows to identify the structure and to estimate the reactivity of active short-lived paramagnetic intermediates with the lifetimes in the range from nano- to microseconds. Research on the intermediates formed in the reactions involving single-electron transfer steps is of greatest importance. Suffice it to mention the nucleophilic substitution processes, where the possibility of single-electron transfer has been discussed for years, and it was CIDNP technique that has provided unambiguous solution of this problem.

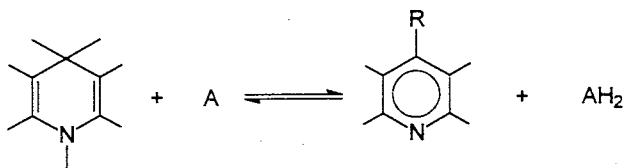
Nowadays, the appearance of single-electron steps in various biologically relevant processes is intensively studied and discussed. The processes are, first of all, the reactions catalyzed by oxygenase enzymes (peroxidase, glutamate dehydrogenase, alcohol dehydrogenase, cytochromes, etc.), as well as photoinduced transformations of some vitamins.

The present report also describes the attempts to apply spin chemistry techniques to the investigations of elementary mechanisms of several chemical reactions which are considered to be separate stages of important biochemical processes.

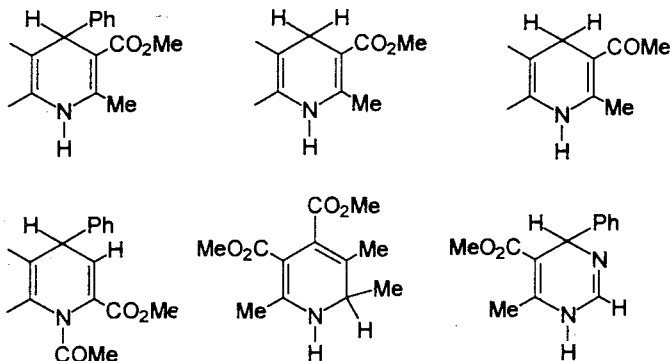
Oxidation of native NADH coenzymes and their synthetic analogs, N-benzyl nicotinamide (BNAH) and 1,4-dihydropyridines (DHP), may proceed due to various factors:



In this case, the 1,4-dihydropyridine skeleton, characteristic for all above mentioned compounds, transforms into pyridine (or pyridinium cation). In principle, three possible mechanisms discussed in the literature could be proposed for the brutto-process in the presence of oxidant A.



These are one-step hydride transfer (ionic mechanism) [1] and two types of radical processes, two-stage ( $e^-$ ,  $H^\cdot$  or  $H^\cdot$ ,  $e^-$ ) and three-stage ( $e^-$ ,  $H^\cdot$ ,  $e^-$ ; or  $e^-$ ,  $e^-$ ,  $H^\cdot$ ; or  $H^\cdot$ ,  $e^-$ ,  $e^-$ ) ones [2].  $^1\text{H}$  CIDNP experiments have confirmed the existence of the electron transfer step in photo-oxidation reactions of BNAH with flavin [3], and 1,4-DHP with onium salts [4]. Results of the present research - applications of time-resolved and stationary  $^1\text{H}$  and  $^{15}\text{N}$  CIDNP techniques - have made it possible to define the whole sequence of radical stages and to establish the structure of paramagnetic intermediates of photoinduced oxidation of 1,4- and 1,2-DHPs, and 1,4-dihydropyrimidines in the presence of various electron acceptors. Compounds studied in the present work are



Following electron acceptors have been used: chloranil, duroquinone, benzoquinone, 2,5-dichlorobenzoquinone, 1-chloroanthraquinone,

## PL-7

9-cyanophenanthrene. It has been found that the reaction of N-unsubstituted 1,4-DHPs with quinones proceed via sequential transfer of  $e^-$ ,  $H^+$  (from the first position of radical cation) and  $H^+$ . The process is preceded by the formation of charge transfer complex. When it comes to use aromatic hydrocarbons as acceptors, the reaction starts with hydrogen atom abstraction from the fourth position of DHP. In the case of N-substituted 1,4-DHPs, in addition to the first step of single-electron transfer we have managed to detect the transformations of radical cations in the bulk (oxidation for N-methyl substituted 1,4-DHP and disproportionation with the elimination of acetyl group for N-COMe derivative). All the reactions under study are sensitive to the polarity of medium and the presence of oxygen in solution. Thermal mixing reactions of 1,4-DHPs with electron acceptors result in the same set of products, but CIDNP effects are absent. However, ESR and UV-spectroscopic studies have shown the formation of charge transfer complexes [5] and radical anions of the acceptors, thiobenzophenone and quinones [5,6].

According to literature data [7], single-electron transfer step also plays a role in enzymatic oxidation of NADH. To observe the electron transfer stages, the kinetics of aerobic oxidation of NADH and 2-methyl-1-(trimethylsilyloxy)-1-propene by horseradish peroxidase has been studied in various magnetic fields. We have observed magnetic field effects formed at the stage of transformations of active peroxidase intermediates, Compound I and Compound II which constitute the main catalytic cycle of the enzyme.

The last part of the report is devoted to studies of the role of radical ion stages in *cis-trans* isomerization of all-*trans*-retinal. This process is considered to be a part of the image formation in mammalian eye [8]. Recently, the photoreactions of carotenoids, the species closely related to retinal, were successfully studied by means of spin chemistry techniques (CIDEP [9], magnetic effects [10]). However, there is a lack of literature data on direct participation of radical ions in *cis-trans* isomerization of retinal and other carotenoids, whereas radical ion mechanism of photosensitized *cis-trans* isomerization substituted olefins in the presence of electron donors and acceptors has been definitively proved [11]. Indeed, we have observed  $^1H$  CIDNP effects of the initial retinal and its isomers (9-*cis*, 11-*cis*, and 13-*cis*) in the photoisomerization in deuterioacetonitrile in the presence of electron acceptors. The mechanism of isomerization is discussed.

The financial support of Russian Foundation for Basic Research (grant No. 94-03-08976), International Science Foundation (grant RC7000/RC7300), and NAS of the USA (CAST program) is gratefully acknowledged.

1. Meijer, L.H.P.; van Niel, J.C.G.; Pandit, U.K. *Tetrahedron* **1984**, *40*, 5185.
2. Powell, M.F.; Wu, J.C.; Bruice, T.C. *J. Amer. Chem. Soc.* **1984**, *106*, 3850.
3. Hore, P.J.; Volbeda, A.; Dijkstra, K.; Kaptein, R. *J. Amer. Chem. Soc.* **1982**, *104*, 6262.
4. Ulrich, S.; Pfeifer, D.; Timpe, H.-J. *J. Prakt. Chemie.* **1990**, *332*, 563.
5. Ohno, A.; Kito, N. *Chem. Letters* **1972**, 369.
6. Fukuzumi, S.; Nishizawa, N.; Tanaka, T. *J. Org. Chem.* **1984**, *49*, 3571.
7. Yokota, K.; Yamazaki, I. *Biochemistry* **1977**, *16*, 1913.
8. Goodwin, T.W. *The Biochemistry of Carotenoids*, Chapman and Hall: London, 1980.
9. Jeevarajan, A.; Khaled, M.; Forbes, M.; Kispert, L. *International Symposium on Magnetic Field and Spin Effects in Chemistry and Related Phenomena*, Konstanz, 1992, p. 9.
10. Triebel, M.; Batalov, S.; Frankevich, E.; Anderhofer, A.; Frick, J.; von Schuetz, J.; Wolf, H. *Ibid.* p.48.
11. Leshina, T.V.; Belyaeva, S.G.; Maryasova, V.I.; Sagdeev, R.Z.; Molin, Yu.N. *Chem. Phys. Letters* **1980**, *75*, 438.
12. Leshina, T.V.; Salikhov, K.M.; Sagdeev, R.Z.; Belyaeva, S.G.; Maryasova, V.I.; Purtov, P.A.; Molin, Yu.N. *Chem. Phys. Letters* **1980**, *7*, 228.

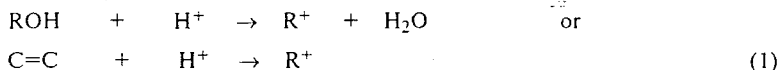
**ON THE REAL MECHANISM OF CARBENIUM ION  
REACTIONS IN SULFURIC ACID**

V.B.Kazansky

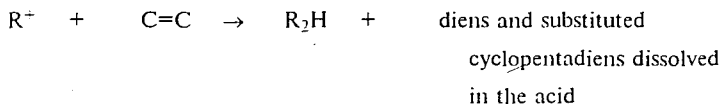
*Zelinsky Institute of Organic Chemistry, RAS, Moscow B-334, Russia.*

Catalytic transformations of hydrocarbons in sulfuric acid are interesting both from theoretical and practical points of view. Indeed, the sulfuric acid catalysed alkylation of olefins by isobutane is still used by chemical industry at the commercial scale, whereas the transformations of olefins and alcohols in sulfuric acid are traditionally considered as classical examples of carbenium-ion reactions.

It is generally believed that the aliphatic carbenium ions are formed in concentrated sulfuric acid according the following reactions:



The corresponding hydrocarbon final products are then yielded by the subsequent transformations of carbenium ions. For instance, in an excess of concentrated 95% sulfuric acid both alcohols and olefins are involved in the so called "conjunct polymerisation" resulting in the complicated mixture of isoparaffins [1,2]. This was explained by the combination of carbenium ion reactions of oligomerisation and hydride transfer:



In more dilute 75-65 % acid the hydride transfer does not take place and the reaction results in olefinic dimers and trimers [2]:



Below we report the results of the "in situ"  $^{13}\text{C}$  NMR study of the reaction mechanism of both polymerisation and "conjunct polymerisation" of olefins and alcohols in sulfuric acid.

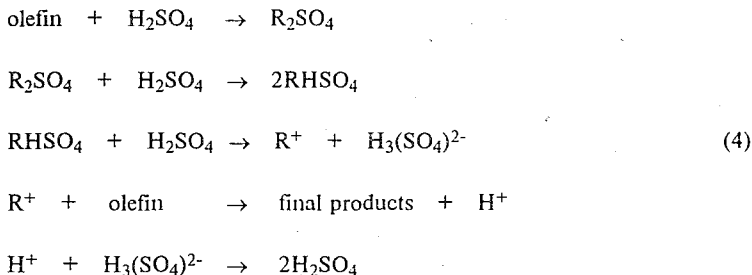
The reaction mixtures of different composition were prepared at 0 °C. Then they were rapidly transferred into ampouls for NMR measurements and the study of kinetics of the corresponding reactions was performed "in situ". In the experiments with concentrated acid, the reaction mixture was gradually separated in two layers. The lower heavier layer represented the reaction mixture of different composition, which was gradually transforming into final products. The upper layer contained the resulting hydrocarbons. In course of NMR measurements only the lower layer was inside the coil of the NMR spectrometer. This allowed both the "in situ" study of the reaction intermediates and of kinetics of their transformations. In addition, the kinetics was also monitored by the amount of hydrocarbon reaction products accumulated in the upper layer. The composition of the final products was analysed after completion of the reaction by chromatography and mass spectrometry and NMR.

The study of "conjunct polymerisation" of 1-pentene demonstrated that this is a consecutive reaction, which proceeds in two steps. The first step results in the mixture of different pentyl-sulfuric acid esters. This was confirmed by  $^{13}\text{C}$  NMR spectra with the chemical shifts of 80-90 ppm from carbon atoms connected with oxygen atoms of the esters and by the chemical shifts of 10-30 ppm from aliphatic carbon atoms. On the other hand, no lines from the aliphatic carbenium ions with the shifts above 300 ppm were observed.

At room temperature the sulfuric acid esters were rather stable and the hydrocarbon final products were formed very slowly. On the other hand, in an excess of 95 % acid the reaction was completed in about only half an hour yielding the complicated mixture of isoparaffinic oligomers and cyclopentadienes

dissolved in sulfuric acid. This indicates the "conjunct polymerisation". However, no NMR lines from aliphatic carbenium ions were observed in this case as well.

The reaction mechanism was explained by the following scheme:



In other words, the sulfuric acid esters act as precursors of aliphatic carbenium ions. However, the steady state concentration of the latter species is far below the sensitivity of  $^{13}\text{C}$  NMR detection.

Thus, the reaction mechanism of catalytic transformations of olefins and alcohols in concentrated sulfuric acid is similar to heterogeneous catalysis on zeolites, where the surface esters also are the precursors of the carbenium ion intermediates [3] and also were not detected by  $^{13}\text{C}$  NMR [4]. On the other hand, the role of the excess of sulfuric acid is specific for the homogeneous acid catalysis. It consists in promotion of formation of carbenium ions due to replacement of alkyl fragments in the sulfuric acid esters by protons instead of the more difficult heterolytic dissociation of the esters:

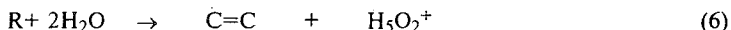


Therefore, in the absence of the excess of 95 % acid or in more dilute acid, where the protonation of the esters does not take place, the reaction rate of conjunct oligomerisation is much lower.

The study of the reaction mechanism in 65-75 % sulfuric acid, was performed for tertial butanol dehydration. In this case the reaction products were quite different from the above "conjunct polymerisation" representing the mixture

of branched C<sub>8</sub>-C<sub>12</sub> olefinic dimers and trimers. Despite the generally accepted carbenium ion mechanism of this reaction, the formation of aliphatic carbenium ions was also not detected by <sup>13</sup>C NMR. Instead only the lines of the tertiary butyl oxonium ions with the chemical shifts of central carbon atoms in the range of 80-83 ppm were observed. The dependence of the shifts on the acid concentration indicated a rapid exchange of protons between oxonium ions and water or alcohol molecules [5].

The obtained results indicated that in dilute sulfuric acid the active intermediates of polymerisation are the oxonium ions, which also are the precursors of the final products. Thus, the polymerisation of tertiary butanol in moderately concentrated sulfuric acid is not a real carbenium ion reaction, but rather an oxonium ion reaction, which probably obeys an S<sub>N</sub> II mechanism. This was explained by the different ways of heterolytic dissociation of hydrated tert-butyl oxonium ions, which unlike sulfuric acid esters, produce olefins and hydrated hydroxonium ions:



This is possible due to the much lower heats of tertiary carbenium ions hydration in comparison with primary and secondary ions.

## REFERENCES

1. L.Smerling, Ind.Eng.Chem 45 (1953) 1447.
2. F.C.Whitmore, Chem.Eng.News 26 (1948) 668.
3. 3.M.T.Arnson, R.J.Gorte, W.E.Farneth, D.White, J.Am.Chem.Soc. 111 (1989) 840.
4. V.B.Kazansky, Acc. Chem. Res. 24 (1991) 317.
5. V.B.Kazansky, F.Figueras, L.C.de Menorval, Catal. Lett. 29 (1994) 311.

## Neutral or Ionic Organometallic Complexes in Homogeneous Catalysis

W. Keim, Institut für Technische Chemie und Petrochemie, RWTH Aachen

Chemical reactions can occur by a cationic, anionic or radical mechanism. When a transition metal is involved the variety increases providing a multitude of additional pathways and opportunities as shown for C-C linkages in Fig. 1

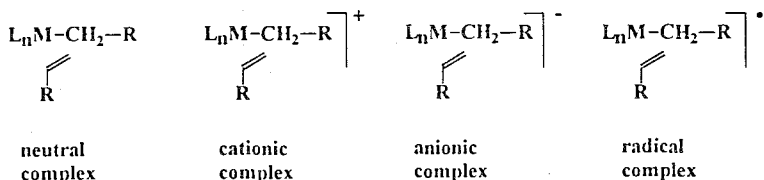


Fig. 1 Ionic, neutral and radical complexes in C-C linkage.

Looking at the literature the majority of reaction mechanisms proposed deal with neutral complexes but there are precedents for all mechanism shown in Fig. 1.

Since many years we are investigating the use of organometallic complexes as catalyst precursors. As is shown in Fig. 2 catalysts can be prepared by various routes [1]

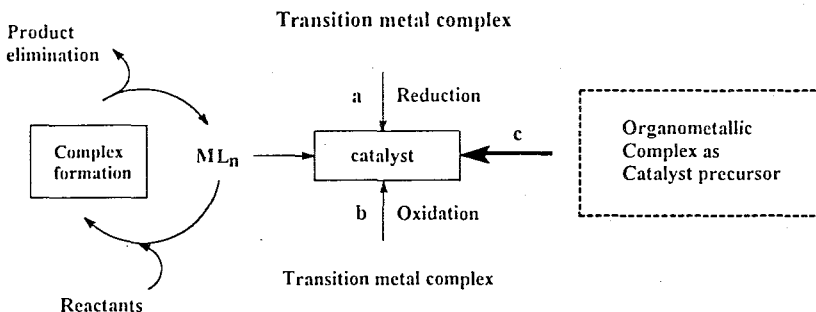


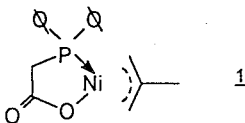
Fig. 2 Preparation of homogeneous catalysts

The reduction route (a) is most frequently used, and its beginnings go back to the work of Karl Ziegler, who found that the combinations of metal alkyls (or hydrides) of Group I - III metals and a transition metal salt of Group IV - VIII metals, such as  $AlEt_3$  plus  $TiCl_4$ , yield active catalysts for olefin polymerisation. Ziegler catalysts can also be prepared in the presence of ligands, thus providing the reduction route with a high degree of applicability and versatility. Whenever possible, industry will use the „in situ“ reduction route, due to its lower cost and ease of catalyst preparation. Multiple reducing agents can be applied, thus giving a high degree of flexibility to this method. The number of papers and patents in this field is nearly unlimited. Less common is the catalyst preparation (b) by oxidizing a low-valent metal complex to a catalytically active higher oxidation state. This route should be also very general and can be conducted in the presence of ligands. Very often isolated and well characterized organometallic complexes are applied in homogeneous catalysis (route c). However, one must be aware that the active catalytic species is not necessarily the same compound that is placed into the reaction mixture as starting complex. Many transformations of the nominal catalyst often occur prior to generating the true catalyst. Here reference to the organometallic starting complex as the catalyst is misleading.

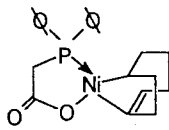
The use of organometallic complexes as catalyst precursors offers many advantages, especially regarding understanding of the reaction mechanism. The individual steps of homogeneous catalytic reactions are usually reactions that are well known from organometallic coordination chemistry. Thus starting from an organometallic complex as a catalyst precursor, the use of *in situ* spectroscopy is possible thus providing some insight into the single reaction steps occurring.

### Neutral complexes

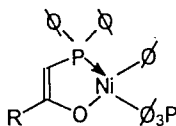
We became interested in comparing the use of neutral and cationic complexes in homogeneous catalysis. The complex **1** is highly active and chemoselective for the linear oligomerization of ethene to  $\alpha$ -olefins as practised in the SHOP-process by Shell [2,3]



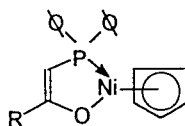
We could demonstrate that catalysis rests with the  $P^{\wedge}O$  chelate ligand. The complexes **1-4** yield identical product slates in ethylene oligomerisation regarding selectivity to linear products.



2



3

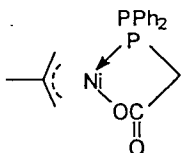


4

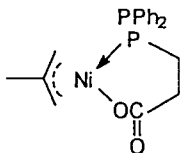
We postulate:

1. All active complexes in the linear oligomerisation of ethylene are square planar. Tetrahedral environment leads to branching or even inactivity.
2. Chain growth occurs always trans to oxygen.
3.  $\beta$ -elimination occurs when the growing chain in trans-position to oxygen is shifted to trans-position to phosphorous.

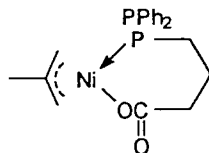
Indeed, by introducing substituents in the chelate part or enlarging the ring size as shown for complexes 1, 5-8 leads to a control of selectivity.



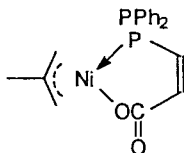
1



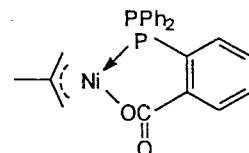
5



6



7



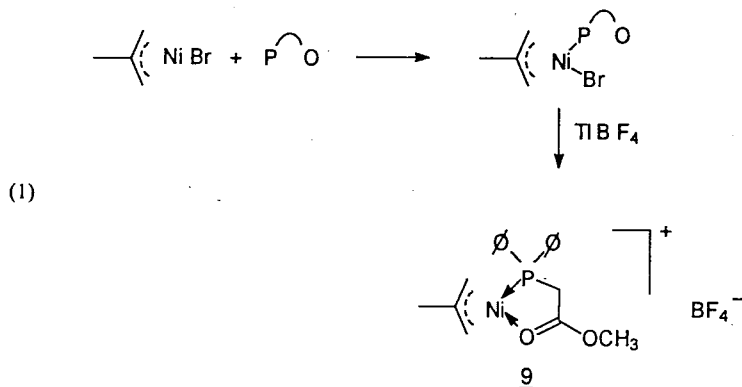
8

Complex 1, 7 and 8 show similar selectivity and activity. Complex 5 is less active and selective and complex 6 possessing a 7-membered ring is nearly inactive.

It can be stated: square planar complexes possessing P<sup>^</sup>O chelates are chemoselective for ethylene only. Introduction of substituents allow a control of the molecular weight. Electron withdrawing substituent in the P<sup>^</sup>O chelate part favour higher molecular weights (waxes) while electron pushing groups favour dimerisation and shorter chain  $\alpha$ -olefins.

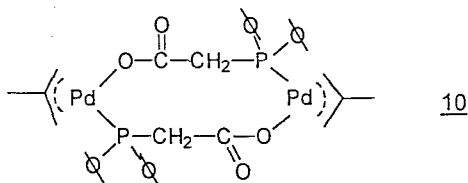
### Cationic complexes

The cationic complex 9 was synthesised according to eq. 1



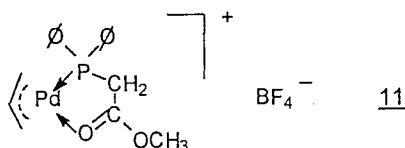
Complex 9 is extremely reactive, even at  $-50\text{ }^{\circ}\text{C}$  for the ethylene oligomerisation and products which are 50 - 60 % linear are obtained. However, complex 9 also reacts with  $\alpha$ -olefin leading to branched products. Complex 1 and 9 show great similarity in the ligands composition, but they differ in the type of bonding.

Attempts to isolate a palladium complex analogous to 1 failed. Instead a new complex 10, in which the P-O ligand is bridged, could be isolated [4].



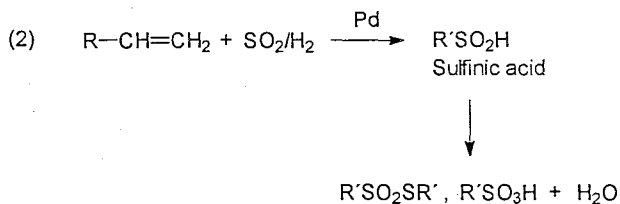
Complex 10 shows no activity in the C-C linkage of olefins.

The cationic complex 11, synthesised similar as shown in eq 1, is active for ethylene dimerization and oligomerization



Complex 11 also catalysed the dimerisation of styrene and ethylene to 3-phenylbut-1-ene. It is also active in the codimerization of ethene and CO to polyketone [4,5].

Cationic complexes of palladium can also be applied to catalyse the hydrosulfination of sulfur dioxide and hydrogen [6,7] according to eq (2), which represents a novel reaction.



cat.:



The sulfenic acids are unstable and disproportionate into thiosulfonates and sulfonic acids. A variety of olefins have been applied. The mechanism proposed is shown in Fig. 2.

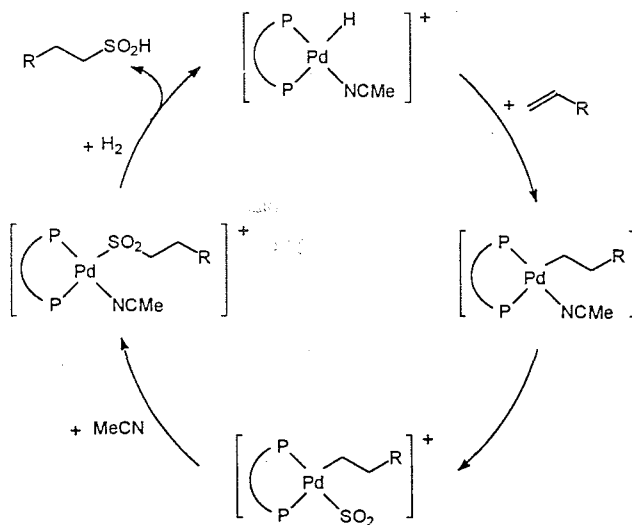


Fig. 2 Mechanism of hydrosulfonation

It can be generalized that cationic complexes open new opportunities in homogeneous catalysis. Compared to the wealth of reactions available from neutral organometallic complexes ionic complexes have been stepchildren. Organometallic chemists are called up to study the chemical reaction behaviour of ionic organometallic complexes thus paving the way for further advancement in homogeneous catalysis.

#### Literature

- [1] W. Keim, *J. of Molec. Catalysis* 52 (1989) 19-25
- [2] M. Peuckert and W. Keim, *Organometallics* 2 (1983) 594
- [3] W. Keim, R.P. Schulz, *J. of Molec. Catalysis* 92 (1994) 21-33
- [4] G.J.P. Britovsek, W. Keim, S. Mecking, D. Sainz, T. Wagner, *J. Chem. Soc. Chem. Commun.* (1993) 1633
- [5] W. Keim, H. Maas, S. Mecking, *Zeitschrift für Naturforschung B*, 50, 430-438 (1995) in English
- [6] W. Keim, J. Herwig, *J. Chem. Soc. Chem. Commun.* (1993) 1592
- [7] J. Herwig, W. Keim, *Inorganica Chimica Acta*, 222 (1994) 381-385

## FIVE-COORDINATE CARBON IN OXIDATION REACTIONS

A. E. Shilov

*Semenov Institute of Chemical Physics, RAS, Chernogolovka, Russia*

High-valent oxygen-containing metal complexes are able to transfer oxygen atom to an acceptor molecule in olefin epoxidation, oxidation of CO, formation of N-oxides from amines, hydroxylation of aromatic and aliphatic hydrocarbons. Enzymatic oxidations performed by monooxygenases include oxygen transfer as the key step in the catalytic process. Direct oxygen atom transfer is believed to occur in the mechanism of the oxidation of unsaturated molecules. Intermediate complexes via oxygen atom bound to the metal are accepted as intermediates in such reactions and this mechanism agrees well with experimental facts.

In the case of hydroxylation of C-H bonds in alkanes saturated character of C-H bond seems to preclude formation of an intermediate complex. Usually two alternative mechanisms are considered for hydroxylation of C-H bonds in saturated molecules:

- 1) concerted insertion of O atom bound to metal into C-H bond, and
- 2) "oxygen rebound mechanism" involving hydrogen atom abstraction followed by recombination of radical formed with OH group on the metal.

It is the latter mechanism that is widely accepted in the literature now although the former is thermodynamically more favourable.

The evidence for the oxygen rebound mechanism involves:

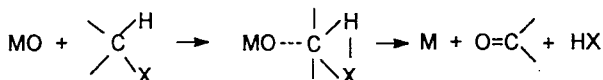
- 1) high isotope effects ( $k_H/k_D > 8$ );
- 2) isomerization observed in the products of hydroxylation;
- 3) the use of radical traps.

However the detailed analysis of the experimental results shows that application of the oxygen rebound mechanism leads to serious contradictions. These contradictions are shown to be removed if to accept a mechanism of *oxygen atom insertion preceded by formation of an intermediate with five-coordinate carbon via O atom bound to metal.*

The mechanism including five-coordinate carbon intermediate is known for alkane reactions with superacids as well as with electron rich transition metal complexes.

The analysis of the results in aerobic biological oxidation and in chemical model systems shows that this mechanism is wide-spread in the systems where oxygen is bound to the active metal center.

A particular case of this mechanism is oxygen addition followed by HX elimination:



This mechanism is particularly favourable in catalytic chemical reactions at high temperatures since it is accompanied by increase of entropy. Concrete examples of the mechanism involving five-coordinate carbon will be considered in the lecture.

The conclusion can be made that this field of catalytic oxidation is very promising for selective catalytic processes of alkane oxidation including methane oxidation.

## Activation of H<sub>2</sub>O<sub>2</sub> and Alkylhydroperoxydes with metal complexes: Achievements and Problems

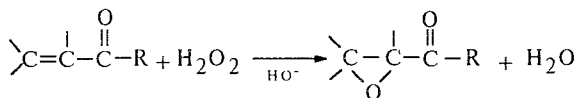
I.I. Moiseev

*N.S.Kurnakov Institute of General and Inorganic Chemistry  
Russian Academy of Sciences,  
Leninsky Prospekt 31, 117907, Moscow GSP-1, Russia*

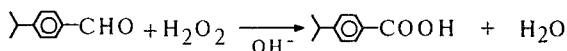
Catalytic oxidation reactions involving peroxide reagents as the oxygen source have provided an attractive alternative to the synthetic approaches based on the use of stoichiometric oxidants like dichromate, permanganate, HNO<sub>3</sub>, H<sub>2</sub>SO<sub>4</sub>, oleum, Cl<sub>2</sub> which were widely employed 50 years ago. The tendency to use cleaner oxidants and cleaner technology to manufacture fine and bulk chemicals is to meet the society demand for both environmental protection and less energy consumption [1-5].

Hydrogen peroxide and organic peroxides are widely used in organic synthesis since the discovery of Fenton chemistry [6]. Until the late 1950 s, the field of metal-catalyzed peroxide oxidation was influenced by the development of the free radical chain theory of autoxidation. Nowadays, the approach based on the oxidation with peroxides is enlarged tremendously encompassing many reactions catalyzed with bases, acids and metal complexes and rationalized within polar mechanistic schemes [1-3,7,8,9]. The following reactions will be taken as a starting point for the discussion in the paper:

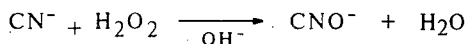
- Epoxidation of  $\alpha,\beta$ -unsaturated carbonyl compounds, carboxylic acids and their derivatives [8,9]:



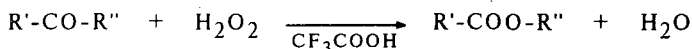
- Oxidation of aromatic aldehydes [4]:



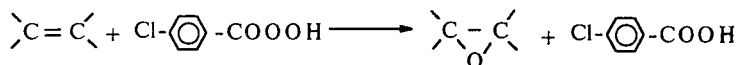
- Oxidation of cyanide ion [1]:



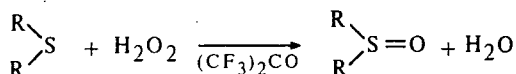
- Baeyer-Villiger oxidation [8,9]:



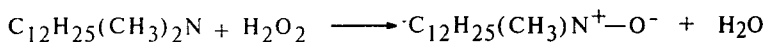
- Epoxidation of alkenes after N.A.Prilezhaev, e.g. [10]:



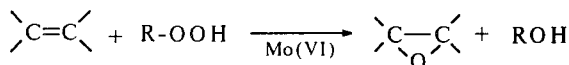
- Oxidations of sulfides [1]:



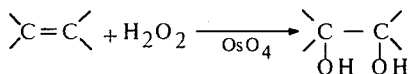
- Oxidation of amines: [4]:



- Epoxidation of alkenes after Halcon/Arco process [1,2,3,7,11]:

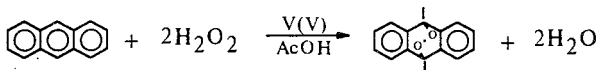


- Milas dihydroxylation [1,2,12]:

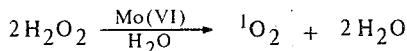


PL-11

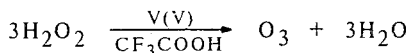
- Singlet oxygen transfer [13]:



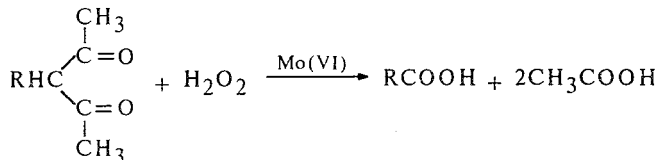
- A singlet dioxygen formation [14]:



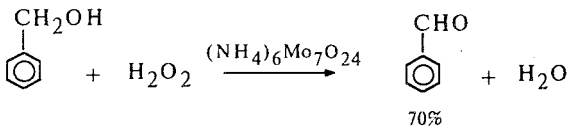
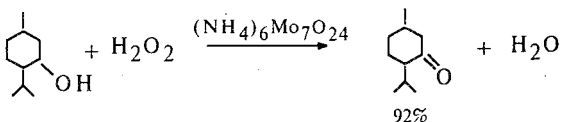
- Ozone formation [15]:



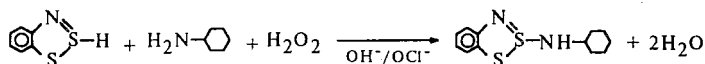
- Oxidation of  $\beta$ -diketones [16]:



- Oxidation of alcohols [1,4,17]:



Synthesis of sulphenamides [4]:



The reactivity of hydrogen peroxide and its organic derivatives, the properties of peroxocomplexes and modes of peroxides activation will be discussed in the paper.

1. R.A. Sheldon, J.K. Kochi. *Metal-Catalyzed Oxidations of Organic Compounds*, Academic Press: New York, 1981; Chapter 9.
2. R.A. Sheldon, in R. Ugo (Ed.) *Aspects of Homogeneous Catalysis*, vol. 4, Reidel, Dordrecht, 1981, p. 1.
3. R.A. Sheldon, in W.A. Herrmann (Ed.) *Topics in Current Chemistry*, vol. 164, Springer-Verlag, Berlin, Heidelberg, New York, 1993, p. 21.
4. K. Dear, *ibid.*, p. 115.
5. G. Franz, R.A. Sheldon, in *Ullmann's Encyclopedia of Industrial Chemistry*, vol. A18, 1991, p. 261.
6. H. Fenton. *J. Chem. Soc.*, 1894, **65**, 899.
7. G.A. Tolstikov, V.P. Yur'ev, U.M. Dzhemilev, *Russ. Chem. Rev. (Usp. Khim.)*, 1975, **44**, 319.
8. Ya.K. Syrkin and I.I. Moiseev, *Russ. Chem. Rev. (Usp. Khim.)*, 1960, **29**, 425.
9. O. Edwards, Ed. "*Peroxide Reaction Mechanisms*", Wiley Intersc., New York, 1962.
10. N. Prieschajew, *Ber.*, 1900, **42**, 4811;  
D. Swern in D. Swern (Ed.) *Organic Peroxides*, vol. II, Wiley Intersc., New York-London, Sydney, Toronto, 1971, p. 355-534;  
P.D. Bartlett, *Rec. Chem. Progr.*, 1950, **11**, 47.
11. W.F. Brill, *J. Amer. Chem. Soc.*, 1968, **85**, 141;  
W.F. Brill and N. Indictor, *J. Org. Chem.*, 1964, **30**, 710.
12. N. Milas. *J. Amer. Chem. Soc.*, 1937, **59**, 2342.
13. A.E. Gekhman, A.P. Makarov, V.M. Nekipelov, E.P. Talsi, O.Ya. Polotniuk, K.I. Zamaraev, I.I. Moiseev, *Bull. Acad. Sci. USSR (Izv. AN SSSR)*, **1985**, 1686.
14. J.M. Aubry, *J. Amer. Chem. Soc.*, 1985, **107**, 5844;  
J.M. Aubry, B. Cazin, *J. Inorg. Chem.*, 1988, **27**, 2013.
15. A.E. Gekhman, N.I. Moiseeva, E.A. Bliumberg, I.I. Moiseev, *Bull. Acad. Sci. USSR (Izv. AN SSSR)*, **1985**, 2653.
16. I.I. Moiseev, V.A. Bochkareva, A.E. Gekhman, Yu.V. Kokunov, Yu.A. Buslaev, *Dokl. Akad. Nauk USSR*, 1977, **233**, 375.
17. O. Bortolini, V. Conte, F.DiFuria, G. Modena, *New J. Chem.*, 1985, **9**, 147;  
*J. Org. Chem.*, 1985, **51**, 2661.

## Phase transfer catalysis in the synthesis of organic chlorine compounds. Some fundamental aspects and industrial use

G.A.Tolstikov, S.S.Shavanov

*Institute of Organic chemistry Ufa Scientific Center RAS  
Novosibirsk Institute of Organic Chemistry Siberian Branch RAS*

Many technological processes producing organic chlorine compounds do not satisfy modern ecological require. In particular, high temperature chlorination and dehydrochlorination give amounts of toxic wastes.

We have created scientific bases for environmentally balanced technologies producing unsaturated C<sub>2</sub> - C<sub>4</sub> - chlorohydrocarbons and some practically important organic compounds related.

Our approaches use liquid phase catalytical reactions realized by means of phase transfer catalysts.

We have elucidated the common principals of elimination reactions catalysis in the bi-phase systems. We have found tetraalkylammonium (or benzyltrialkylammonium) alkoxides to be the most active reagents.

Thus, triethylammonium ethoxide in the form of a concentrated solution in ethanol interacts with polychloroalkanes almost immediately at -20°C resulting in chloralkanes. Tetraalkylammoniumalkoxides are highly active catalysts of polychloroalkanes dehydrochlorination in the presence of NaOH. Table 1 represents alkoxianion structure effect on the rate of vinyl chloride formation from 1,2-dichloroethane. Benzyloxianion is evident to increase the reaction rate.

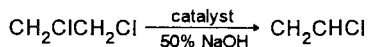


**Table 1**

t=50-55°C, C<sub>2</sub>H<sub>4</sub>Cl<sub>2</sub>; NaOH = 1:2, [NaOH] 50%,  
time 30 min. Catalyst 0,3% mol.

Catalyst	W. 10 <sup>4</sup> M/L.sec	C <sub>2</sub> H <sub>4</sub> Cl <sub>2</sub> conversion %
(C <sub>2</sub> H <sub>5</sub> ) <sub>3</sub> NCH <sub>2</sub> C <sub>6</sub> H <sub>5</sub> Cl	8.6	28.5
(C <sub>2</sub> H <sub>5</sub> ) <sub>3</sub> NCH <sub>2</sub> C <sub>6</sub> H <sub>5</sub> CH <sub>3</sub> O	13.9	45.7
(C <sub>2</sub> H <sub>5</sub> ) <sub>3</sub> NCH <sub>2</sub> C <sub>6</sub> H <sub>5</sub> C <sub>4</sub> H <sub>9</sub> O	20.7	68.1
(C <sub>2</sub> H <sub>5</sub> ) <sub>3</sub> NCH <sub>2</sub> C <sub>6</sub> H <sub>5</sub> C <sub>6</sub> H <sub>5</sub> CH <sub>2</sub> O	31.6	99.5
(C <sub>4</sub> H <sub>9</sub> ) <sub>4</sub> NCl	9.2	30.6

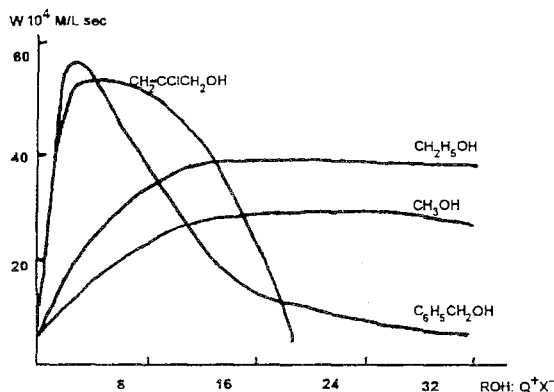
Cation structure effect the catalysts activity including benzylate anion, is shown on Table 2. The reaction rate increases with cation lypophilicity rises to a certain extent. The effect of nitrogen atom electron density is evidenced by the comparison of reaction rates in the presence of catalysts, including *p*-ClC<sub>6</sub>H<sub>4</sub>CH<sub>2</sub> and CH<sub>2</sub>=CHCH<sub>2</sub> substituents ( Table 2, № 1,4,5,6)

Table 2

No	Catalyst	W. 10 <sup>4</sup> M/L.sec	C <sub>2</sub> H <sub>4</sub> Cl <sub>2</sub> conversion %
1	(C <sub>4</sub> H <sub>9</sub> ) <sub>4</sub> NC <sub>6</sub> H <sub>5</sub> CH <sub>2</sub> O	26.2	82.4
2	(CH <sub>3</sub> ) <sub>2</sub> C <sub>12</sub> H <sub>25</sub> NCH <sub>2</sub> C <sub>6</sub> H <sub>5</sub> C <sub>6</sub> H <sub>5</sub> CH <sub>2</sub> O	17.3	54.5
3	(CH <sub>3</sub> ) <sub>2</sub> NCH <sub>2</sub> OHC <sub>6</sub> H <sub>5</sub> CH <sub>2</sub> O	9.0	28.3
4	(C <sub>2</sub> H <sub>5</sub> ) <sub>3</sub> NCH <sub>2</sub> C <sub>6</sub> H <sub>5</sub> C <sub>6</sub> H <sub>5</sub> CH <sub>2</sub> O	31.6	99.5
5	(C <sub>2</sub> H <sub>5</sub> ) <sub>2</sub> (CH <sub>2</sub> =CHCH <sub>2</sub> )NCH <sub>2</sub> C <sub>6</sub> H <sub>5</sub> C <sub>6</sub> H <sub>5</sub> CH <sub>2</sub> O	77.3	99.5
6	(C <sub>2</sub> H <sub>5</sub> ) <sub>3</sub> NCH <sub>2</sub> C <sub>6</sub> H <sub>4</sub> Cl <sub>(n)</sub> C <sub>6</sub> H <sub>5</sub> CH <sub>2</sub> O	28.4	89.4

Catalysts of a similar activity with tetraalkyl ammonium alcoxides are available from quaternary ammonium salt (Q+X-) and alcohol (Alc) inversion into 1,2-dichloroethane. As Fig.1 suggests, catalytic systems activity depends on both alcohol structure and Q+X-:Alc ratio.

Fig. 1



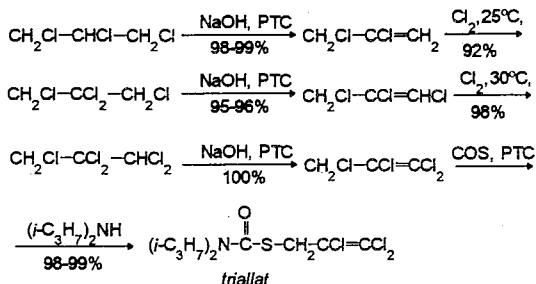
$t = 50-55^{\circ}\text{C}$ ,  $\text{C}_2\text{H}_4\text{Cl}:\text{NaOH} = 1:2$ ,  $[\text{NaOH}] 50\%$   
 $(\text{C}_2\text{H}_5)_3\text{NCH}_2\text{C}_6\text{H}_5\text{Cl}(\text{Q}^+\text{X}^-) 0.4\% \text{ mol}$ .

Basing on kinetic experiments we suggest a scheme of dehydrochlorination mechanism. According to this scheme complexes  $\text{Q}^+\text{X}^- \cdot \text{nAlc}$  form during the induction period. Then organic chlorine substrate enters the ligand sphere, coordinates to the base within the interphase thus producing associates.

Finally, HCl splits out of the interphase and organic phase.

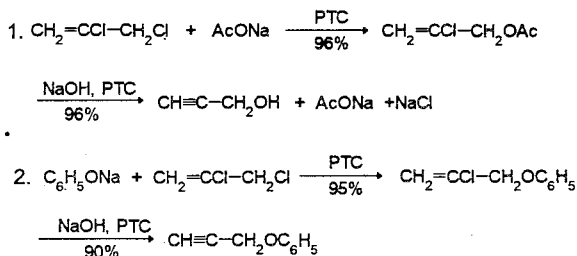
We have designed efficient catalysts for industrial processes producing vinylchloride, vinylidene chloride, trichloroethylene, 1,2,3,3-tetrachloropropene-2, herbicide triallate and insecticide bensultap.

Reactions used as the basis for a new industrial process of triallate herbicide production are cited below. The absence of substitutional chlorination and highly effective catalysts provide a 6-7 - fold reduction in amounts of chlororganic wastes and sewage.



We offer industrially perspective methods for preparing propargyl chloride, propargyl alcohol and propargyl ethers.

These methods use 1,2,3-trichloropropene and / or 2,3-dichloropropene and do not require acetylene.



We suggest a concept how to organize industrial production of organic chlorine compounds.

The environmentally balanced technology producing vinyl chloride and sodium hydroxide is designed.

Vinyl chloride production has already been arranged at plant "Kaustic" in Sterlitamak ( Bashkortostan).

## CATALYSIS BY SUPPORTED TRANSITION METAL CLUSTERS

B. C. Cates

*Department of Chemical Engineering and Materials Science  
University of California  
Davis, CA 95616  
USA*

Some supported metal catalysts consist of clusters (particles smaller than about 10 Å in diameter) dispersed on internal surfaces of high-area porous supports. This class of catalyst is important in technology: Pt<sub>n</sub> clusters (n = 6) supported in zeolite KLTL are used commercially for reforming of naphtha to give high yields of aromatics such as benzene. These clusters in such catalysts have been difficult to identify because of their smallness and the nonuniformity of the materials. The research summarized here is concerned with preparation, physical characterization, and catalytic testing of nearly uniform supported metal clusters, illustrated by Ir<sub>4</sub> and Ir<sub>6</sub> on amorphous and zeolitic supports.

A number of successful attempts have been made to prepare supported metal clusters < 10 Å in size from metal carbonyl precursors, and these are the subject of the present review. For example, [Ir<sub>6</sub>(CO)<sub>15</sub>]<sup>2-</sup> was formed by surface-mediated synthesis on γ-Al<sub>2</sub>O<sub>3</sub> powder by treatment of adsorbed [Ir(CO)<sub>2</sub>(acac)] in CO at 100 °C and 1 atm. The supported clusters were characterized by infrared spectroscopy, by extended X-ray absorption fine structure (EXAFS) spectroscopy, and by extraction into solution by cation metathesis. Treatment of γ-Al<sub>2</sub>O<sub>3</sub>-supported [Ir<sub>6</sub>(CO)<sub>15</sub>]<sup>2-</sup> in He at 300 °C led to decarbonylation without disruption of the cluster frame, giving Ir<sub>6</sub>/γ-Al<sub>2</sub>O<sub>3</sub>, as indicated by EXAFS data determining a first-shell Ir-Ir coordination number of 4.05 ± 0.07, matching that of the supported [Ir<sub>6</sub>(CO)<sub>15</sub>]<sup>2-</sup>, with a first-shell Ir-Ir coordination number of 4.07 ± 0.03. The supported Ir<sub>6</sub> clusters were found to be catalytically active for toluene hydrogenation at temperatures in the range of 60-100 °C; the turnover

### PL-13

frequency at 60 °C with a toluene partial pressure of 50 Torr and a H<sub>2</sub> partial pressure of 710 Torr was  $1.7 \times 10^{-3} \text{ s}^{-1}$ . The catalyst was stable in operation in a flow reactor, and, consistent with this observation, EXAFS results for the used catalyst indicated that the nuclearity of the supported Ir<sub>6</sub> clusters was unchanged during catalysis. The  $\gamma$ -Al<sub>2</sub>O<sub>3</sub>-supported Ir<sub>6</sub> catalyst is an order of magnitude less active (per total Ir atom) for toluene hydrogenation than a catalyst consisting of small aggregates of iridium (with an average of about 30-40 atoms each) supported on  $\gamma$ -Al<sub>2</sub>O<sub>3</sub>.

Similarly, supported Ir<sub>4</sub> catalysts have been prepared from [HIr<sub>4</sub>(CO<sub>11</sub>)]<sup>-</sup> on MgO, from [Ir<sub>4</sub>(CO)<sub>12</sub>] on  $\gamma$ -Al<sub>2</sub>O<sub>3</sub>, and from [Ir<sub>4</sub>(CO)<sub>12</sub>] on NaY zeolite. These clusters are active for toluene hydrogenation and for cyclohexene hydrogenation, and they stable under the mild catalytic reaction conditions stated above for toluene hydrogenation. The supported Ir<sub>4</sub> clusters retained their metal frameworks during catalysis, as indicated by EXAFS results for the used catalysts. The activity increased monotonically from zero as CO ligands were removed from the precursor [HIr<sub>4</sub>(CO<sub>11</sub>)]<sup>-</sup> on MgO, consistent with the conclusion that the Ir<sub>4</sub> clusters themselves were catalytic species. Ir<sub>6</sub> clusters are several fold less active than Ir<sub>4</sub> clusters. The orders of reaction in toluene and in H<sub>2</sub> were found to be approximately 0 and 1, respectively, for all the catalysts.

The low catalytic activity of Ir<sub>4</sub> and Ir<sub>6</sub> relative to metallic Ir correlates with the capacities of these structures for adsorption of H<sub>2</sub>. Although the extremely small Ir clusters catalyze at least two of the same reactions as metallic Ir, their catalytic character is different. The clusters are metal-like but evidently not metallic. The concept of structure insensitivity is limited to catalysis by metallic surfaces and does not extend to clusters as small as Ir<sub>4</sub> and Ir<sub>6</sub>. The supported clusters are thus regarded as quasi molecular, with the metal oxide support providing part of a ligand shell, which affects the activity as ligands affect the activities of molecular metal-complex and cluster catalysts.

## References

1. "Size-dependent Catalytic Activity of Supported Metal Clusters," Z. Xu, F.-S. Xiao, S.K. Purnell, O. Alexeev, S. Kawi, S.E. Deutsch, and B.C. Gates, *Nature (London)* **372**, 346 (1994).
2. "Reactions of Tetrairidium Clusters on the Surface of MgO: Characterization by Infrared Spectroscopy and Chemisorption Measurements," F.-S. Xiao, Z. Xu, O. Alexeev and B.C. Gates, *J. Phys. Chem.*, **99**, 1549 (1995).
3. "Cyclohexene Hydrogenation Catalyzed by MgO-supported Tetrairidium Clusters," Z. Xu and B.C. Gates, *J. Catal.*, **154**, 335 (1995).
4. "Supported Metal Clusters: Synthesis, Characterization, and Catalysis," B.C. Gates, *Chem. Rev.*, **95**, 511 (1995).
5. "Hexairidium Clusters Supported on  $\gamma$ -Al<sub>2</sub>O<sub>3</sub>: Synthesis, Structure, and Catalytic Activity for Toluene Hydrogenation," A. Zhao and B.C. Gates, submitted for publication.

**The Role of Solid-phase Interaction in Formation of Oxide Catalyst Surface on Supports.**

V.V.Lunin.

Chemistry Department of M.V.Lomonosov Moscow State University, Vorobyovy Gory, 119899, Moscow, Russia.

Formation of an active surface of oxide catalyst usually includes the stage of solid-phase interaction of components. Such an interaction can take various ways what is caused by the nature of components, reaction environment, and treatment conditions. The interphase processes can lead to the formation of solid solutions, and/or start new phases. Prognosis of the results and control of proceeding of the process is one of fundamental problem of the heterogeneous catalysis.

In this paper we discuss that problem for zirconia doped by rare-earth metal oxides and ferruginous systems applied on  $Al_2O_3$ ,  $SiO_2$ ,  $ZrO_2$ . The doping of  $ZrO_2$  by alkaline-earth and rare-earth elements is used to increase thermostability of zirconia. The doping considerably increases mechanical properties of  $ZrO_2$ , stabilizes the specific surface area.

We have found out by using BET, XRD, and IR diffuse reflectance spectroscopy that the solid solution  $Me_2O_3-ZrO_2$  ( $Me=Y, La$ ) of tetragonal zirconia structure forms in the surface layers of samples obtained with supporting doped cations to the monoclinic zirconium dioxide surface from nitrate solution with following calcination. The stability of the formed structure mostly depends on the dopant concentration and treatment conditions.

Accumulation of dopants on the surface leads to a change of acidic and basic surface properties: decrease of electron-acceptor site concentration, and increase of electron-donor properties of the surface.

During the formation of the surface of a ferruginous catalysts the topochemical processes are also of the great importance. After the calcination at the high

temperature there can be observed the formation of  $Fe_xAl_yO_z$  spinels in  $Fe_2O_3-Al_2O_3$  systems, and ferrisilicate  $FeSiO_3$  in  $Fe_2O_3-SiO_2$  system. The formation of these compounds makes difficult the reduction of iron oxide.

On the base of the obtained results and summarized literary data we discuss the mechanism of the formation of adsorbtion-catalytic sites on the heterogencous oxide supported catalyst surfaces.

## THE ROLE OF SUPPORT IN FORMATION AND STABILIZATION OF CLUSTER METAL COMPOUNDS

*V.A.Likholobov**Boreshkov Institute of Catalysis SB RAS, Novosibirsk, Russia*

Researchers, dealing with catalysts containing anchored complexes or a supported ultradispersed phase of an active component, usually assume the support not to take part in the formation of active sites. Typically, silica and active carbon are reported as these «inert» supports.

With the systems containing palladium compounds supported on active carbon and substructural characteri silica surfaces taken as examples, the catalytic properties are shown to depend remarkably on both support surface chemistry and substructural properties of the particles or crystallites constituting the porous bodies.

**1. Palladium compounds on carbon supports.**

The role the support plays in the process of formation of the active sites is discussed. Among the most important effects is the influence of the so-called substructural characteristics of the carbon material on physico-chemical state of the precursor adsorbed. The following substructural characteristics can be referred to in the case of carbon materials: interlayer distance  $d_{002}$ , size of graphite crystallites  $L_a \times L_c$ , degree of three-dimensional ordering  $\gamma$ , as well as the ratio of basal and edge planes building the surface of the porous space.

Adsorption of palladium chloride from hydrochloric acid solutions on porous carbon materials were studied [1, 2]. The isotherms measured for this process allowed the conclusion about non-uniform properties of carbon surface for sorption of  $H_2PdCl_4$ . It was found using the elution methods that there are at least three sorts of adsorption sites on the carbon surface, their adsorption constants  $K_i$ , where  $i$  is the sort, being greatly different (by more than two orders of magnitude). There are strong arguments in favor of localization of these sites ( $A_i$ ) on basal ( $A_1$ ) and edge ( $A_2$  and  $A_3$ ) planes of the graphite-like crystallites;  $A_3$  sites are situated in micropores, likely, they are the slit-like faults in the layer packing of carbon atoms. The stability constants  $K_1$  and  $K_2$  of  $(H_2O)_nPdCl_2 \cdot C$  complexes (where C is an active carbon surface) was shown to be affected by not only oxidation state of the surface and nature of oxygen-containing functional groups but also substructural characteristics of the carbon material such as interlayer distance  $d_{002}$ , crystallite size  $L_a$ , three-dimensional ordering  $\gamma$  [3].

Upon dehydration of the complexes, anchored clusters  $(PdCl_2)_n \cdot C$  are formed on carbon surface. XPS, WAXS, and RDF data were used to make a conclusion that the clusters are bonded through  $\pi$ -allyl species to the surface; in the process the structural array of the support matrix accommodates to geometry of the «flat»

polynuclear allyl anchor  $(C-PdCl)_k$  where rhomboidal structure  $(PdCl_2)_{n-k}$  is then built [4].

Direct resolution of clusters  $(PdCl_2)_n$  obtained using HREM technique allows us to know that the polynuclear allyl anchors are allocated over edge plane steps of the carbon matrix, and the rhomboidal species are set out of the anchor along or normally to basal plane. The clusters stabilized through epitaxial interaction with basal planes are larger in size, and, thus, carbon supports which are more contributed by edge planes to their surfaces allow a smaller  $(PdCl_2)_n$  clusters. This phenomenon can affect the size and catalytic behaviour of metal palladium particles produced via gas phase reduction of  $(PdCl_2)_n-C$  precursors.

The surface structure of carbon material influences the process of formation of anchored polynuclear compounds from polynuclear precursors too. For instance, in the course of adsorption of polynuclear palladium hydroxo complexes  $[Pd(OH)_2 \cdot Na_{k/n}^+]_n Cl_k^-$  (according to data obtained by us [5]), they have thread-like structure, the threads being rolled up to spherical globules due to «bounding» individual fragments  $=Pd(OH)_2Pd=$  of the threads with sodium ions) both three-dimensional ultradispersed particles of palladium oxide and extended structural species duplicating the shape of surface steps can appear on the surface. These processes may be explained if take into account hydrophobic and hydrophilic properties of various surface fragments of the carbon matrix surface [6].

Specific substructural properties of carbon supports make specific bodies(????) involving various palladium-containing species in Pd/C catalysts. For instance, XPS studies of Pd/C catalysts prepared using various carbon materials and different precursors showed four predominant states of palladium in these catalysts:  $Pd^0$ ,  $Pd^{+1}$ ,  $Pd^{+2}$ , and  $PdO$ . The species form associates the size of which increases, normally, in the row  $Pd^{+1} < Pd^{+2} < Pd^0 \sim PdO$ ; the ratio of these palladium species depends strongly on the micro- and mesopore proportions and seems to be sensitive to the ratio of basal and edge planes contributing to the carbon surface [7].

## 2. Palladium and copper compounds on silica

Other objects illustrating the effect of texture and substructural properties of supports are palladium complexes anchored onto phosphinated silica. Available experimental observations demonstrate that both dimensions of primary silica globules and the surface «mosaic» of the globules (caused by various kinds of packing of silicon and oxygen atoms exposed on their surface; this kind of packing can be detected by  $^{29}Si$  NMR and CP MAS techniques [7a, b]) influence the catalytic properties of systems in the reactions of hydrogenation and hydroformylation of olefins in gas phase or hydrocarbon media [8]. Generally, the data obtained using IR, ESR, NMR, XPS, RDF, HREM techniques and computer simulation allow the conclusion that in the above mentioned reactions the polynuclear species constituted by palladium atoms and organic ligand molecules (or the products of its transformations) were the catalytically active sites [9]. Hence, the size and composition of the polynuclear species may be supposed to depend on not only reaction conditions but also nature of the silica matrix.

A system which demonstrated the influence of substructural characteristics of the support on catalytic properties of the active component was 2%Cu/SiO<sub>2</sub>. The sample, in which the support surface was mainly contributed by the structure of  $\alpha$ -quartz type [7b], showed superior activity and selectivity for hydrolysis of benzonitril to benzamid.

Account of substructural and texture properties of supports should be the most important new item of «catalyst tailoring ideology». With hydrodechlorination of aromatic chlorides as an example, there are shown how peculiarities of surface structure of carbon matrices can be employed to intensify the process.

### **Acknowledgments**

The results of the works funded by the Russian Foundation for Basic Research (Project 93-03-4836), the International Science Foundation and Russian Government (Projects RP 0300 and RP 5300) are reported in this communication.

### **REFERENCES**

1. P.A.Simonov, V.A.Semikolenov, V.A.Likholobov, A.I.Boronin, Yu.I.Yermakov//Izv.AN SSSR, 1988, p.2719.
2. P.A.Simonov, A.L.Chuvilin, V.A.Likholobov// Izv.AN SSSR, 1989, p.1952.
3. P.A.Simonov, E.M.Moroz, G.V.Plaksin, V.A.Likholobov// Izv.AN SSSR, 1990, p.1477.
4. P.A.Simonov, E.M.Moroz, A.L.Chuvilin, V.N.Kolomiichuk, A.I.Boronin, V.A.Likholobov, in: Scientific Bases for the Preparation of Heterogeneous Catalysts, Prepr. of 6th Inter.Symp, Vol.3, Louvain-la-Neuve, 1994, p.201-210.
5. S.Yu.Troitskii, M.A.Fedotov, V.A.Likholobov// Izv.RAN, 1993, p.675.
6. S.Yu.Troitskii, E.M.Moroz, D.I.Kochubei, A.L.Chuvilin, V.A.Likholobov// Izv.RAN (in press).
7. (a) B.Pfleiderer, K.Albert, E.Bayer, et al.// J.Phys.Chem., 1990, v.94, p.4189; (b) V.M.Mastikhin, V.V.Tersikh (personal communication).
8. V.A.Likholobov// Design of catalysts based on metal complexes, in: Perspectives in Catalysis, Eds.J.A.Thomas and K.I.Zamaraev, Blackwell Scientific Publications, p.67-90, 1992
9. B.L.Moroz, V.A.Likholobov// Handbook of Heterogeneous Catalysis. Part 4.5. Hydroformylation, Eds. G.Ertl, H.Knozinger, J.Weitkamp (in press).

## PHOTOASSOCIATION - THE PHOTON ASSISTED TWO-BODY RECOMBINATION OF ATOMS, IONS, AND FREE RADICALS

E.B.Gordon, V.S.Pavlenko, O.S.Rzhevsky

*Institute of Energy Problems of Chemical Physics (Branch)  
Chernogolovka, Moscow Region, 142432, Russia*

Any chemical reactions of recombination or attachment of atoms, free radicals, ions or molecules are related to a stabilization of a final product by removing a part of the energy released. As a rule, this energy is taken up by a third particle, and practically every its collision with an intermediate complex results in stabilization. Therefore, such reactions are described by a third order kinetics and in the case of atoms and diatomic molecules indeed occur in termolecular collisions. This means the elementary act has a time scale comparable with both the time of collision and the molecular vibration period,  $\tau \approx 10^{-13}$  s. Besides, although the recombination products being just formed in an elementary act are highly excited, the selectivity in sense of determinancy of a product quantum state is quite low.

In principle, the stabilization could occur by a photon emission during a pair collision of reactants, however the probability of this process is small: since even for allowed optical transitions the spontaneous emission time is  $\tau_{sp} \approx 10^{-8}$  s, just one of  $10^5$  collisions will result in a product stabilization, i.e. in a chemical reaction occurrence (in practice, such a probability does not exceed  $10^{-7}$  ).

However, a product can be stabilized as well by photon absorption during the impact, provoking an optical transition into a chemically bound, but electronically excited state of a product. Further, the latter could convert into bound unexcited state at the expense of either a photon spontaneous emission or a subsequent collision.

The dynamics of such elementary process, the so called photoassociation, differs significantly from termolecular one - it proceeds so quickly,  $\tau_{pa} \approx 10^{-15}$  s, that in elementary act neither positions nor momenta of colliding particles have

time to be changed. In the spectroscopy language such reactions may be qualified as free-bound molecular transitions followed to Franck-Condon principle. As a rule, their selectivity is rather high, and the photon energy determines quantum, electronic-vibrational-rotational state of a product. On one hand, the demand for coincidence of positions and momenta of colliding particles and those in a molecule formed diminishes the process cross-section, but on the other hand - large dimension of a photon being considered as a particle,  $\sigma \approx 10^5 \text{ nm}^2$  promotes its increase. Really, the corresponding "rate constants" for optimal energies of a stabilizing quantum are about  $10^{-28} \text{ cm}^6 \text{ s}^{-1}$ , that is by three orders of magnitude greater than the values inherent to ordinary termolecular reactions. Since the spectroscopic approach is suitable for describing photoassociation, the corresponding rate constants and their spectral dependences can be simulated theoretically, provided the knowledge of the potential curves for upper and lower states as well as transition dipole momenta.

Extremely interesting, however not investigated yet are the reactions of photoassociation of a heavy particle (atom or molecule) with an electron, which represent the intermediate case in elementary act dynamics. In view of small electron mass the time of structure rearrangement from that intrinsic to a neutral reactant to that for ionic product should be close to the free-bound transition duration. Therefore for such reactions one should expect high rate constants of the order of  $10^{-25} \text{ cm}^6 \text{ s}^{-1}$  and quasiline spectral structure reflecting the structure of the meta-stable negative ion energy levels. In principle, the photon induced electron-ion recombination can take place as well.

The ratio of ordinary and photoinduced recombination rates is clearly seen to be proportional to  $I/[M]$  ( $I$  is a light flux intensity,  $\text{cm}^{-2} \text{ s}^{-1}$ ,  $[M]$  is a buffer gas concentration). Therefore at low densities under intense irradiation the rate of photoinduced recombination will noticeably exceed the rate of termolecular one. Such processes can play the considerable role as a mechanism of small molecules formation in interstellar space and upper layers of the Earth atmosphere. In principle, the same situation can be brought about in laboratory conditions.

However, in practice it is more convenient to work with the systems which have no bound state correlating with the ground state of reactants, except weak

van-der-waals bonding. In this case the basic features of photoinduced process should be the same as for particles chemically active in their ground state. But since the bypass channel of ordinary recombination is absent for this systems, one can utilize stationary reactors, short pulse lasers and allow high concentrations of reactants.

The only but important difficulty in such experiments carried out in quasi-equilibrium conditions is the presence of bound-bound transitions from the corresponding weakly bound van-der-waals states, which are in the equilibrium with free reactants and contribute to a total excitation spectrum.

In the present lecture the following items will be considered on the basis of calculations and experiments carried out in our laboratory.

1. The atoms - van-der-waals diatom equilibrium constant calculations and the choice of a criterion for bound and free states separation in equilibrium conditions (on the example of  $\text{Xe}+\text{Cl}$  and  $\text{Xe}+\text{F}$  systems) [1].

2. Calculation of absolute photoassociation (fb-transitions) and photoabsorption (bb-transitions) cross-sections ( $\text{Xe}+\text{Cl}$  and  $\text{Xe}+\text{F}$  systems) [2].

3. The results of experimental investigation of  $\text{Xe}+\text{Cl}$  and  $\text{Xe}+\text{F}$  systems, and the comparison of experimental and calculated data [3].

4. The experiments on distinguishing photoabsorption and photo-association contributions into total excitation cross-section in  $\text{Xe}+\text{Cl}$  system [4].

5. Theoretical approaches to calculating rate constants of photo associative recombination in a system of "atom + diatomic molecule".

6. The application of experimental approaches developed to the measurement of halogen atoms termolecular recombination rate constants [5].

7. The analysis of the possibilities of measuring the absolute atom concentrations by a photoassociation method.

8. Qualitative consideration of the processes of electron photo-associative attachment and photoassociative recombination.

The work is supported by the Russian Foundation for Basic Researches (project 95-03-09429) and the International Science Foundation (grant Ph3-3352-0925).

## PL-16

### References

1. E.B. Gordon, O.S. Rzhnevsky, *Khimicheskaya Fizika* 12 (1993) 1571 (Chemical Physics, in Russian).
2. E.B. Gordon, O.S. Rzhnevsky, *Optika i Spektroskopiya* 78, 360 (1995) (Optics and Spectroscopy, in Russian).
3. V.S. Pavlenko, S.E. Nalivaiko, V.G. Egorov, E.B. Gordon, O.S. Rzhnevsky, *Quantum Electronics* 24, 199 (1994).
4. E.B. Gordon, V.G. Egorov, S.E. Nalivaiko, V.S. Pavlenko, O.S. Rzhnevsky, *Chem. Phys. Lett.*, in press.
5. V.S. Pavlenko, S.E. Nalivaiko, V.G. Egorov, E.B. Gordon,
6. *Kinetika i Kataliz* (Kinetics and Catalysis, in Russian), in press.

## New Trends in the Study of Carbene Analogs by Modern Physico-Chemical Techniques

O.M.Nefedov, M.P.Egorov, V.A.Kuzmin \*, M.B.Taraban\*\*, T.V.Leshina\*\*,  
V.F.Plusnin\*\*, R.Walsh\*\*\*

*Institute of Organic Chemistry, Russian Academy of Sciences, Moscow, Russia*

*\*Institute of Chemical Physics, Russian Academy of Sciences, Moscow, Russia*

*\*\*Institute of Chemical Kinetics and Combustion, Russian Academy of Sciences,  
Novosibirsk, Russia*

*\*\*\*University of Reading, UK*

Like carbenes, their IVB group element analogs - silylenes, germylenes, stannylenes are very important class of reactive intermediates both from theoretical and synthetic points of view. The modern stage of the investigation of these short-lived species is characterized by wide use of sophisticated physico-chemical methods for the study of their structure, spectral properties, reactivity and detailed mechanisms of chemical reactions. However, an information concerning the properties of short-lived species and their reaction mechanisms obtained by each of these methods alone usually contains a certain degree of uncertainty. Therefore only a complex approach based on a combination of the different methods applied to the same system studied provides a true picture.

In this report we will discuss the results of a complex study of mechanisms of generation, spectral properties and reactivity of short-lived carbene analogs by different methods - CIDNP, laser flash photolysis in liquid and gas phase, low temperature matrix isolation techniques.

Quantum-chemical semi-empirical (MNDO, AM1, PM3) and ab initio calculations have been widely used in our studies.

The mechanism of photochemical generation of dimethylgermylene and dimethylsilylene from the 7-heteronorbomadienes of the same structure, the 7,7-dimethyl-1,4,5,6-tetraphenyl-2,3-benzo-7-sila(germa)-norbomadienes (1a (1b)) was studied by CIDNP and flash photolysis techniques. The data obtained by both methods are mutually complementary. They show that photochemical decomposition of

## PL-17

these precursors occurs via stepwise mechanism including the reversible formation of a singlet biradical at the first stage of the reaction. The triplet biradical obtained as a result of S-T evolution of the singlet biradical irreversibly decomposes with the formation of  $\text{Me}_2\text{E}$  ( $\text{E}=\text{Si}, \text{Ge}$ ) in excited triplet state. The multiplicity of  $\text{Me}_2\text{E}$  formed was confirmed by the analysis of CIDNP effects detected in the reaction of  $\text{Me}_2\text{E}$ , photochemically generated from 1a(1b) with 3,3,6,6-tetra-methyl-1-thiacycloheptyne.

Transient species with an absorption maximum at 380 nm was detected upon flash photolysis of the solutions of 1a (heptane, 20°C). The results of trapping reactions and kinetic data let us assign this transient absorption to dimethylgermylene or to a complex between  $\text{Me}_2\text{Ge}$  and 1,2,3,4-tetra-phenylnaphthalene, the stable decomposition product of 1b. Indeed, our further investigation of the generation of dimethylgermylene in gas phase by 193 nm laser flash photolysis of the two different precursors (pentamethyldigermene and 1,1-dimethyl-1-germacyclopentene-3) that do not contain fragments capable of forming complexes with  $\text{Me}_2\text{Ge}$  showed that a "free" dimethylgermylene has an absorption maximum at 480 nm. Complexation with 1,2,3,4-tetra-phenylnaphthalene results in a blue shift of the absorption maximum of  $\text{Me}_2\text{Ge}$ .

Kinetics of the reaction between  $\text{Me}_2\text{Ge}$  and different trapping agents in liquid and gas phases will be discussed.

In a singlet state, carbene analogs have a vacant  $\pi$ -orbital and an occupied  $\sigma$ -orbital providing a possibility to form complexes with different substrates. We also report the results of our experimental and theoretical study of complexation between carbene analogs and unsaturated substrates (alkenes, alkynes, aromatics) as well as n-donor agents (phosphines, alkyl halides).

Flash photolysis of the solutions of 1a with  $\text{PPh}_3$  (heptane, 20°C) gives rise to a transient species with an absorption maximum at 370 nm. Both the trapping reactions and kinetic data (second-order kinetics for the decay of this species, the increase of the lifetime and decrease of its reactivity) show that the 370 nm species is a complex of  $\text{Me}_2\text{Ge}$  with  $\text{PPh}_3$ . In a similar manner, a complex between dimethylsilylene and  $\text{CHBr}_3$  was detected upon flash photolysis of the solutions of

1a with  $\text{CHBr}_3$  (hexane,  $20^\circ\text{C}$ ). It has an absorption maximum at 338 nm. The absorption maximums of both complexes with n-donor agents are blue shifted as compared with those of "free"  $\text{Me}_2\text{E}$  (E=Si, Ge) species.

Complexation of  $\text{Me}_2\text{E}$  (E=Si, Ge) with n-donor agents results in the decrease of their reactivity. For example, the  $k_r$  values for the reactions of  $\text{Me}_2\text{Ge} \cdot \text{PPh}_3$  with different trapping agents was found to be smaller than those for a "free"  $\text{Me}_2\text{Ge}$ .

Complexation with a Lewis base can change in some cases the pathways and the mechanisms of dimethylgermylene (dimethylsilylene) reactions. As an example, the reactions of  $\text{Me}_2\text{E}$  and their complexes  $\text{Me}_2\text{E} \cdot \text{PPh}_3$  (E=Si, Ge) with  $\text{CCl}_4$  will be considered.

The reactions of difluorostannylene (generated by sublimation of  $(\text{SnF}_2)_x$  in high vacuum at  $400\text{-}600^\circ\text{C}$ ) with heptyne-1, benzene, toluene, chlorobenzene, methyl chloride, nitrogen, etc. have been studied by matrix IR spectroscopy. For this purpose difluorostannylene and a substrate were codeposited in argon matrix at 12K. The formation of complexes have been detected for all substrates mentioned above.

AM1, PM3 and ab initio quantum-chemical calculations confirm the existence of such complexes. The calculated shifts of vibrations in complexes with respect to starting materials are in a good agreement with experimentally observed. Optimized geometries, electronic structures, heats of formation of the complexes as well as activation energies of the reactions studied will be discussed. The main trends in an ability of carbene analogs  $\text{EX}_2$  (E=Si, Ge, Sn; X=H, F, Cl, Me, etc.) to form complexes will be considered.

This work was supported by the Russian Foundation for Basic Research (Project No 95-03-09042), International Science Foundation (grant MHL 000) and the Royal Society of Chemistry (UK).

**Multifrequency EPR of site-selectively  $^{13}\text{C}$ -labelled quinone and tyrosine electron transport compounds *in vivo* and *in vitro*.**

R.J. Hulsebosch,<sup>a</sup> J.S. van den Brink,<sup>a</sup> P. Gast,<sup>a</sup> T.N. Kropacheva,<sup>b</sup> R.I. Samoilova,<sup>c</sup> J. Raap,<sup>d</sup> J. Lugtenburg,<sup>d</sup> Yu.D. Tsvetkov<sup>c</sup> and A.J. Hoff.<sup>a</sup>

<sup>a</sup>Department of Biophysics, Huygens Laboratory, Leiden University, Leiden, The Netherlands.

<sup>b</sup>Department of Chemistry, Udmurt University, Izhevsk, Udmurtia, Russia.

<sup>c</sup>Institute of Chemical Kinetics and Combustion, Academy of Sciences, Novosibirsk, Russia.

<sup>d</sup>Department of Chemistry, Gorlaeus Laboratory, Leiden University, Leiden, The Netherlands.

The unique efficiency of photosynthetic energy conversion is largely due to an electron transfer chain fine-tuned by protein-cofactor interactions. Mapping these interactions is currently of much interest. One very promising technique is the study of photosynthetic reaction centers (RCs) containing cofactors selectively labelled with a spin isotope ( $^2\text{H}$ ,  $^{13}\text{C}$ ,  $^{15}\text{N}$ ), with EPR at several frequencies (9.5, 35, 95 GHz) and with ESEEM. Especially the isotropic and anisotropic  $^{13}\text{C}$ -hyperfine couplings are a sensitive probe of environmental interactions, such as hydrogen bonding, and of molecular distortions produced by the environment, which in turn determine cofactor functioning in the electron transport chain. We have determined hyperfine tensor elements of the  $^{13}\text{C}$ -nucleus at several positions of the carbon skeleton for the quinone cofactor *in vitro* and in bacterial RCs. Furthermore we have determined such elements for oxidized tyrosine *in vitro*, with the aim to compare the *in vitro* data with future *in vivo* data of the tyrosine electron donors in the RC of plant Photosystem II. It will be shown that the first acceptor quinone  $\text{Q}_\text{A}$  in bacterial RCs interacts asymmetrically with the protein matrix, the 4C-carbonyl position being strongly hydrogen bonded to the  $\text{N}^{\text{H}}\text{-H}$  of Histidine M219, whereas the 1C-carbonyl is more or less free. This contrasts with the practically symmetrical binding of the secondary acceptor quinone  $\text{Q}_\text{B}$ , which has both carbonyls weakly hydrogen bonded to the protein. This remarkable difference between the quinone cofactors will be discussed in terms of their different functions,  $\text{Q}_\text{A}$  being a firmly bound, non-protonable one-electron port, whereas  $\text{Q}_\text{B}$  is a protonable two-electron port, which after double reduction and protonation leaves the RC.

# Electron Spin Echo Spectroscopy Applied to Intermediate States of Photosynthetic Reaction Centers

Sergei A. Dzuba

*Institute of Chemical Kinetics and Combustion, Russian Academy of Sciences  
Novosibirsk 630090, RUSSIA*

Electron spin echo (ESE) spectroscopy is nowadays a powerful method which allows a valuable information on structure and dynamics of paramagnetic species to be obtained. Its applications are based on studying of (i) magnetic relaxation induced by spin or molecular dynamics, (ii) chemical kinetics, (iii) ESE envelope modulation (ESEEM) induced by the electron-nuclear hyperfine interaction, and some other phenomena. This communication presents two new approaches in ESE experiment which have been applied to study transient states of photosynthetic reaction centers (RCs).

## **Selective hole burning in EPR for studying dipolar-induced spectral diffusion.**

In these experiments a narrow hole in an EPR spectrum is produced initially by applying a low-amplitude microwave pulse. This hole later becomes broader because of spectral diffusion. At low temperature only one source of spectral diffusion usually remains; it is local magnetic field fluctuations which are induced by relaxing paramagnetic ions. The scale of the hole broadening reflects directly the value of dipolar coupling with these ions. Hence, the distances between different paramagnetic species could be obtained. This provides a valuable structural information on the reaction center.

The pulse sequence ( $180^\circ - T - 90^\circ - \tau - 90^\circ$ ) used in experiment is shown in Fig. 1. The hole shape is determined by the FID after the first  $P_0$  pulse. The temporary echo shape is constructed by two FIDs "back-to-back" and therefore reflects the hole shape too. The advantage of using the echo shape is that the dead-time problem in the FID acquisition is lifted.

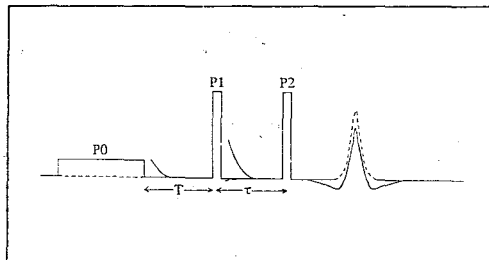


Fig. 1. The pulse sequence for the selective hole burning experiment. The low-amplitude P0 pulse produces a narrow hole in the EPR spectrum which results in appearance of the strong FID signal following the P1 pulse. The echo temporary shape also is changed. The dashed line shows the pattern with the P0 pulse off.

This method has been applied to measure dipolar interactions of tyrosine  $D^+$  radical with the Mn-cluster in oxygen-evolving center and with  $Fe^{2+}$  ion on the acceptor side of photosystem II. The distance from  $D^+$  to  $Fe^{2+}$  ion has been determined to be less than 52 Å. The distance from  $D^+$  to the Mn-cluster was determined to be 28 - 30 Å. Moreover, the distribution of distances could be evaluated using this method. In the latter case it turned out to be not more than 6 Å.

#### **ESEEM induced by electron-electron interaction in spin-polarised radical pairs.**

Charge separation in photosynthetic reaction centers leads to formation of radical pairs. Dark electron transfer from the electronically excited state of the primary donor P, a bacteriochlorophyll dimer, to  $Q_A$ , the primary acceptor quinone, creates the radical pair  $P^+Q_A^-$ . This reaction occurs within 200 ps and the radicals in the pair are spin-polarised. The study of magnetic dipole-dipole and spin-exchange interactions between radicals in the pairs could reveal important structural information. The dipole-dipole interaction reflects mutual radical positions in the pair, while the exchange interaction is related to the overlap of electronic wavefunctions, which correlates with the rate of electron-transfer.

Theory predicts strong modulation of primary echo of spin-polarised radical pair which is induced by dipolar and exchange interactions between the electron spins. The in-phase signal is absent and the out-of-phase echo is determined by the analytical expression (for pairs that are formed originally in a singlet state):

$$E_x(\tau) = (\Delta\omega^2 B^2 / R^4) \sin A\tau [1 - \cos(R\tau)], \quad (1)$$

where

$$A = -2D(3\cos^2\theta - 1)/3 + 2J, B = D(3\cos^2\theta - 1)/3 + 2J, R^2 = \Delta\omega^2 + B^2,$$

and  $\Delta\omega$  is the difference of resonance frequencies for two spins in the absence of dipolar and exchange interactions,  $D$  and  $J$  are the values of dipolar and exchange coupling correspondingly,  $\theta$  is the angle between direction of the external magnetic field and vector joining two species. Eq. (1) is to be averaged over all spectral and spatial positions of both radicals in the pair.

These theoretical predictions have been confirmed in the experimental investigation of the  $P^+Q_A^-$  spin-polarised pairs in the photosynthetic RC of the purple bacterium *Rhodobacter sphaeroides* R26, in which the native non-heme iron was replaced by the diamagnetic  $Zn^{2+}$ -ion. (Removing the magnetic coupling between the  $Fe^{2+}$ -ion and  $Q_A^-$  in this way allows the observation of spin polarisation.) It has been found that the system under study produce very strong modulation of the echo signal - see Fig. 2.

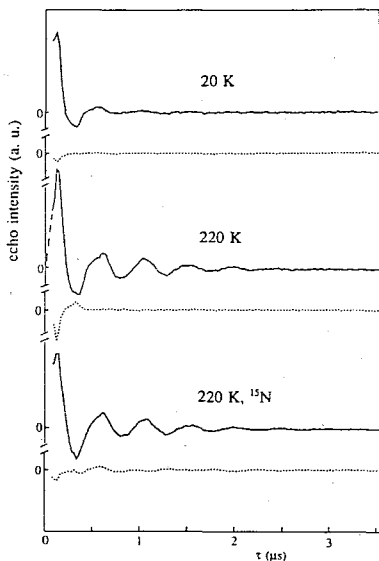


Fig. 2. Echo signal as a function of the time separation  $\tau$  between two microwave pulses at two different temperatures for RCs with natural-abundant nitrogen and for those  $^{15}N$ -enriched. The solid lines represent the out-of-phase signal, the dotted lines the in-phase one.

Fourier-transformed echo envelopes are to be compared with Fourier transformation of the theoretical expression (1). This allows to obtain readily the D and J values. It is interesting to note that the obtained distance between the two species differs remarkably from those found in X-ray studies for the crystalline RC. This difference could be attributed probably to the different phase state (amorphous and crystalline) and to different temperatures of investigation.

### **Acknowledgments**

This work has been performed in close collaboration with Prof. A. Kawamori (selective hole burning) and with Prof. A.J. Hoff (ESEEM of spin-polarised radical pairs) when the author joined their labs at Kwansai Gakuin University (Nishinomiya, Japan) and at Huygens Laboratory (Leiden University, The Netherlands) correspondingly.

## SURFACE RECONSTRUCTION AND RATE PROCESSES IN ADSORBED OVERLAYERS

V.P. Zhdanov<sup>a</sup> and P.R. Norton<sup>b</sup>

<sup>a</sup>Boreskov Institute of Catalysis, Novosibirsk 630090, Russia

and

<sup>b</sup>Interface Science Western, Department of Physics and Chemistry,  
University of Western Ontario, London, Ontario, Canada N6A 3K7

Rate processes in adsorbed overlayers at finite coverages represent an example of a nontrivial phenomenon in many-body dynamical systems. To simulate these processes, the lattice-gas models are customarily used [1]. In the framework of these models, the surface lattice is usually assumed to be rigid and to possess a well-defined two-dimensional periodicity closely resembling the atomic ordering in the bulk.

In many instances, however, the surface reconstructs spontaneously or as a result of adsorbate induced effects. In particular, the adsorbate-induced buckling and lateral shifts of substrate atoms are now found experimentally even for close-packed surfaces [2]. More significant changes in the arrangement of substrate atoms can accompany adsorption on many more open surfaces [3-7]. The influence of such changes on elementary rate processes in adsorbed overlayers is expected to be significant because typical energies involved into surface reconstruction are usually much higher than the thermal energy. Adsorbate-induced restructuring of the surface may thus play a crucial role in such interesting and important phenomena as bistability, kinetic oscillations, and promotion and poisoning of surface reactions [7,8].

In our lecture, we will consider a few examples illustrating the role of surface reconstruction in thermal desorption and surface diffusion. Our goal is to discuss the available results of simulations based on microscopic statistical models of surface reconstruction. Such simulations are presently limited because the development of statistical models of surface reconstruction is in its infancy [1,6,7]. The formulation and analysis of these models are usually

rather cumbersome. For this reason, we will consider only the main physical ideas and approximations employed in calculations and will not represent in detail the formalism.

In general, the relationship between microscopic statistical models of surface reconstruction and kinetic processes is straightforward [1]. As a rule, the rate constants for elementary rate processes in adsorbed overlayers can be represented via the probabilities of different arrangements of adsorbed particles and substrate atoms and the lateral interactions between them, including the interactions in the ground and activated states. Often, the latter interaction (i.e., the interaction of the activated complex with adjacent particles) is negligible. In this case, the coverage dependence of a rate constant can usually be expressed via the chemical potential of adsorbed particles. Employing a statistical model of surface reconstruction, it is possible to calculate the desired probabilities or the chemical potential and then to obtain the rate constants for desorption, diffusion or elementary chemical reactions.

If restructuring of the surface is spontaneous and the structure formed is stable with respect to adsorption (i.e., adsorbate-induced changes in the surface are negligible), the effect of surface reconstruction on rate processes in adsorbed overlayers can often be described in the framework of the lattice-gas approximation simply by redefining a lattice structure. As an example, we will consider hydrogen adsorption on Si(001). The most attention will be paid to examples when the surface structure changes with increasing or decreasing adsorbate coverage. In particular, we will discuss the following systems: H/W(001) (hydrogen adsorption on bridge sites stabilizes the reconstructed  $c(2 \times 2)$  structure of the clean surface), CO/Pt(110) (CO adsorbs primarily on top sites and destroys the missing-row structure of the clean surface), H/Cu(110) (hydrogen adsorption results in formation of the missing-row structure), and H/Pt(001) (hydrogen adsorption on the Pt(001)-hex surface recovers the  $(1 \times 1)$  structure). The role of restructuring of the surface in the kinetic processes occurring in these systems is nontrivial, and the results predicted by microscopic statistical models are rather instructive.

even if the models employed are usually simplified and do not describe all the details observed in real systems.

Surface reconstruction is known to be an important ingredient contributing to oscillatory kinetics observed for different chemical reactions on metal surfaces under UHV conditions (e.g., CO oxidation on Pt(001) and Pt(110)). The available models describing oscillatory kinetics (see the reviews [8] and a recent paper [9]) however introduce surface reconstruction into the mean-field kinetic equations "by hands", i.e. without underlying physics. Such models are an important tool in understanding of kinetic oscillations. Their description is however beyond the present review.

A brief summary of our lecture is as follows:

(i) Statistical models of surface reconstruction developed originally for describing the phase diagrams of the adsorbate/substrate systems can be employed (with minor modifications) to analyze the influence of restructuring of surfaces on thermal desorption and surface diffusion.

(ii) In the case of desorption, the available results of simulations indicate that at present there are no general rules connecting the type of reconstruction with the special features of the thermal desorption spectra. Sometimes, the effect of surface reconstruction on desorption is well manifested. For example, formation of dimers on Si(001) or effectively one-dimensional rows on Cu(110) results in the first-order kinetics of associative desorption of hydrogen from these surfaces. Sometimes, however, adsorption is accompanied by dramatic changes in the surface, but the manifestation of these changes in the TPD spectra is hidden. For instance, during CO adsorption on Pt(110), the structure of the surface is directly governed by adsorption due to adsorbate-adsorbate and adsorbate-substrate interactions, but the calculated thermal desorption spectra for the CO/Pt(110) system are qualitatively the same as in the experiment even if surface reconstruction is neglected in simulations (i.e., the desorption kinetics might be formally described by taking into account only adsorbate-adsorbate lateral interactions). Almost the same situation takes place for hydrogen adsorption on W(001).

(iii) The effect of surface reconstruction on surface diffusion is quite obvious: restructuring of the surface results often in anisotropy of this process.

The whole text of the lecture will be published elsewhere [10].

### References

- [1] Zhdanov, V.P. *Elementary Physicochemical Processes on Solid Surfaces*; Plenum: New York, 1991.
- [2] Lindros, M.; Pfnur, H.; Held, G.; Menzel, D. *Surf. Sci.* 1989, 222, 451.
- [3] Somorjai, G.A.; Van Hove, M.A. *Prog. Surf. Sci.* 1989, 30, 201.
- [4] Pick, S. *Surf. Sci. Rep.* 1990, 12, 99.
- [5] Lafemina, J.P. *Surf. Sci. Rep.* 1992, 16, 133.
- [6] Bernasconi, M.; Tosatti, E. *Surf. Sci. Rep.* 1993, 17, 363;  
Lapujoulade, J. *Surf. Sci. Rep.* 1994, 20, 191.
- [7] Phase Transitions and Adsorbate Restructuring at Metal Surfaces;  
*The Chemical Physics of Solid Surfaces*; King, D.A., Woodruff, D.P.,  
Eds.; Elsevier: Amsterdam, 1994; Vol. 7.
- [8] Ertl, G. *Adv. Catal.* 1990, 37, 231;  
Schuth, F.; Henry, B.E.; Schmidt, L.D. *Adv. Catal.* 1993, 39, 51;  
Imbihl, R. *Prog. Surf. Sci.* 1993, 44, 185.
- [9] Hopkinson, A.; King, D.A. *Chem. Phys.* 1993, 177, 433.
- [10] Zhdanov, V.P.; Norton, P.R. *Langmuir*, in press.

**Cluster and slab model studies of catalysis-relevant adsorption phenomena on  
metal and metal oxide surfaces**

N. Roesch

*Lehrstuhl fuer Theoretische Chemie, Technische Universitaet  
Muenchen D-85747 Garching, Germany*

Several examples of recent density functional studies of molecular interactions with catalytic materials like transition metals, perfect and defect metal oxides as well as with zeolites will be presented. Among them are investigations devoted to the spectroscopic manifestation of NO and NH species on Ru(001), the analysis of bonding and vibrations of di- $\sigma$  and  $\pi$ -complexes of ethylene at Ni(110), the rationalisation of the interactions of CO molecules with a perfect MgO(001) surface and with low-coordinated sites of MgO, complexes of Brønsted and Lewis acidic sites with probe molecules as well as with highly-dispersed platinum species in zeolites.

The possibilities offered by modern quantum chemical methods to describe adsorption and catalytic phenomena will thus be evaluated.

## Mechanism of Chemical Waves Propagation during the CO and H<sub>2</sub> - Oxidation on Platinum Surface

V.Gorodetskii, W.Drachsel<sup>1</sup> and J.H. Block<sup>1</sup>

*Boreskov Institute of Catalysis, Prospect Lavrentieva 5, Novosibirsk, 630090 Russia*

<sup>1</sup>*Fritz-Haber-Institut der Max-Planck-Gesellschaft, Faradayweg 4-6, D-14195 Berlin, Germany*

One of the most surprising phenomena in catalysis-related surface science research is the appearance of self-sustained isothermal oscillations with the formation of surface chemical waves [1]. In numerous investigations such nonlinear surface reactions have been characterized and imaged on a mesoscopic scale (1 $\mu$ m) [2]. Only recently, field electron microscope (FEM) with a resolution of  $\sim 20$  Å and field ion microscope (FIM) with a resolution  $\sim 3$ -6 Å have been applied for imaging oscillating catalytic surface reactions thus opening a direct atomic view into the molecular behavior at reaction sites [3-5]. In the present work the mechanism of the appearance of chemical waves during CO+O<sub>2</sub>/Pt and H<sub>2</sub>+O<sub>2</sub>/Pt oscillatory reactions will be investigated on a nanometer scale with FEM, FIM and mass spectroscopic analysis.

A field ion microscope is simultaneously used as a catalytic flow reactor. The platinum field emitter is a model catalyst grain (diameter  $> 200$  Å) that exposes different small single-crystal planes with well-defined crystallographic orientations. The molecules reacting on the catalyst surface are also used as the FIM imaging gas. Due to preferential O<sub>2</sub> field ionization on O<sub>(ad)</sub> layers, the different surface sites (O<sub>(ad)</sub> and CO<sub>(ad)</sub>) can be discriminated *in situ* and in real time during on-going catalytic CO oxidation. H<sub>2</sub> oxidation on the Pt field emitter is distinguished by preferential imaging of the catalytically active surface sites with the product molecule H<sub>2</sub>O (desorbed mainly as H<sub>3</sub>O<sup>+</sup>). In field electron microscopy (FEM) the different local work functions (WF) lead to areas with different brightness, characterizing CO<sub>(ad)</sub>, O<sub>(ad)</sub>, H<sub>(ad)</sub> and H<sub>2</sub>O

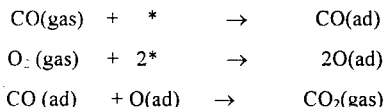
-covered surfaces. Isothermal, non-linear dynamic processes of CO- and H<sub>2</sub> oxidation reactions on Pt are investigated, involving the formation of face-specific adsorption islands, mobility of reaction/diffusion fronts and the creation of chemical waves. The electric fields ( $\approx 0.4$  V/Å) in the FEM and ( $\approx 1.5$  V/Å) in the FIM appear to have a minor influence on the catalytic behavior of the Pt surface planes.

## EXPERIMENTAL

Experiments were performed in an UHV chamber (base pressure  $10^{-10}$  mbar). The catalyst was a platinum field emitter supported on a tungsten loop. The temperature at the tip could be controlled within 1 K. The Pt surface was cleaned by field evaporation. The CO, H<sub>2</sub> and O<sub>2</sub> reaction gases of the highest purity were supplied and controlled by a spinning rotor gauge (visco-vac manometer) and a quadrupole mass spectrometer. The total field electron (ion) current and the FEM (FIM) image were continuously monitored during the catalytic surface reaction at an oxygen partial pressure of  $\approx 5 \times 10^{-4}$  mbar and CO partial pressure of  $\approx 5 \times 10^{-5}$  mbar ( $P_{H_2} \approx 5 \times 10^{-5}$  mbar). A single channel plate was used as image amplifier and a CCD camera recorded the propagation of the surface waves.

## CO OXIDATION

The catalytic CO oxidation proceeds via a Langmuir-Hinshelwood mechanism:



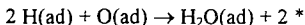
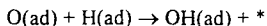
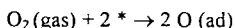
Experimental observations with FEM/FIM on the Pt surface strongly suggest that the CO oxidation is a face-specific reaction which displays isothermal oscillations under particular conditions in the parameter space, as determined by a kinetic phase diagram [6]. For Pt-field emitter surface kinetic oscillations are observed for (100), (110) and (210) but not for (111) planes. The transition from the low (CO ad-layer) to high (O ad-layer) activity is accompanied by local oscillations in the surface coverage. The catalytic activity is higher at the border line between (Oad) and CO(ad) islands. Within the CO(ad) islands the O<sub>2</sub> adsorption is prevented and therefore the catalytic reaction is poisoned. Chemical waves appear on the emitter surface and propagate in phase with self-sustained isothermal oscillations. Two spatially separated adlayers are formed

## PL-22

on the surface under oscillating conditions. The  $\text{CO}_{\text{ad}}$ -covered layers are formed only on the  $\{111\}$ ,  $\{112\}$ ,  $\{113\}$  planes, whereas  $\text{O}_{\text{ad}}$ -covered areas are formed on the  $\{100\}$ ,  $\{012\}$ ,  $\{011\}$  planes. During the catalytic reaction on these areas, the  $\text{CO}_{\text{ad}}$ - and  $\text{O}_{\text{ad}}$ -wave fronts move alternately in opposite directions and display the different velocities of propagation. In the case of Pt (100), the oscillations are associated with a CO-induced surface phase transition  $\text{hex} \leftrightarrow 1 \times 1$ . This phase transition can be directly observed by FEM and FIM as an interface (a sharp reaction zone at a width of  $\approx 50 \text{ \AA}$ ) between the  $\text{CO}_{\text{ad}}$ - and  $\text{O}_{\text{ad}}$ -layers on the (100) plane. The travelling reaction zone during the oscillation cycle was further mass-analyzed by a probe hole technique, providing a sharpness of  $\approx 20 \text{ \AA}$  and a maximum in  $\text{CO}_2$  rate, detected as a  $\text{CO}_2^-$  current. The lifting of the surface reconstruction by CO increases the sticking probability of oxygen by hundred times with a consequent increase in catalytic activity within the reaction zone. As a result, the surface O-wave front originates on the (100) plane and moves to the  $\text{CO}_{\text{ad}}$ -covered (111) plane.

## $\text{H}_2$ OXIDATION

The imaging situation (FIM) for the  $\text{H}_2$  oxidation on Pt is even more challenging because the product molecule of the catalytic reaction,  $\text{HO}$ , serves as the imaging gas [5]. There is known the sequence of six reaction steps:



The character of the  $\text{H}_2/\text{O}_2$  oscillating reaction differs remarkably from that in CO-oxidation: (i) the imaging product molecules ( $\text{H}_2\text{O} + (\text{H}_3\text{O}^+)$  ions) directly locate reactive sites; (ii) a front travelling in the reverse directions, starts fast from the central Pt(100) plane and propagates to the peripheral  $\{111\}$  planes, and then starts again slowly from  $\{111\}$  to (100). The reactivities of the oxygen adlayer on the hex- and  $1 \times 1$ -phase during the  $\text{H}_2 + \text{O}$  titration reaction is studied. The diffusion reaction front on a  $\text{O}_{\text{ad}}$ -precovered (100)-hex surface starts at  $\{331\}$  planes and proceeds in an anisotropic re-

action sequence of planes until finally the (100) plane is covered by hydrogen adatoms. The reaction with  $O_{ad}$ -1x1 surface starts in the reverse direction from the central Pt(100) plane (as in oscillations) and propagates to the peripheral {111} planes. This means, that in an oscillation the drive mechanism would include the hydrogen inducing transformations between the hex-phase and the (1x1) phase.

### OXYGEN ADSORPTION

The role of the oxygen was studied in a separate HREELS experiment where the conversion of the molecular peroxide  $O_2^{2-}$  ad-state and superoxide  $O_2^-$  ad-state into the dissociated  $O_{ad}$  state was observed. The formation of hot O-adatoms by the exothermic adsorption leading to a motion parallel to the Pt surface will be discussed as another possible mechanism describing such a sharp reaction zone formation.

### References

- [1] G.Ertl, Adv.Catal. 37 (1990) 213
- [2] R.Imbihl, Progr. Surf. Sci. 44 (1993) 185
- [3] V.Gorodetskii, J.H. Block, W. Drachsel and M. Ehsasi, Appl. Surface Sci. 67 (1993) 198
- [4] V.Gorodetskii, W. Drachsel and J.H. Block, Catal. Lett. 19 (1993) 223
- [5] V.Gorodetskii, J. Lauterbach, H.-H. Rotermund, J.H. Block and G.Ertl, Nature 370 (1994) 276
- [6] Y.-S. Lim, M. Berdau, M. Naschitzki, M. Ehsasi and J.H. Block, J. of Catal. 149 (1994) 292

### Acknowledgments

This work was in part supported by INTAS (93-964).

TUNNELING REACTION AND HIGH RESOLUTION ESR SPECTROSCOPY IN  
QUANTUM SOLID PARAHYDROGEN AT 4 K

Tetsuo Miyazaki

Department of Applied Chemistry, School of Engineering,  
Nagoya University, Chikusa-ku, Nagoya 464-01, JAPAN;  
Advanced Science Research Center, Japan Atomic Energy  
Research Institute, Tokai-mura, Ibaraki 319-11, JAPAN

The solid hydrogen is a well-known quantum solid. The reactive species in quantum solid hydrogen are fascinating problems in chemistry and physics at low temperature. Hydrogen atoms in solid hydrogen react with neighboring hydrogen molecules by quantum mechanical tunneling even at 4.2 K [1]. Since the total nuclear spin of  $p\text{-H}_2$  is zero, the dipole interactions of the electron spin magnetic moments of the surrounding  $p\text{-H}_2$  molecules vanish and thus the radicals are expected to show very narrow ESR spectra. Then, the  $p\text{-H}_2$  matrix can be used as a new matrix for the high resolution analysis of ESR spectra with high sensitivity.

## 1. Tunneling Reaction of H(D) Atoms in Solid Hydrogen

### (1) Evidence for tunneling reaction

When solid HD is irradiated by  $\gamma$ -rays at 4.2 K, H and D atoms produced are measured by ESR. Upon storage of the irradiated HD at 4.2 K, the amounts of H atoms increase while those of D atoms decrease complementally. The results indicate clearly the occurrence of a reaction  $\text{HD} + \text{D} \rightarrow \text{H} + \text{D}_2$  at 4.2 K. The reaction takes place also at 1.9 K with the same rate as that at 4.2 K, indicating no activation energy for the reaction, though the potential energy barrier for the reaction is 10 Kcal/mol. The rate constant for a reaction  $\text{D} + \text{HD}$  was measured experimentally as  $0.0021 \text{ cm}^3 \text{ mol}^{-1} \text{ s}^{-1}$ .

The rate constant obtained here is much larger than the rate constant ( $10^{-454} \text{ cm}^3 \text{ mol}^{-1} \text{ s}^{-1}$ ) for the reaction that takes place by passing over the energy barrier. The rate constant obtained here is approximately similar to the rate constant (0.0027;  $0.039 \text{ cm}^3 \text{ mol}^{-1} \text{ s}^{-1}$ ) calculated for a tunneling reaction [2,3], where the reaction takes place by passing through the barrier by a tunneling effect.

## (2) Effect of rotational quantum states ( $J=0,1$ ) on tunneling reactions

There are two kinds of  $\text{H}_2$ , i.e., para- $\text{H}_2$  and ortho- $\text{H}_2$ . Rotational quantum states ( $J$ ) of p- $\text{H}_2$  and o- $\text{H}_2$  at 4 K are 0 and 1, respectively. The effect of rotational quantum states on tunneling reaction  $\text{H}(\text{T}) + \text{H}_2(\text{J}=0,1)$  was studied by use of p- $\text{H}_2$  and n- $\text{H}_2$  that contains 75 % o- $\text{H}_2$ .  $\text{H}(\text{T})$  atoms react about 4 times faster with  $\text{H}_2(\text{J}=0)$  than  $\text{H}_2(\text{J}=1)$ .

## 2. High Resolution ESR Spectroscopy in Solid p- $\text{H}_2$

### (1) Alkyl radicals produced by photolysis

ESR spectra of  $\text{CH}_3$ ,  $\text{CD}_3$  and  $\text{C}_2\text{H}_5$  radicals, produced by the photolysis of the alkyl iodides, have been measured in solid  $\text{H}_2$  at 4.2 K. The ESR spectra of the radicals in a n- $\text{H}_2$  matrix containing 75 % o- $\text{H}_2$  (nuclear spin = 1) and 25 % p- $\text{H}_2$  consist of broad peaks, while spectra in the p- $\text{H}_2$  (nuclear spin = 0) matrix consist of extremely narrow lines and the hyperfine structures can be clearly observed in the spectra [4]. Since the total nuclear magnetic moment of p- $\text{H}_2$  is zero, the dipole interactions of electron spin magnetic moments of an alkyl radical with the surrounding p- $\text{H}_2$  molecules disappear completely, resulting in the narrowing of the ESR spectra. When  $\text{C}_2\text{H}_5$  radicals are produced in the p- $\text{H}_2$  matrix, the hyperfine structures of ESR spectra can be observed clearly. The most stable structure of  $\text{C}_2\text{H}_5$  radicals was determined by the analysis of ESR spectra.

## (2) Ion-pair of an electron bubble and a hole produced by radiolysis

Since ESR spectra of radicals in the p-H<sub>2</sub> matrix are narrowed drastically, the sensitivity of ESR measurement in the p-H<sub>2</sub> matrix is increased by about 100 times that in the n-H<sub>2</sub> matrix. When p-H<sub>2</sub> is irradiated at 4.2 K with  $\gamma$ -rays, the new reactive species that show narrow doublet ESR lines, indicated by arrows, with a separation of 12.4 G have been observed (Fig. 1A). The intense spectra, which appear in the right-hand side of the figure, are due to color centers produced in the irradiated quartz cell. The sharp doublet line, however, were not observed in the n-H<sub>2</sub> matrix probably because of broadening of the spectra caused by the superhyperfine interactions with neighboring o-H<sub>2</sub> molecules (Fig. 1B). The yield of the new species is 0.0001 G-unit. The new species decay in several hours upon storage of the irradiated solid p-H<sub>2</sub> at 4.2 K. The doublet lines were interpreted in terms of an ion-pair of an electron bubble and a hole ( $e^-_{\text{bubble}} \cdots p\text{-H}_2^+$ ) separated by 12 Å [5].

In conclusion, solid parahydrogen can be used as a new matrix for study of reaction intermediates.

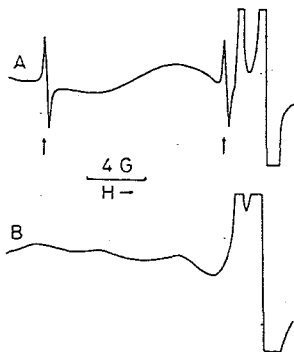


Fig. 1. ESR spectra of  $\gamma$ -irradiated solid hydrogen at 4.2 K. (A) p-H<sub>2</sub>, (B) n-H<sub>2</sub>.

## References

- [1] T.Miyazaki, S.Kitamura, H.Morikita and K.Fueki, J. Phys. Chem., 96, 10331 (1992), and references therein.
- [2] T.Takayanagi and S.Sato, J. Chem. Phys., 92, 2862 (1990).
- [3] G.C.Hancock, C.A.Mead, D.G.Truhlar and A.J.C.Varandas, J. Chem. Phys., 91, 3492 (1989).
- [4] T.Miyazaki, K.Yamamoto and J.Arai, Chem. Phys. Letters, 219, 405 (1994).
- [5] T.Miyazaki, K.Yamamoto, and Y.Aratono, Chem. Phys. Letters, 232, 229 (1995).

## MECHANISM OF MECHANICAL ACTIVATION OF SOLIDS

V.V. Boldyrev

*Institute of Solid State Chemistry and Mineral Raw Processing,  
SB RAS, Novosibirsk, 630128, Russia*

1. Reactivity of solids. Features in evaluation of the reactivity of solids and methods to control it. Crystal defects and their role in evaluation and control of reactivity.
2. Mechanical activation. Mechanical activation in one-component systems. Routes of stress field relaxation at the tip of a moving crack and at contacts. Initiation of defect formation, of phase and chemical transformations during a stress field relaxation. Unusual states of solids occurring during mechanical activation. Structures with anomalous redistribution of ions in cation and anion sublattices. Icosahedral structures.
3. Mechanical activation of multicomponent systems. Liquid-solid systems. Possibilities of realization of hydrothermal transformations. Soft mechanochemical synthesis. Solid-solid system. Mechanical alloying. Mechanism of interaction between components. Diffusion in the solid phase in a stress field.  
Possible role of the fluid phase. Mechanism of interaction due to the contact melting.
4. Problems and prospects in studies of mechanical activation.

FRACTAL-TIME DYNAMICS OF ELEMENTARY REACTIONS  
IN CONDENSED MEDIA

Andrzej Plonka

Institute of Applied Radiation Chemistry  
Wroblewskiego 15, 93-590 Lodz, Poland

Nowadays deviations from classical rate laws are seen to be endemic even for elementary reactions followed at very short time scales and/or low temperatures in condensed media. Unnecessarily, in many instances these deviations are related to complex mechanisms as simple reaction schemes are recovered by accounting for the dispersion of reactivity in condensed media.

The dispersion of reactivity becomes evident only when it is changing during the reaction course. Reactions, by their very nature, have to disturb reactivity distributions of reactant in condensed media. The extent of disturbance depends on the ratio of the rates of reactions to the rate of internal rearrangements in the system restoring the initial distribution in reactivity of reactants. If the rates of chemical reactions exceed markedly the rates of internal rearrangements, then the initial distribution in reactant reactivity is not preserved during the course of reaction and one has to account both for the initial distribution and for the changes in reactivity distribution during the reaction course. If, however, the rates of internal rearrangements exceed markedly the rates of chemical reactions, then the extent of disturbance is negligible and the classical kinetics may be valid.

Following this idea, it is convenient to begin with reaction modelling in static systems, then to account for the dynamical effects and to conclude with the survey of experimental results for fluids, solids and for some heterogeneous systems.

Starting with rigid matrix approximation one finds reaction kinetics in condensed media to be scale invariant, like the processes of relaxation and transport. Scale invariance means that the rate processes are not characterized by any particular scale of time, all temporal scales are present. This phenomenon, accounted for by fractal-time rate laws discussed below, is commonly believed to be an effect of a large number of degrees of freedom in disordered media and this approach will be preferred in the presentation given below. The large number of degrees of freedom in

## PL-25

condensed media is linked directly to their disorder. Phenomenologically, accounting for static aspects of disorder one finds the mean number of distinct sites visited by a random walker  $S(t)$  to be given by

$$S(t) = (t/\zeta)^\alpha, \quad 0 < \alpha < 1$$

where  $\alpha$  denotes the dispersion parameter and  $\zeta$  is the parameter defining the time scale. The specific reaction rate  $k(t)$  related to  $S(t)$  by

$$k(t) \sim dS(t)/dt$$

is of the form

$$k(t) \sim (\alpha/\zeta)(t/\zeta)^{\alpha-1}$$

This specific reaction rate introduces the fractal time,  $t^\alpha$ , into the kinetic equations. The dispersion parameter  $\alpha$  originates e.g. from continuous time random walk (CTRW) models which incorporate the distribution of waiting times for a walker

$$\Psi(t) \sim t^{-\alpha-1}$$

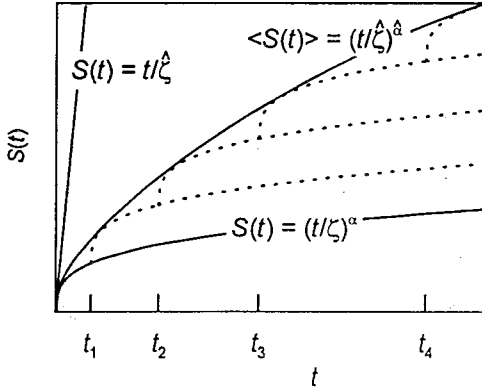
to account for temporal disorder in the condensed medium. This is paralleled by the result of random walk modelling on fractal structures exemplifying the spatial disorder,  $\alpha = \min(\bar{d}/2, 1)$ , where  $\bar{d}$  is the spectral dimension of the system, and by the result of random walk modelling on ultrametric spaces which exemplify the energetic disorder of the system,  $\alpha = \min(\delta, 1)$ , where  $\delta = (kT/\Delta) \ln b$  for consecutive energy levels differing by  $\Delta$  and for branching ratio  $b$ .

Here it seems relevant to note that even for random walk modelling on regular lattices  $S(t)$  is linear in time only for dimensions  $d > 2$ .

$$S(t) \sim \begin{cases} t^{1/2} & d = 1 \\ t/\ln t & d = 2 \\ t & d = 3 \end{cases}$$

This means that for  $d \leq 2$  specific reaction rate is time-dependent even for regular lattices and reflects the fact that diffusion is not an effective mixing mechanism in low dimensions.

In all models of statically disordered systems the mean number of distinct sites visited  $S(t)$  is sublinear in time



The less dispersive is the kinetics the smaller is the deviation from linear dependence on time of the mean number of distinct sites visited by the walker. Thus, in the language of the above picture, the problem of accounting for host matrix effects, giving in the limit the classical kinetics, is equivalent to showing how to go from sublinear dependence of  $S(t)$  on time to the linear one. This was achieved by imposing upon the static disorder model the additional assumption that at certain random instants reinitialization occurs, consisting of a random reassignment of hopping rates with the values having the some statistical distribution as before. It is seen in the picture that due to a sequence of reassignment events, the effective number of distinct sites visited approaches the linear dependence on time. To evaluate this effect quantitatively we have to consider possible sequences of times at which reassignments occur and to average  $S(t)$  over all of them. For  $S(t)$  given above and reinitialization events given by a set of fractal time events, resulting from the use of Kohlrausch function

$$\Phi(t) = \exp[-(t / \tau_0)^\beta], \quad 0 < \beta \leq 1$$

to describe the structural relaxation of the host matrix, the result is

$$\langle S(t) \rangle = (t/\hat{\zeta})^{\hat{\alpha}}$$

This leads to

$$k(t) \sim (\hat{\alpha}/\hat{\zeta})(t/\hat{\zeta})^{\hat{\alpha}-1}$$

where  $\hat{\alpha}$  denotes the dynamically averaged dispersion parameter

$$\hat{\alpha} = 1 - (1 - \alpha)(1 - \beta)$$

which we do observe experimentally, and  $\hat{\zeta}$  is given by

$$\hat{\zeta} = \zeta^{(\alpha/\hat{\alpha})} \tau_0^{(1-\alpha/\hat{\alpha})}$$

The numerical value of  $\hat{\alpha}$  is seen to depend on the numerical value of  $\beta$  which depends on the time scale of the experiment in the following way

$$\beta = \begin{cases} 1/3 & \text{or less for } t \ll \tau_0 \\ 1/2 & \text{for } t \sim \tau_0 \\ 2/3 & \text{or more for } t \gg \tau_0 \end{cases}$$

In the model, the time scale  $t$  has to be directly related to the characteristic time  $\zeta$ . Therefore, for  $\tau_0 \gg \zeta$  one can take  $\beta \rightarrow 0$  to get

$$\hat{\alpha} \rightarrow \alpha$$

$$\hat{\zeta} \rightarrow \zeta$$

i.e. the limit for kinetics on time scales short compared with those of matrix relaxation. On the other hand, for  $\tau_0 \ll \zeta$  one can take  $\beta \rightarrow 1$  to get

$$\hat{\alpha} \rightarrow 1$$

$$\hat{\zeta} \rightarrow \zeta^\alpha \tau_0^{(1-\alpha)}$$

i.e. the limit for kinetics on time scales long compared with those of matrix relaxation. If both processes, i.e. guest movement and host matrix relaxation, are thermally activated with activation energies  $E(\zeta)$  and  $E(\tau_0)$  then

$$E(\hat{\zeta}) \sim \begin{cases} E(\zeta) & \text{for } \hat{\alpha} \rightarrow \alpha \\ \alpha E(\zeta) + (1-\alpha)E(\tau_0) & \text{for } \hat{\alpha} \rightarrow 1 \end{cases}$$

For reactive species there is, in general,  $E(\zeta) < E(\tau_0)$ . Therefore the above given model rationalizes the marked increase of activation energy with the change of reaction pattern from dispersive to classical in numerous systems. This point will be illustrated by a number of experimental results displaying the change from "liquid-like" to "solid-like" behaviour.

For fractal time kinetics there is no mean value of the specific reaction rate. For any reaction order there are, however, moments of the distributions of the logarithms of lifetimes which are directly related to the moments of distributions of parameters like activation energy used to describe the thermally activated transitions over the potential barrier (Arrhenius, Eyring, Kramers) or tunnelling distance for quantum mechanical transitions under the barrier (Gamov). For  $\hat{\alpha} \rightarrow 1$  the second moments of these distributions turn out to be zero. Thus it is shown that nowadays commonly encountered deviations from classical patterns do not necessarily call for specific mechanisms or complex kinetic schemes.

#### References

1. A. Plonka, Time-Dependent Reactivity of Species in Condensed Media, Lecture Notes in Chemistry, vol. 40, Springer-Verlag, Berlin 1986.
2. A. Plonka, Developments in Dispersive Kinetics, Prog. Reaction Kinetics, **16**, 157 (1991).
3. A. Plonka, Dispersive Kinetics in Condensed Phases, Annu. Rep. Prog. Chem., **85**, 47 (1988)
4. A. Plonka, Dispersive Kinetics, Annu. Rep. Prog. Chem. **89**, 37 (1992).
5. A. Plonka, Dispersive Kinetics, Annu. Rep. Prog. Chem. **91**, 172 (1994).

## CHEMICAL DYNAMICS AT LOW TEMPERATURES

Y. A. Benderskii and S. Yu. Grebenshchikov

Institute of Chemical Physics at Chernogolovka, Russian Academy of Sciences,  
Chernogolovka, Moscow Region, 142432 Russia

Preliminary development of the concept of low-temperature dynamics was supported by experimental studies of solid-state chemical reactions, rate constants of which deviate from the Arrhenius law [1, 2]. There existed also a set of examples, in which tunneling is observable in the spectroscopy of non-rigid molecules. Among them, inversion of ammonia molecule is mostly well-known. The number of molecules and molecular complexes grew considerably after the appearance of supercooled jet technique and development of tunable laser far-IR spectroscopy. Combining these two methods, one can study vibration-rotation-tunneling (VRT) spectra for vibration and rotation temperatures below 10 - 20 K.

Conditions, in which rate constants of chemical reactions and tunneling splittings in VRT spectra are measured correspond to two limiting tunneling regimes: an incoherent regime of chemical reaction and a coherent one of spectroscopy. What regime is realized, depends upon the interaction between the tunneling motion and low-frequency motions along the non-tunneling modes, forming the "bath" [3, 4]. The part of the "bath" is played either by low-frequency phonons and librational modes (in solids) or by multiple collisions (in gas). Weak interaction does not destroy the coherence of tunneling transitions, and the probability of finding the particle in either potential well oscillates in time with the tunneling frequency. Coherence is spoiled by strong interaction with the bath, and the dissipative tunneling transition is characterized by a rate constant (transition probability). According to the Fermi golden rule, this probability is proportional to the square of the tunneling frequency. Therefore, the both limits are described by the latter quantity.

Modern far-IR and microwave spectroscopy, inelastic neutron scattering spectroscopy, and NMR in low fields allow measuring tunneling frequencies in the range of 10 -  $10^{-4}$   $\text{cm}^{-1}$ . Corresponding range of rate constants ( $10^5$  -  $10^{-5}$   $\text{s}^{-1}$ ) is also available to direct measurements. This correlation enables one to observe the same system in both the tunneling regimes, experimentally changing the interaction between the reaction complex and its environment.

The correlation between tunneling splittings in VRT-spectra and rate constants of tunneling reaction implies, that a unified theoretical description of them can be given. Upon the transition from the tunneling rate constant to the thermally-activated one, vibrationally-excited states become populated, and their tunneling splittings must also be calculated.

Like the majority of chemical dynamics' problems, the tunneling spectra are to be computed for a multidimensional potential energy surfaces (PES). Apart from interactions with low-frequency "bath", the tunneling coordinate is strongly influenced by a limited

number of non-tunneling modes of the reaction complex itself. The effect of intramolecular modes on tunneling splitting depends on the symmetry of coupling and may be revealed from two-dimensional (2D) model PES. There are three basic types of 2D PES with two equivalent minima and one saddle point. For "linear" (antisymmetric) coupling, the interaction renormalizes the tunneling matrix element by a Frank-Condon factor, smaller than unity [5]. This is typical of the diffusion of a light impurity in solids. Non-correlated jumps between the neighboring sites are accompanied by environmental reorganization, that equalizes the initially different occupied and empty sites in the lattice. For "gated" (symmetric only with respect to tunneling coordinate) coupling, vibrationally-assisting tunneling (VAT) regime is realized [6]. This PES is characteristic of the exchange chemical reactions. The transverse vibration cannot be considered within the Condon approximation because of the equivalence of the initial and final states. Displacements along the soft transverse mode lower the barrier height. Purely dynamical VAT takes place for positive "squeezed" (symmetric in both the coordinates) coupling [7, 8]. The frequency of the transverse oscillator varies in the course of the tunneling transition, but its equilibrium position remains unchanged. Softening of the transverse mode forces the tunneling transition probability to grow. The 2D problem can be reduced to the one-dimensional (1D) one in two ways [4]. If the frequency of the tunneling motion is much greater than the transverse one, "sudden" approximation [7], treating transverse mode as frozen out, can be used. In the opposite case, the problem may be simplified by invoking the vibrationally-adiabatic approximation. However, these approximations have a very limited range of applicability to real objects. The obvious reason for non-tunneling modes to take part in the transition is strong distortion of molecular skeleton in the transition state. For example, the O...O distance in malonaldehyde molecule is shortened by 0.4 Å in the transition state with respect to the equilibrium distance [6, 9]. The contraction leads to VAT, resulting in the increase in the tunneling probability. Threefold decrease in the bending frequency of the cyclopentanone molecule in the planar transition state results in a two-orders-of-magnitude growth of the tunneling splitting with the transverse quantum number changing from 0 to 6.

For different symmetries of coupling, the dependences of tunneling splitting on the transverse quantum number are different [5 - 8]. This is an experimentally observed vibrational selectivity of tunneling splitting. VAT regime is characterized by a sharp growth of tunneling splitting in the vibrational progressions.

Intra- and intermolecular hydrogen transfer in OH...O [5, 6], NH...N, CH...C fragments, hindered rotation of methyl groups, interconversion of saturated cyclic organic molecules [7] and HF dimer and van der Waals complex  $H_2F^-$  [10] can be treated within these 2D models. However, there is a number of examples in which two coupled tunneling motions occur simultaneously: two-proton transfer, combined inversion-rotation in methylamine, two coupled inversions in hydrazine and hydrogen pyroxide, two coupled hindered rotations in

water and ammonia dimers. Commonly used symmetry considerations are insufficient, because symmetries of the transition and equilibrium states are different. Inversion of the amine group in methyl amine is energetically allowed only after  $60^\circ$  rotation of the methyl group. Additionally, strong coupling of torsion and low-frequency bending modes is characteristic of inverting and rotating molecular subunits. In these systems, there are more than one transition states and more than two equilibrium configurations. As a result, the tunneling path suffers a bifurcation at certain quantum numbers (or temperatures), and, thus, the transfer mechanism changes. Such case was earlier observed for two-proton transfer [11, 12]. At  $T = 0$ , the transfer is synchronous, while the transitions above the barrier correspond to asynchronous (step-wise) case.

Within the semiclassical approximation, the tunneling trajectory may be introduced, much like that in the transition state theory for overbarrier transitions. However, it is calculated in the upside-down potential (or, equivalently, in imaginary time and with imaginary momenta). The tunneling channel, centered around the tunneling path, has a certain width due to transverse small-amplitude vibrations. The main peculiarity of tunneling trajectories is that, unlike classical ones, they deviate from the minimum energy path (MEP). The deviation arises, because the path is a compromise between the barrier height and the length of path. In particular, "cutting corner" paths appear in the "gated" potential. We note, however, that for large mass tunneling trajectory follows MEP closely, and goes away from it with diminishing mass. This is a dynamical cause of large isotope effects on tunneling splittings [10] and rate constants [4].

Full semiclassical consideration of multidimensional tunneling in the ground and vibrationally-excited states [5] goes beyond the sudden and adiabatic approximations. It employs the widely accepted in molecular spectroscopy approximation of uncoupled small-amplitude vibrations near the equilibrium position. Vibrational energy of the unsplit state is a sum of individual vibration quanta, while the wave function is approximately a product of the linear oscillator wave functions along each mode. The orthogonal "moving" frame, consisting of a coordinate, running along the tunneling trajectory, and a set of transverse coordinates is introduced in the spirit of the reaction path Hamiltonian method due to Miller. Tunneling path, however, is computed from the coupled equations of motion, rather than postulated to be the MEP. Transverse to this calculated path modes turn out to be uncoupled dynamically, their motion being correlated to the tunneling coordinate only. This is a substantial simplification with respect to the reaction path Hamiltonian method, in which transverse to the MEP modes actively influence each other.

Common vibration-rotation spectra of rigid molecules with the only equilibrium conformation contain frequencies of small-amplitude vibrations near the PES minimum. At the same time, modern chemical dynamics concentrates on the behaviour of system far from equilibrium, in the vicinity of the transition state. This region of PES cannot be reconstructed

uniquely only from the spectral information about the reactants. For instance, the transfer distance remains unknown. Tunneling wide-amplitude motions are directly related to the barrier region of PES. For this reason, the spectroscopy of non-rigid molecules allows reconstruction of whole PES of the reacting system.

We thank Professors V.I. Gol'danskii, L.I. Trakhtenberg, C.A. Wight, J. Simons, Drs. D.E. Makarov, P.G. Grinevitch, G.V. Mil'nikov A.I. Boldyrev, and E.V. Vetoshkin for collaboration.

Authors thank Russian Fund of Fundamental Investigations (Grants No. 94-03-08863 and No. 94-03-08862) and the International Science Foundation (Grant RE 3000) for the financial support of this work.

#### REFERENCES

1. Gol'danskii V.I., Benderskii V.A., and Trakhtenberg L.I., *Quantum Cryochemical Reactivity of Solids*, Adv. Chem. Phys. **85** (1989) 349.
2. Benderskii V.A. and Gol'danskii V.I., *Tunneling Effects in Low-Temperature Chemistry*, Int. Rev. Phys. Chem. **11** (1992) 1.
3. Benderskii V.A., Gol'danskii V.I., and Makarov D.E., *Tunneling Dynamics in Low-Temperature Chemistry*, Phys. Repts. **233** (1994) 197.
4. Benderskii V.A., Makarov D.E., and Wight C.A., *Chemical Dynamics at Low Temperatures*, J.Wiley, N.Y., 1994.
5. Benderskii V.A., Grebenshchikov S.Yu., and Mil'nikov G.V., *Tunneling Splittings in Model 2D Potentials. III. Generalization to N-Dimensional Case*, Chem. Phys. 1995, in press.
6. Benderskii V.A., Grebenshchikov S.Yu., and Mil'nikov G.V., *Tunneling Splittings in Model 2D Potentials. II. "Gated" Potential.*, Chem. Phys. 1995, in press.
7. 1. Benderskii V.A., Grebenshchikov S.Yu., Mil'nikov G.V., and Vetoshkin, E.V., *Tunneling Splittings in Model 2D Potentials. I. "Squeezed" Potential.*, Chem. Phys. **188** (1994) 19.
8. Benderskii V.A., Grebenshchikov S.Yu., Vetoshkin, E.V., Mil'nikov G.V., and Makarov D.E., *Two-Dimensional Tunneling: Bifurcations and Competing Trajectories*, J. Phys. Chem. **98** (1994) 3300.
9. Benderskii V.A. Makarov D.E., and Grinevich P.G., *Quantum Chemical Dynamics in Two Dimensions*, Chem. Phys. **170** (1993) 275.
10. A.I. Boldyrev, J. Simons, G.V. Mil'nikov, V.A. Benderskii, S.Yu. Grebenshchikov, and E.V. Vetoshkin, *Ab initio Vibration-Rotation-Tunneling Spectra and Dynamics of H<sub>2</sub>F<sup>+</sup> and its isotopomers*, J. Chem. Phys. **102** (1995) 1295.
11. Benderskii V.A., Gol'danskii V.I., and Makarov D.E., *Two-Dimensional Tunneling in a Potential with Two Transition States*, Chem. Phys. Lett. **186** (1992) 29.
12. Benderskii V.A., Grebenshchikov S.Yu., Makarov D.E., and Vetoshkin E.V., *Tunneling Trajectories of Two-Proton Transfer*, Chem. Phys. **185** (1994) 101.

DIFFUSION MOBILITY IN QUENCHING REACTION OF ELECTRONIC EXCITED STATES OF ORGANIC SYSTEM AT LOW TEMPERATURES.

N.M.Bazhin, V.V.Korolev

Institute of Chemical Kinetics and Combustion, SB RAS, Novosibirsk,  
630090, Russia.

The diffusion of the small molecules of gaseous substances and, first of all, those of oxygen, determines the aging of many materials, particularly, polymers. The mechanism of small molecules mobility in disordered matrices controls the reaction kinetic behaviour and many peculiarities in kinetic curves in solid state. Every reaction act between two molecules include two stages: approach and reaction at small distance. If you study the reaction kinetics via product formation or disappearance you will observe the sum of two processes: approach and reaction. It is very important to discriminate between two stages. We decided to begin with mobility study at distances more than reactive radii and to compare this mobility results with reaction products data.

The luminescence methods are much more preferable in studying the microscopic mobility of molecular oxygen because the information on the value of diffusion coefficient is extracted upon displacements of partners over the distances from fractions to tens of angstrom. In this case, advantageous are the processes of the exchange quenching of electronic excited singlet and triplet states accelerated by particle motion, because the range of the changes of exchange interaction is 1-2 Å which is close to the sizes of small molecules.

We developed in this presentation two techniques for molecular oxygen slow mobility determination in low-molecular glasses:

1. Exchange quenching of phenanthrene phosphorescence ( $T_1$  -quenching) for  $D \sim 10^{-17}$  cm<sup>2</sup>/s. A lower value of the mobility depends on the lifetime of

an aromatic molecule in the triplet state ( $\sim 1$  s) and a characteristic range of exchange interaction decay ( $\sim 1$  Å) [1,2].

2. Luminescence quenching ( $S_1$ -quenching) during the separation process of the specially created geminate pairs. In this case, much lower diffusion coefficients (by three-six orders of magnitude) can be measured than by the quenching of triplet states [3,4].

The aim of our work is:

1. To analyze and to compare the process of the diffusion measurement by both techniques.
2. To determine the relaxation matrix processes.
3. To compare the time dependent diffusion with time dependent reaction constant.

#### 1. Diffusion coefficient measurements.

Diffusion coefficient measurements were made for phenanthrene phosphorescence quenching at alcohol and squalane low temperature glasses [2,4].

We used steady-state and pulse phosphorescence excitation. The steady-state method has been based on the comparison between the experimental dependence of the value of the quantum yield of phenanthrene phosphorescence quenching and that calculated for the different values of  $O_2$  molecule mobility. The pulse excitation method allow not only calculate the diffusion coefficient but to verify the initial proposals about oxygen mobility [4].

Much more slow diffusion coefficient can be measured with the new technique via luminescence quenching during separation of the specially created geminate pairs. This has been demonstrated [3,4] by the separation of the geminate pair of anthracene and oxygen molecules. The geminate pairs have been obtained by photolysis of anthracene endoperoxide in a glassy alcohol and squalane. The diffusion has been studied at temperatures close to 77 K. The motion of oxygen molecules can be recorded by the decreasing efficiency of anthracene fluorescence quenching.

The diffusion coefficient data are listed in Table 1 [4].

TABLE 1.

The values of diffusion coefficients obtained by stationary measurements of the quantum yield of phenanthrene phosphorescence ( $D_{st}$ ), during numerical analysis of the kinetic curves ( $D_{kin}$ ), in the analytical approximation ( $D_{appr}$ ) and by the separation of geminate pairs ( $D_{pair}$ ).

T, K	$D \cdot 10^{16}$ , $\text{cm}^2/\text{s}$			
	$D_{st}$	$D_{kin}$	$D_{appr}$	$D_{pair}$
77				$0.9 \cdot 10^{-7}$
90				$1.0 \cdot 10^{-4}$
100	$0.085 \pm 0.015$	0.08		$5.1 \cdot 10^{-3}$
105	$0.24 \pm 0.04$	0.28	0.24	$2.4 \cdot 10^{-2}$
110	$0.58 \pm 0.1$	0.7	0.58	
120	$6.4 \pm 1.2$	6.0	5.5	
130	$46.0 \pm 10.0$	54	57	
140		480	500	
150		3000	3200	
155		10000	13000	

This techniques can measure the diffusion coefficient in a range  $10^{-12} - 10^{-23} \text{ cm}^2/\text{s}$ .

## 2. Matrix relaxation processes.

The steady state phenanthrene phosphorescence in alcohol matrixes increase in time during annealing [2]. It can be interpreted as slowing oxygen mobility due to relaxation. Relaxation can occur via matrix relaxation or due to redistribution of oxygen molecules from shallow traps to more deep traps. Geminate pair separation was used for discrimination between two possibilities. Photolysis of the anthracene epoxide after annealing allow to introduce oxygen in preliminary aged matrix. The result of the experiment is slowing down of pair separation in alcohol matrix [3]. It denotes that slowing

down oxygen mobility in alcohol matrix take place via matrix relaxation rather than via redistribution. No relaxation take place in squalane as in luminescence quenching [4] and oxidation reaction [5].

3. Comparison between the time dependent diffusion and time dependent rate constant.

It is very interesting to compare time dependent diffusion coefficient and time dependent rate constant. Oxidation reactions of free radicals by oxygen in glassy low temperature matrixes control by diffusion. Some of this reactions show slowing down in reaction rate.[6]. Comparison of the oxygen mobility and reaction rate constant in the same alcohol matrix show the same time dependence of diffusion coefficient and rate constant [6]. Thus there are the reactions which demonstrate that the slowing down take place due to decreasing in time rate constant rather than rate constant distribution

#### REFERENCES.

1. Bazhin N.M. J.Luminescence, 42 (1988) 211
2. V. V. Korolev, N. P. Gritsan, N. M. Bazhin, Khim. Fiz. 5 (1986) 730.
3. V. V. Korolev, D. G. Sushkov, N. M. Bazhin, Chem. Phys. 158 (1991) 129.
4. V. V. Korolev, V.V.Bolotsky, N.V.Shkhirev, E.B.Krissinel', V.A.Bagryansky, N. M. Bazhin Chem. Phys. (1995).
6. S. V. Vasenkov, V. A. Bagryansky, V. V. Korolev, . A. Tolkachev. Radiat. Phys. Chem. 38 (1991) 191.
7. E. L. Zapadinsky, V. V. Korolev, N. P. Gritsan, N. M. Bazhin, V. A. Tolkachev, Chem. Phys. 108 (1986) 373.

## In-situ Controlled Promotion of Catalyst Surfaces: Non-Faradaic Electrochemical Modification of Catalytic Activity

S.G. Neophytides, I.V. Yentekakis, S. Bebelis, and C. G. Vayenas

Department of Chemical Engineering  
University of Patras,  
Patras, GR-26500, Greece

The effect of Non-Faradaic Electrochemical Modification of Catalytic Activity (NEMCA) has been described during the last four years for some twenty-five catalytic reactions on Pt, Pd, Ag, Rh, Au and Ni surfaces [1-6]. It appears to be a general effect, not restricted to any particular catalytic reaction, metal catalyst or solid electrolyte. The NEMCA literature has been reviewed [6]. In brief it has been found that the catalytic activity and selectivity of metal films deposited on solid electrolytes, such as yttria-stabilized-zirconia (YSZ), an  $O^{2-}$  conductor, or  $\beta''\text{-Al}_2\text{O}_3$ , a  $\text{Na}^+$  conductor, can be altered dramatically and reversibly by applying currents or potentials to galvanic cells of the type:

gaseous	metal	solid	counter	reference
reactants,	catalyst	electrolyte	electrode,	gas

and by thus changing the catalyst potential  $V_{WR}$  with respect to a reference electrode (Fig. 1) via supply or removal of ions from/to the solid electrolyte to/from the catalyst surface.

The induced change in catalytic rate can be up to a factor of 200 higher than the open-circuit, i.e. regular, catalytic rate on the metal catalyst [5,6] and up to  $3 \times 10^5$  times higher than the rate of ion supply or removal through the solid electrolyte [4,6]. Significant changes in product selectivity have also been observed for several catalytic reactions [6].

More recently the NEMCA effect has been demonstrated using  $F^-$  conducting solid electrolytes [7] and also in aqueous alkaline solutions during  $H_2$  oxidation [8]. Earlier studies of ester hydrolysis had also shown some Non-Faradaic characteristics [9].

Figure 2 provides a typical example of NEMCA. It shows a galvanostatic transient, i.e., it depicts the transient effect of a constant applied current on the rate of a catalytic reaction. The figure refers to the oxidation of  $C_2H_4$  on Pt which is one of the first reactions for which NEMCA was found and

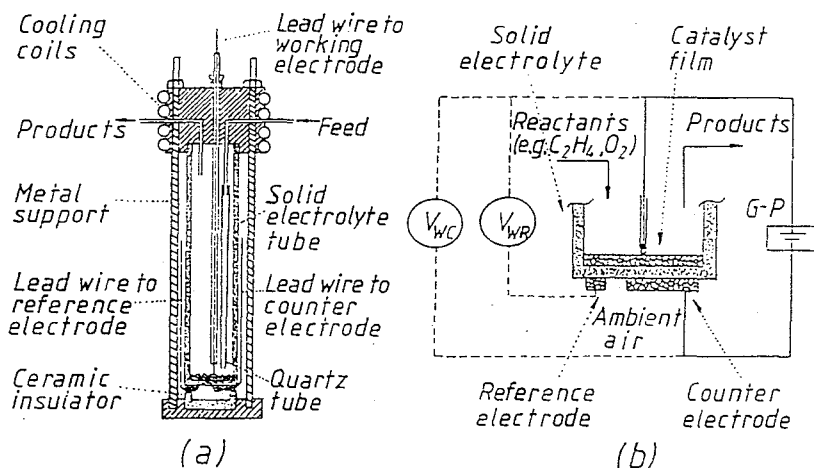


Figure 1. Reactor cell (a) and electrode configuration (b) for NEMCA studies; G-P: Galvanostat-Potentiostat.

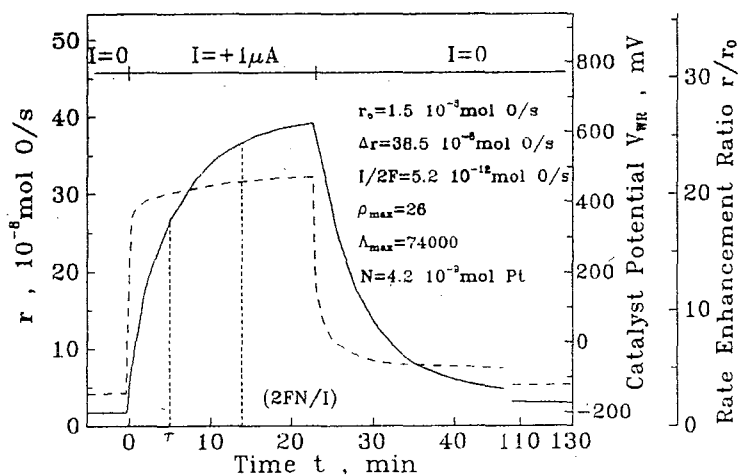


Figure 2. NEMCA: Rate and catalyst potential response to step changes in applied current during  $\text{C}_2\text{H}_4$  oxidation on Pt;  $T=370^\circ\text{C}$ ,  $P_{\text{O}_2}=4.6$  kPa,  $P_{\text{C}_2\text{H}_4}=0.36$  kPa; comparison of experimental ( $\tau$ ) and computed  $(2FN/I)$  rate relaxation time constants; see text for discussion.

studied in detail [2,4]. A Pt film with a surface area corresponding to  $N=4.2 \cdot 10^{-9}$  g-atom Pt as measured by surface titration techniques [3-6], is exposed to  $P_{O_2}=4.6$  kPa,  $P_{C_2H_4}=0.36$  kPa in the CSTR-type flow reactor depicted in Fig. 1. Initially ( $t < 0$ ) the circuit is open ( $I=0$ ) and the open-circuit catalytic rate  $r_0$  is  $1.5 \cdot 10^{-8}$  g-atom O/s. (In order to have a consistent way of comparing the rates of different reactions we express their rates in g-atom O/s). The corresponding turnover frequency (TOF), i.e., oxygen atoms reacting per site per s is  $3.57 \text{ s}^{-1}$ .

Then at  $t=0$  the galvanostat is used to apply a constant current of  $+1 \mu\text{A}$  between the catalyst and the counter electrode (Fig. 1). Now oxygen ions  $O^{2-}$  are supplied to the catalyst-gas-solid electrolyte tpb at a rate  $G_O=I/2F=5.2 \cdot 10^{-12}$  g-atom O/s. The catalytic rate starts increasing and within 25 min gradually reaches a value  $r=40 \cdot 10^{-8}$  g-atom O/s, which is 26 times larger than  $r_0$ . The new TOF is  $95.2 \text{ s}^{-1}$ . The increase in catalytic rate  $\Delta r=r-r_0=38.5 \cdot 10^{-8}$  g-atom O/s is 74,000 times larger than  $I/2F$ . This means that each  $O^{2-}$  supplied to the catalyst causes at steady-state 74,000 additional chemisorbed oxygen atoms to react with  $C_2H_4$  to form  $CO_2$  and  $H_2O$ . This is why this novel effect has been termed Non-faradaic Electrochemical Modification of Catalytic Activity (NEMCA). It is worth noting that the rate relaxation time  $\tau$  is of the order of  $2FN/I$ .

As shown on Fig. 2 NEMCA is reversible, i.e., upon current interruption the catalytic rate returns to its initial value within roughly 100 min. Negative current application has practically no effect on the rate of this particular reaction.

The main features of the NEMCA effect have been summarized elsewhere [6]. It has been shown by in situ work function measurements [1,6], X-ray photoelectron spectroscopic (XPS) [13,14] and surface enhanced Raman spectroscopic (SERS) [15] studies that NEMCA is due to the electrochemically controlled backspillover of promoting ions ( $O^{\delta-}$ ,  $Na^{\delta+}$  etc.) from the solid electrolyte onto the catalyst surface. These backspillover ions act as promoters by changing the work function of the gas-exposed catalytic electrode surface and affecting the chemisorptive bond strength of chemisorbed reactants and intermediates [6,14]. This novel effect appears to be one of the most promising new applications of electrochemistry as recently discussed by Bockris [16].

## References

- 1 C.G. Vayenas, S. Bebelis and S. Ladas, Nature (London) 343 (1990) 625.
- 2 C.G. Vayenas, S. Bebelis and S. Neophytides, J. Phys. Chem. 92 (1988) 5083.

- 3 I.V. Yentekakis and C.G. Vayenas, *J. Catalysis* 111 (1988) 170.
- 4 S. Bebelis and C.G. Vayenas, *J. Catal.* 118 (1989) 125.
- 5 C.G. Vayenas, S. Ladas, S. Bebelis, I.V. Yentekakis, S. Neophytides, Y. Jiang, C. Karavassilis, C. Pliangos, *Electrochimica Acta* 39(11/12) (1994) 1849
- 6 C.G. Vayenas, S. Bebelis, I.V. Yentekakis and H.-G. Lintz, *Catalysis Today* 11(3) (1992) 303-442.
- 7 I.V. Yentekakis and C.G. Vayenas, *J. Catal.* 149, (1994) 238.
- 8 S. Neophytides, D. Tsiplakides, P. Stonehart, M.M. Jaksic and C.G. Vayenas, *Nature* 370 (1994) 45.
- 9 Despic, A.R., Drazic, D.M., Mihailovic, M.L. Lorenz, L., Adzic, R. and Ivic, M., *J. Electroanal. Chem.* 100 (1979) 913.
- 10 I.V. Yentekakis, G. Moggridge, C.G. Vayenas and R.M. Lambert, *J. Catal.* 146 (1994) 292
- 11 C.G. Vayenas, S. Bebelis and M. Despotopoulou, *J. Catal.* 128 (1991) 415 .
- 12 S. Ladas, S. Bebelis and C.G. Vayenas, *Surf. Science* 251/252 (1991) 1062.
- 13 T. Arakawa, A. Saito and J. Shiokawa, *Chem. Phys. Lett.* 94 (1983) 250.
- 14 S. Ladas, S. Kennou, S. Bebelis and C.G. Vayenas, *J. Phys. Chem.* 97 (1993) 8845.
- 15 L. Basini, C. Cavalca, G. Larsen and G.L. Haller, *J. Phys. Chem.* 98 (1994) 10853.
- 16 J.O' M. Bockris and Z.S. Minevski, *Electrochimica Acta* 39(11/12) (1994) 1471.

**Reactivity Patterns Among Substituted Pentacyanoiron(II) Compounds in Aqueous Solution**

John M. Malin

*International Activities, American Chemical Society**1155 16th St., NW, Washington, DC 20036 USA*

Studies of the properties of aqueous pentacyanoiron(II) complexes of 4-methylpyridine, pyridine, isonicotinamide, pyrazine and the N-methylpyrazinium ion are presented. Each complex has a strong absorption band in the visible region which is assigned to a metal-to-ligand charge-transfer (MLCT) electronic transition. The complexes can be reversibly protonated at a cyanide with measured  $pK_a$  values which vary according to the identity of the ligand. The kinetics of exchange of the heterocyclic ligand yield clear evidence for a limiting  $S_N1$  substitution mechanism. Rates of dissociation vary in the range  $11.5 \times 10^{-4} \text{ sec}^{-1}$  to  $2.8 \times 10^{-4} \text{ sec}^{-1}$  (25 °C, 1.0 M ionic strength) in the order of ligands specified above. Rates of association starting with the free ligand and the pentacyano-(aqua)iron(II) complex are first-order in the complex and also the ligand concentration, with the rate constant of formation varying from  $3.6 \times 10^2$  to  $5.5 \times 10^2 \text{ M}^{-1} \text{ sec}^{-1}$ . The calculated oscillator strengths of the MLCT bands and the measured Fe(III)/Fe(II) redox couples for the complexes have been determined. Spectra, and the thermodynamic and kinetics data are interpreted in terms of  $d\pi$ - $\pi$  backbonding from the pentacyanoiron(II) moiety to the aromatic ligand.

Since the dissociation rates are governed by relative metal-ligand bond strength, the backbonding hypothesis has been tested by studying dissociation of two pentacyanoiron(II) complexes of ligands incapable of backbonding, i.e., ammine and methylamine. For pentacyano(ammine)iron(II) and pentacyano-(methylamine)iron(II) the specific rates of dissociation are  $1.75 \times 10^{-2} \text{ sec}^{-1}$  and  $2.8 \times 10^{-3} \text{ sec}^{-1}$ , respectively. Comparison with the rates of dissociation for the complexes of 4-methylpyridine, pyridine, isonicotinamide and pyrazine, respectively allows one to estimate backbonding stabilization energies of 4.1, 4.7, 6.3 and 8.9 kcal/mol, respectively, for the complexes of those ligands.

The complex ion pentacyano(dimethylsulfoxide)iron(II) has been prepared in aqueous solution and its sodium salt isolated. Infrared and NMR measurements indicate that the dimethylsulfoxide (DMSO) ligand is coordinated to iron(II) through the sulfur atom. The kinetics of formation of the complex in aqueous solution are first order in each of the reactants, DMSO and pentacyano(aqua)iron(II), with a specific rate of  $2.4 \times 10^2 \text{ M}^{-1} \text{ sec}^{-1}$ . An investigation of the kinetics of exchange of coordinated dimethyl sulfoxide for N-methylpyrazinium yields rate saturation, typical of a limiting dissociative exchange mechanism, with a specific rate of  $7.5 \times 10^{-5} \text{ sec}^{-1}$ . The results are interpreted as signifying a substantial  $\pi$ -bonding interaction between the pentacyanoiron(II) moiety and the sulfur atom of dimethylsulfoxide.

It has been possible to study intramolecular thermal and light-induced electron transfer between iron(II) and cobalt(III) through use of these complexes. The first-order, specific rates of reduction of Co(III) in complexes of the type  $[(\text{NH}_3)_{(4 \text{ or } 5)}\text{CoLFe}(\text{CN})_5]$  with L as chelating 2-carboxylatopyrazine, pyrazine and 2-methylpyrazine are  $1.3 \times 10^{-2}$ ,  $5.5 \times 10^{-2}$ , and  $30 \times 10^{-2} \text{ sec}^{-1}$ , respectively. Photoinduced electron transfer occurs upon irradiation of the iron(II)-to-heterocycle MLCT bands near 620 nm. Within experimental error, the quantum yield is unity for the first two species. The complexes are formed by aqueous reaction of pentacyano(aqua)iron(II) with the appropriate cobalt(III) ammine incorporating the bridging ligand. Kinetics of formation are first-order in each of the two reactants with specific rates of  $3.1 \times 10^3$ ,  $7.0 \times 10^3$  and  $3.7 \times 10^3 \text{ M}^{-1} \text{ sec}^{-1}$ , respectively.

The influence of the pentacyanoiron(II) substituent on the ligand hydration equilibrium in the complex pentacyano(4-formylpyridine)iron(II) has been studied spectrophotometrically by following the shifts with temperature of the MLCT bands in the visible-UV region. In the complex, the hydration constant, 0.48, measured at 37 °C is lower than that reported for 4-formylpyridine, yet higher than that for the pentaammine(4-formylpyridine)ruthenium(II) species. The phenomenon is attributed to moderate backbonding stabilization of the aldehyde relative to the hydrated form of the ligand.

The kinetics of oxidation of ferrocyanide by a series of substituted pentacyano(pyridine)iron(III) complexes have been studied in aqueous solution. Second-order rate constants for the complexes of pyridine, 4-methylpyridine, isonicotinamide, 4-phenylpyridine and 4-tert-butylpyridine are, respectively,  $6 \times 10^7$ ,  $1.7 \times 10^7$ ,  $5.7 \times 10^7$ ,  $8.2 \times 10^7$  and  $2.8 \times 10^7 \text{ M}^{-1} \text{ sec}^{-1}$ . The rates of reaction of the same series of reactants with aqueous ferrocyanide ion are, respectively,  $1.7 \times 10^5$ ,  $5.5 \times 10^4$ ,  $2.8 \times 10^5$ ,  $5.5 \times 10^4$  and  $1.9 \times 10^4 \text{ M}^{-1} \text{ sec}^{-1}$ . Using the Marcus theory, the rate constant for self-exchange in pentacyano(pyridine)iron(II)/(III) is calculated to be  $2.4 \times 10^6 \text{ M}^{-1} \text{ sec}^{-1}$  at 25 °C. The results are interpreted in terms of the steric and hydrophobic influences of the 4-pyridine substituents on the stability of electron transfer precursor complexes.

## Photocatalysis and Global Chemistry of Atmosphere

V.N.Parmon, K.I.Zamaraev

Boreskov Institute of Catalysis, 630090, Novosibirsk, Russia.

Direct photochemical reactions in the stratosphere induced by far ultraviolet solar light are very important for the chemistry of the atmosphere. However, only a small portion of the solar energy flux is in this spectral region.

Nevertheless, according to our recent semiquantitative estimates [1,2] one can suggest that an impact on the Global Chemistry of the Earth Atmosphere of indirect heterogeneous photochemical (both photocatalytic and photosorption) reactions under the action of much more abundant visible, near ultraviolet and near infrared solar light may be also non-negligible. As photocatalysts and photoadsorbents may serve atmospheric aerosols, i.e. water droplets or ensembles of ultrasmall solid particles that sometimes are also embedded into liquid droplets. Reactions over them are expected to occur mainly in the troposphere.

Direct experimental studies on photocatalysis and photoadsorption over real atmospheric aerosols are just starting. Therefore, today the estimates of their expected role can be made only on the ground of numerous *in vitro* experimental studies of the reactions over certain model photocatalysts and photoadsorbents, and some known characteristics of the atmosphere as a sort of a global photocatalytic reactor.

The principal components of the atmosphere are nitrogen, oxygen, argon, carbon dioxide, and water. However, there are some other components which in spite of their low concentrations exert strong influence on the chemistry of the atmosphere. The Table shows the natural content (i.e. average stationary concentrations) of the principal trace components, their average residence time and rates of supply and removal from the atmosphere.

As most probable photocatalysts for atmospheric reactions may serve dust particles of soil that contain metal oxides or ions of transition metals captured by water aerosols. Reactions over such photocatalytically active particles may occur in all layers of the atmosphere, in contrast to the direct photochemical processes under the far ultraviolet radiation that occur only in the upper layer of the atmosphere.

Table

The average natural concentration C of main trace gases in the Earth atmosphere, their residence time  $\tau$  and rate of their removal (supply) R, and values  $\phi_{0.1}$  of the quantum yield at which the rate of photocatalytic removal (supply) of the same gases over natural aerosols containing  $Fe_2O_3$ ,  $TiO_2$  and  $ZnO$  would make 10% of their total removal (supply) rate R (according to refs. [1,2])

Gas	C		$\tau$	R/mol·l <sup>-1</sup> ·s <sup>-1</sup>	$\phi_{0.1}$		
	ppb	mol·l <sup>-1</sup> /(P=1 bar, T=273 K)			$Fe_2O_3$	$TiO_2$	ZnO
CO <sub>2</sub>	3.3·10 <sup>5</sup>	1.5·10 <sup>-5</sup>	4 years	1.2·10 <sup>-13</sup>	0.17	11	6.0·10 <sup>2</sup>
CO	100	4.5·10 <sup>-9</sup>	0.1 year	1.4·10 <sup>-15</sup>	2.0·10 <sup>-4</sup>	1.3·10 <sup>-2</sup>	0.7
CH <sub>4</sub>	1600	7.1·10 <sup>-8</sup>	3.6 years	6.3·10 <sup>-16</sup>	9.0·10 <sup>-5</sup>	5.7·10 <sup>-3</sup>	0.32
CH <sub>2</sub> O	0.1-1	4.5·10 <sup>-11-12</sup>	5-10 days	(1.0-20)·10 <sup>-17</sup>	(0.1-2.9)·10 <sup>-5</sup>	(0.9-18)·10 <sup>-4</sup>	(0.5-10)·10 <sup>-2</sup>
N <sub>2</sub> O	0.3	1.3·10 <sup>-11</sup>	20-30 years	(1.4-2.0)·10 <sup>-20</sup>	(2.0-2.9)·10 <sup>-9</sup>	(1.3-1.8)·10 <sup>-7</sup>	(0.7-10)·10 <sup>-5</sup>
NO	0.1	4.5·10 <sup>-12</sup>	4 days	1.3·10 <sup>-17</sup>	1.9·10 <sup>-6</sup>	1.2·10 <sup>-4</sup>	6.5·10 <sup>-3</sup>
NO <sub>2</sub>	0.3	1.3·10 <sup>-11</sup>	4 days	3.9·10 <sup>-17</sup>	5.7·10 <sup>-6</sup>	3.6·10 <sup>-4</sup>	2.0·10 <sup>-2</sup>
NH <sub>3</sub>	1	4.5·10 <sup>-11</sup>	2 days	2.6·10 <sup>-16</sup>	3.7·10 <sup>-5</sup>	2.4·10 <sup>-3</sup>	0.13
SO <sub>2</sub>	0.01-0.1	4.5·10 <sup>-12-13</sup>	3-7 days	(0.7-17)·10 <sup>-18</sup>	(1-24)·10 <sup>-7</sup>	(0.6-16)·10 <sup>-5</sup>	(0.4-8.5)·10 <sup>-3</sup>
H <sub>2</sub> S	0.05	2.2·10 <sup>-12</sup>	1 day	2.6·10 <sup>-17</sup>	3.7·10 <sup>-6</sup>	2.4·10 <sup>-4</sup>	1.3·10 <sup>-2</sup>
CS <sub>2</sub>	0.02	8.9·10 <sup>-13</sup>	40 days	2.6·10 <sup>-19</sup>	3.7·10 <sup>-8</sup>	2.4·10 <sup>-6</sup>	1.3·10 <sup>-4</sup>
COS	0.5	2.2·10 <sup>-11</sup>	1 year	7.0·10 <sup>-19</sup>	1.0·10 <sup>-7</sup>	6.5·10 <sup>-6</sup>	3.5·10 <sup>-4</sup>
(CH <sub>3</sub> ) <sub>2</sub> S	0.001	4.5·10 <sup>-14</sup>	1 day	5.2·10 <sup>-19</sup>	7.4·10 <sup>-8</sup>	4.8·10 <sup>-6</sup>	2.6·10 <sup>-4</sup>
H <sub>2</sub>	550	2.5·10 <sup>-8</sup>	6-8 years	(9.9-13)·10 <sup>-17</sup>	(1.4-1.9)·10 <sup>-5</sup>	(9.2-12)·10 <sup>-4</sup>	(4.9-6.5)·10 <sup>-2</sup>
H <sub>2</sub> O <sub>2</sub>	0.1-10	4.5·10 <sup>-10-12</sup>	1 day	(0.5-52)·10 <sup>-16</sup>	(0.7-7.4)·10 <sup>-5</sup>	(0.5-48)·10 <sup>-3</sup>	(0.3-26)·10 <sup>-1</sup>
CH <sub>3</sub> Cl	0.7	3.1·10 <sup>-11</sup>	3 years	3.3·10 <sup>-19</sup>	4.7·10 <sup>-8</sup>	3.0·10 <sup>-6</sup>	1.7·10 <sup>-4</sup>
HCl	0.001	4.5·10 <sup>-14</sup>	4 days	1.3·10 <sup>-19</sup>	1.9·10 <sup>-8</sup>	1.2·10 <sup>-6</sup>	6.5·10 <sup>-5</sup>

The most important solid materials, that present in the atmosphere and have photocatalytic properties, are transition metal oxides. Many of them are semiconductors, and some of them absorb visible and near infrared light. The most abundant in natural continental aerosols are semiconductor oxides  $\text{Fe}_2\text{O}_3$ ,  $\text{TiO}_2$  and  $\text{ZnO}$ .

In order to estimate quantitatively a possible influence of heterogeneous photocatalytic processes on the composition of the atmosphere, one can compare the rates of the expected light-generated reactions of various atmospheric components over aerosol photocatalysts with the rates of the actual removal of these components from (or supply into) the atmosphere (see the Table). Immediate calculation of such rates needs a knowledge of both fluxes of solar light quanta absorbed by particular photocatalytically active components of aerosols (e.g., at their background concentrations) and the expected quantum yields  $\phi$  of the processes under consideration.

There are no problems to estimate typical value of the above fluxes for the main expected constituents of solid aerosols [1,2]. However, unfortunately, at present it is impossible to forecast *a priori*  $\phi$  of photocatalytic reactions over solid surfaces.

For this reason, for estimation of the role of photocatalysis in the global chemistry of the atmosphere, the following way was chosen [1,2]. It was estimated, how big must be  $\phi$  to provide removal or supply of a noticeable part (for example, 10%) of an atmospheric component via a photocatalytic route. This evaluation of  $\phi$  was based on the removal (supply) rates of the Table and has shown at which values of such "critical" quantum yield  $\phi_{0.1}$  the photocatalytic formation or decomposition of a particular compound should become important for composition of the atmosphere. Then these estimates were compared with the values of  $\phi$  that are actually known for photocatalytic formation or decomposition of some compounds. From this comparison one can draw conclusions, whether the known values of  $\phi$  are high enough for particular photocatalytic processes to be expected important for the global chemistry of the atmosphere.

*Reactions of the Main Atmospheric Components.* The following reactions belong to this group : formation of ammonia and hydrazine from molecular nitrogen and water; oxidation of molecular nitrogen with water or oxygen to

nitrogen oxides; decomposition of water into hydrogen and oxygen; oxidation of water by oxygen into hydrogen peroxide; formation of organic compounds from  $\text{CO}_2$  and  $\text{H}_2\text{O}$ . All these reactions are well known from laboratory-scale studies.

*Reactions of Trace Components of the Atmosphere.* The most important should be the following photocatalytic reactions: complete oxidation of hydrocarbons and halogenated hydrocarbons, as well as of oxygen-containing volatile organic compounds, for example, alcohols, aldehydes, carbonic acids, phenols, etc. Such reactions may be also decomposition of  $\text{H}_2\text{S}$  and  $\text{NO}_x$  into elements, oxidation of  $\text{SO}_2$  with oxygen, reactions of partial oxidation of organic substances. All these reactions are also well-known from photocatalytic research. One should take into account, however, that some new harmful compounds can be generated in the latter case.

Note, that the published values on the mentioned reactions exceed quite substantially the "critical" values  $\phi_{0,1}$  for many of the photocatalytic reactions on, e.g.,  $\text{TiO}_2$  (see Table). This may be regarded as an evidence for, rather than against the importance of photocatalysis for the global chemistry of the atmosphere.

In addition to semiconductor oxides, dielectric compounds may also contribute to photocatalysis and photoadsorption in both troposphere and stratosphere. A most important contribution to cleaning the atmosphere from the ozone layer depleting halogenated hydrocarbons may be expected from MgO- and CaO-containing aerosols that are present in large amount in volcanic clouds as well as soil, fire or industrial aerosols. Indeed, MgO was found recently to be an efficient photoadsorbent of  $\text{CH}_2\text{FCF}_3$  (i.e. freon 134a), performing most probably photogenerated stoichiometric substitution of the oxide oxygen anions for halogen anions with quantum yield of several percent even under visible or mild UV light [3].

A contribution of the UV-induced photocatalysis by the cations of such transition metals as iron, copper, manganese, etc. dissolved in water droplets or in a water layer that may cover a solid aerosol, is also expected. UV is able also to generate on solid surfaces new states of transition metal ions that can serve as active sites for thermal catalytic reactions even as very mild conditions of the atmosphere. A typical example here is generation of long-

lived low valence states of vanadium and copper on the surface of  $\text{SiO}_2$ . These states catalyze thermal oxidation of alkenes even at room temperatures.

The summary on the above analysis allows to suggest that both photocatalytic and photoadsorption reactions on aerosol particles can play an essential role in the global chemistry of the atmosphere. In contrast to the noncatalytic photochemistry which takes place mostly in the stratosphere and mesosphere under the action of far UV-light, the photocatalytic (and photoadsorption) chemistry should take place mainly in the troposphere under near UV, visible and even near IR light, though its contribution to the chemistry of the stratosphere and mesosphere, perhaps, should not be neglected as well.

So, one can suggest that in fact the dust may clean photocatalytically the atmosphere from harmful compounds, as well as affect the intensity of acid rains, concentration of "greenhouse" and "ozone-depleting" gases. *Thus, large desert areas which are the main generator of the continental dust, perhaps, play the role of the "kidneys" of the planet.*

Atmospheric components on atmospheric aerosols containing  $\text{Fe}_2\text{O}_3$ ,  $\text{TiO}_2$  and  $\text{ZnO}$ , as well as  $\text{MgO}$  and, perhaps,  $\text{CaO}$  are the most plausible candidates for the role of photocatalysts and photoadsorbents due to their appropriate photochemical properties and rather high concentration in the troposphere.

#### REFERENCES

1. K.I. Zamaraev, M.I. Khramov and V.N. Parmon, *Catal.Rev.-Sci.Eng.*, **36**, 17-644 (1994).
2. V.N. Parmon and K.I. Zamaraev, in G.Ertl, H.Knezingner and J.Weitkamp (Eds.), *Handbook of heterogeneous catalysis*. VCH, Weinheim (1995) (in press).
3. V.S.Zakharenko, V.N.Parmon and K.I.Zamaraev., *Kinet.Katal.*, (1995) (to be published).

**ORAL PRESENTATION**

**SECTION CATALYSIS**

## **Different Types of Oscillatory Behaviour in Heterogeneous Catalytic Systems**

**M.M.Slin'ko**

**Institute of Chemical Physics, Moscow 117334, Russia**

There are many observations of self-sustained oscillations in heterogeneous catalytic systems. This phenomenon may be observed in various reactions on different classes of catalysts including massive and supported metallic catalysts, oxides and zeolites. Self-sustained reaction rate oscillations may be isothermal and the amplitude of catalyst temperature variation may be as large as 100-200 C. The frequency of self-sustained oscillations may vary from seconds to some hours. The large variations in properties of reaction rate oscillations indicate, that different types of oscillatory behaviour may exist in heterogeneous catalytic systems.

The present paper analyses different types of oscillations due to the various causes of their origin. It is demonstrated, that different types of oscillations arise on different levels of heterogeneous catalytic system. The properties of different types of oscillations are defined by various processes. This fact helps greatly in the discriminating of different types of oscillatory behaviour. The procedure of the experimental recognition of different types of oscillations observed experimentally is developed.

The most interesting are kinetic oscillations, which arise due to the peculiarities of the reaction mechanism. They originate on the first level of heterogeneous catalytic system- an element of the single crystal plane. The observation of global kinetic oscillations on the reactor level demands the complete synchronization between the local oscillators on each sublevel of heterogeneous catalytic system. Different mechanisms of synchronization of local oscillators on various levels of heterogeneous catalytic system are analysed.

## THEORY OF COMPLEX KINETIC BEHAVIOUR OF CATALYTIC REACTIONS

Gregory S.Yablonskii, A.V. Myshlyavtsev\*

*Kiev Polytechnic Institute, Kiev, Ukraine*  
*\*Tuvinnian Complex Institute, SB RAS, Kyzyl, Tuva, Russia*

New approaches to the theory of complex kinetic behaviour of catalytic reactions are developed. They take into account both detailed mechanisms and surface phase transitions. Different important cases are analyzed:

### 1. "Pure kinetic" phase transitions. Complex catalytic mechanisms (ideal isothermal case)

The main theoretical result is the close correspondence between complex kinetic behaviour (multiplicity of steady states, self-oscillations, discontinuities, etc.) that is observed in a lot of catalytic oxidation systems and the type of the detailed mechanism of catalytic reaction. It is proved that the necessary condition for the kinetic critical phenomena is the presence of steps of interaction between different adspecies [1].

This statement was proven mathematically rigorously for any kinetic model of catalytic reactions, under the surface action law.

The well-known Langmuir-Hinshelwood (L.-H.) mechanism is the simplest one with multiplicity of steady states. This general result for explanation of critical phenomena in different catalytic systems (multiplicity of steady states in CO-oxidation's over Pt and discontinuities of steady-state rate in H<sub>2</sub>-oxidation over Pt and Ir at high vacuum conditions, multiplicity and self-oscillations in CO-oxidation over supported Pt at normal conditions, etc.) was applied [2].

A new conception of chemical kinetics, the kinetic polynomial (k.p.) is worked out. This result was obtained by means of modern algebraic methods and computer analytic methods. The structure of the k.p. does not depend on the detailed mechanism of complex catalytic reaction. In fact, the k.p. can be defined as an equation of the state of an open chemical system relating the reaction rate to the parameters of the processes (temperature and composition of the reaction mixture).

For the L.-H. mechanism by the help of k.p. some interesting phenomena were described:

- 'critical simplifying'
- 'thermodynamics of the hysteresis'
- simple algebraic correlation's between bifurcation reaction rates

## 2. The phase transition in the adsorbed layer.

The lattice-gas model (LGM) with the help of different statistical physics methods, first of all transfer-matrix method (TMM) was analyzed (Myshlyavtsev, Yablonskii)

TMM as a key method for the deterministic modeling of non-ideal adsorbed layer is chosen. As result the complicated dependencies of rate coefficients (adsorption, desorption, diffusion, reaction) on surface coverage namely non-monotonous dependencies of activation energy and pre-exponential factor as well as the peculiarities of the thermodesorption spectra for some well-known model surface systems with surface reconstruction H/W (100), CO/Pt (100), CO/Pt (111), CO/Ni (100) were obtained.

## 3. L.-H. mechanism + Surface reconstruction.

The modified L.-H. mechanism namely mechanism with surface reconstruction (second order phase transition) is the simplest mechanism for catalytic self-organization [3].

Monte-Carlo modelling allows one to find different spatio-temporal structures including those of non-diffusion and non-lateral origin.

There were found different regions of the oscillations particularly the region where the oscillations are governed by the formation of a steady compact cluster which controls the frequency and amplitude.

## 4. Temkin-Boudart mechanism + 'lateral phase transition' (Myshlyavtsev, Yablonskii)

The close correspondence between complicated dynamics in open catalytic system and phase coexistence system on the phase diagram of the adsorbed layer is shown.

It is interesting that critical kinetic behavior may occur in the wide region of the parameters even in the absence of phase transition which is governed by the lateral interaction of the adspecies and even for linear Temkin-Boudart mechanism. The reasons of that are some peculiarities of chemical potential of adspecies.

## 5. New model of the surface catalyst reconstruction (Shechtman, Yablonskii)

New model of the surface reconstruction is developed. This model ('modified Frenkel-Kontorova model') takes into account both lateral interaction between adspecies and interaction of adspecies with skeleton of crystal.

The classification of possible situations of surface reconstruction is obtained.

Literature

1. Yablonskii, V.I. Bykov, A.N. Gorban', V.I. Elochin, Kinetic models of catalytic reactions, in *Comprehensive Chemical Kinetics*, v32. Edited by R.G. Compton, Elsevier, Amsterdam-Oxford-New-York-Tokio, 392p. (1991)
2. G.S. Yablonskii, V.I. Elochin, Kinetic models of heterogeneous catalysis, in *Perspective in catalysis*, ed. by J.A. Thomas and K.I. Zamaraev, Blackwell Sci Publication, p.191-249 (1992)
3. L.V. Lutsevich, V.I. Elochin, S.V. Ragozinskii, G.S. Yablonskii, Trigger Mechanism of self-oscillations and Effect of Molecyle Self-organization in the Course of Monte-Carlo Modelling of a Bimolecular Catalytic Reaction, *J. of Catalysis*, 142, 198-205 (1993).

## MULTI - CENTER CATALYSIS - THE WAY TO GOVERN CATALYTIC ACTIVITY

V.I.Savchenko, E.A.Ivanov, S.I.Fadeev\*, N.I.Efremova, A.V.Kalinkin,

A.N.Salanov, A.V.Pashis, S.N.Pavlova, V.A.Sadykov

Institute of Catalysis and \*Institute of Mathematics, Siberian Branch, Russian Academy of Sciences, 630090, Novosibirsk, Russia

The surface of real catalysts is heterogeneous by its structure (different metal faces) and chemical composition (metal on catalyst support, oxide mixture, etc.). One can assume that various reaction stages proceed on different surface patches (phases) with different rates and kinetic conjugation of the stages occurs via surface diffusion (spillover) of intermediate adsorbed particles. The problem is what effects in reaction kinetics can appear with surface patches conjugation via spillover and what properties various phases must possess for new active catalysts designing.

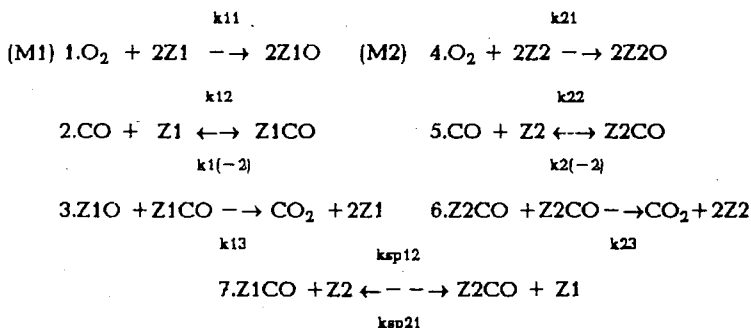
Present paper concerns a role of adparticles migration between various surface patches 1) in general form for the Eley-Rideal (impact mechanism) and the Langmuir - Hinshelwood (adsorption mechanism) for CO oxidation.

The key concept of heterogeneous catalysis of Balandin, Boreskov on the decisive role of binding energy of reacting molecules and a catalyst and on a vulkano-like reaction rate dependence is based on the idea of "one-center" catalysis, i.e. adsorption and interaction are assumed to proceed on the same center. We have considered a possible role of diffusion on the discrete heterophase surface of the main reactant, for which adsorption  $A_2 \rightarrow 2A_{ads}$  (I) or interaction  $A_{ads} + B_{gas} \rightarrow P_{gas}$  (II) are the limiting stages. The kinetic reaction conjugation between the surface patches  $M_1$  and  $M_2$  with adsorption heats  $q_{opt} - \Delta q$  and  $q_{opt} + \Delta q$  via  $A_{ads}$  spillover can increase or decrease the reaction rate comparing with that on isolated patches. Rate increase at  $\alpha_1 > \alpha_2$  ( $\alpha_1, \alpha_2$  are the constants in Brenstead - Polany equation for the I and II reaction stages) occurs due to  $A_{ads}$  overflow

OP-3

from the patches with higher ( $M_2$ ) to those with lower binding energy ( $M_1$ ) and higher adparticles reactivity. When  $\alpha_1 < \alpha_2$ ,  $A_{ads}$  spillover slightly decreases the reaction rate.

For the adsorption (LH) mechanism the competing  $A_{ads}$  and  $B_{ads}$  adsorption takes place. For CO oxidation over platinum metals at the insufficient change of adsorption parameters  $s(O_2)$ ,  $s(CO)$  the surface may be covered either with  $O_{ads}$  or  $CO_{ads}$ . Let us assume the reaction to proceed over  $M_1$  and  $M_2$  patches with different parameters via simple 3-stage mechanisms (Scheme I):



For Scheme I a bifurcation analysis of solutions was carried out and the domains of multiplicity (with 1, 3 or 5 steady states) were found. Also the isolated domains of reaction proceeding (i.e. isols) were revealed. For  $M_1$  and  $M_2$  patches with close properties  $CO_{ads}$  spillover "switch-on" leads to smoothing over kinetic dependences and hysteresis disappearance.

It is of great interest to study the situation when the patches  $M_1$  and  $M_2$  sharply differ by their kinetic parameters of oxygen and CO adsorption. In calculations for  $M_1$  patches the reaction parameters typical for Pt were chosen:  $s_1(O_2)=0.3$ ,  $s_1(CO)=1.0$ ,  $E_{1(-2)}=125$  kJ/mol. For  $M_2$  patches:  $s_2(O_2)=0.5$ ,  $s_2(CO)=0.1$ . At 300–400K the isolated  $M_1$  and  $M_2$  patches are covered with  $CO_{ads}$  and  $O_{ads}$ , respectively, but the reaction proceeds only on  $M_1$  (Pt) patches at  $T > 475$ K. When spillover switches on,  $CO_{ads}$  migrates from  $M_1$  to  $M_2$  patches where the reaction starts to proceed at

325K already. At  $T \sim 340\text{K}$  the reaction occurs also on  $M_1$  (Pt) patches. In our previous works the  $M_1$  portion on the surface at various  $P(\text{CO})/P(\text{O}_2)$  ratio in the reaction mixture was calculated.

Calculations via the Monte Carlo method for the lattice (100 x 100) consisting of alternating  $M_1$  and  $M_2$  bands 10 atomic rows wide showed that in the absence of  $\text{CO}_{\text{ads}}$  spillover the reaction rate on  $M_1$  and  $M_2$  is low and the reaction proceeds only at the  $M_1/M_2$  interface. As the rate of  $\text{CO}_{\text{ads}}$  spillover from  $M_1$  to  $M_2$  and back increases, the reaction occurs both on  $M_1$  and  $M_2$  patches at low temperature. When the spillover rate increases,  $\text{O}_{\text{ads}}$  exists as separate islands in the middle of  $M_2$  bonds. The rate dependences on  $P(\text{CO})/P_{\text{sum}}$  obtained via the Monte Carlo method are close to data of the ODE and homotopic methods.

One can assume that the kinetic conjugation of various patches via Scheme I opens the real way for designing a catalyst for low-temperature CO oxidation. As  $M_1$  one can use Pt, Pd and as  $M_2$  - Rh or other metal (or oxide) for which  $s(\text{O}_2) > s(\text{CO})$ . The system noble metal/ reduced oxide (NMRO) seems to be the most promising one for designing catalysts of low-temperature CO oxidation.

Physical modelling and study of heterophase systems was carried out via Pt spraying on  $\text{MO}_x$  support directly in XPS- spectrometer and Scan/ Auger cameras. For heterophase systems  $\text{CuO}_x/\text{Pt}$  and  $\text{NiO}_x/\text{Pd}$  CO oxidation proceeds with high rate at 300-400K already. Catalytic activity of  $\text{Pd}/\text{Al}_2\text{O}_3$ ,  $\alpha\text{-Fe}_2\text{O}_3$ ,  $\text{Pd}/\text{Fe}_2\text{O}_3$  was estimated at  $\text{CO}/\text{O}_2 = 2/1$  by the pulse/ flow method in the reactor with vibroliquefied layer. Activity of  $\alpha\text{-Fe}_2\text{O}_3$  is low only at  $T > 550\text{K}$ . For  $\text{Pd}/\text{Al}_2\text{O}_3$  the process rate increases due to CO desorption from the Pd surface at  $T > 450\text{K}$ . For  $\text{Pd}/\alpha\text{-Fe}_2\text{O}_3$  the catalytic activity is high at 300-400K already, i.e. a synergistic effect takes place.

#### ACKNOWLEDGEMENT

This work is supported by Russian Foundation for Basic Research grant No. 93-03-5098, and ISF. grant RPW 300.

## CATALYTIC DIMERISATION OF FUNCTIONALIZED ALKENES

M.C. Bonnet\*, L. Carmona\*\*, B. Chaudret\*, I. Guibert\*\*\*, D. Neibecker\*\*,  
X.D. He\*\* and I. Tkatchenko\*

\**Institut de Recherches sur la Catalyse, CNRS, 2 avenue Albert Einstein F-69626  
Villeurbanne Cedex (France)*

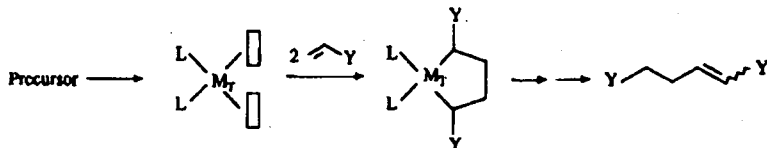
\*\**Laboratoire de Chimie de Coordination, CNRS, 205, route de Narbonne  
F-31077 Toulouse Cedex (France)*

\*\*\* *Present address: CRIT-C, Rhône-Poulenc Industrialisation, BP= 62, F-696129  
Saint Fons Cedex (France)*

The catalytic dimerisation of functionalized alkene could be considered as an alternative route to the production of difunctionalized compounds like adipic acid, hexamethylene diamine or  $\epsilon$ -caprolactame, provided that a high regioselectivity for the tail-to-tail coupling is achieved.

The selective dimerisation of methyl acrylate catalysed by palladium<sup>1</sup> and, more recently, rhodium complexes<sup>2</sup> has been reported. A rationale of the reaction mechanism has been published in the case of rhodium, which corresponds to the classical insertion -  $\beta$ -hydrogen elimination route<sup>3</sup>. The selective dimerisation of acrylonitrile has been reported in the case of ruthenium compounds, under a pressure of hydrogen, with the side production of propionitrile<sup>4</sup>. No evidence for the reaction mechanism has been proposed.

We have considered the possibility of having an oxidative coupling of two molecules of alkene instead of the sequential hydride route, i.e:



This route will require i) two vacant sites in cis-position on the metal centre which are necessary for this elementary process and ii) the tail-to-tail coupling of the alkene units which may be facilitated by the electron-withdrawing character of the substituents Y. Indeed:

-sequential deprotonation/stabilisation of  $\text{Pd}(\text{acac})_2$  with appropriate ligands (phosphines, solvents) provides effective dicationic palladium(II) catalysts which could be optimised by the addition of a protic source ( $\text{HBF}_4 \cdot \text{OEt}_2$ )<sup>5</sup>,

-ruthenium(II) complexes containing  $\eta^2$ -methyl acrylate (ma) or acrylonitrile (acn) ligands, respectively  $[\text{Cp}^*\text{Ru}(\text{ma})\text{Cl}]_2$  or  $[\text{Cp}^*\text{Ru}(\text{acn})\text{Cl}]_3$ , are selective catalysts (in the absence of hydrogen) for the preparation of 1,4-dicyanobutenes<sup>6</sup>.

We will discuss the chemistry associated with these two groups of complexes and catalysts and propose possible catalytic cycles. Catalyst deactivation processes will be also discussed.

1. Oehme G. and Pracejus H, *J. Organometal. Chem.*, 1987, 320, C56 and references therein.
2. Brookhart M, and Sabo-Etienne S, *J. Am. Chem. Soc.*, 1991, 113, 2777.
3. Brookhart M, and Hauptmann E, *J. Am. Chem. Soc.*, 1992, 114, 4434.
4. Rhone-Poulenc, French Pat. 1 472 033 (03.18.1965); *Chem. Abs.* 1967, 66, 85483.
5. Guibert I, Neibecker D, and Tkatchenko I, *J.C.S. Chem. Comm.*, 1989, 1850; Guibert I, Neibecker D, and Tkatchenko I, *Bull. Soc. Chim. France*, in press.
6. Bonnet M.C, Carmona L, Chaudret B, He X.D, Tkatchenko I, *Angew Chem.*, submitted.

## A mechanistic study of the methane reforming reaction with carbon dioxide over Ni/SiO<sub>2</sub> catalyst

*E.C.H. Kroll, H.M. Swaan, S. Lacombe, and C. Mirodatos*  
*Institut de Recherches sur la Catalyse*  
*2, Avenue A. Einstein, F-69626 Villeurbanne Cedex, France*

### ABSTRACT

The mechanism of the carbon dioxide reforming of methane has been investigated over a nickel-on-silica catalyst. Non steady-state and steady-state isotopic transient experiments combined with *in situ* DRIFT spectroscopy investigations were used to quantify the amount of the various adspecies present on the working catalyst surface.

It was found that as soon as contacted with the reacting mixture, the nickel particles are coated with several layers of carbide-like Ni<sub>3</sub>C. These deposits are both formed out from the irreversible initial adsorption of methane and carbon dioxide. Under reaction conditions, a permanent pool of carbide species is continuously fed by methane irreversible activation, while carbon dioxide dissociates reversibly into gaseous CO and adsorbed oxygen atoms on the Ni surface. Adsorption/desorption equilibria ensure a fast inter conversion between gaseous CO<sub>2</sub> and CO, as attested by their isotopic scrambling. A similar adsorption/desorption equilibrium is proposed for H<sub>2</sub>O, the combination of which with the reversible activation of CO<sub>2</sub> and CO leads to the achieved water-gas-shift equilibrium.

Besides the rapid steps which constitute the catalytic cycle, slow side reactions involving the migration of the carbide-like species through the nickel particle and their transformation into structured coke or graphite growing as hollow whiskers are proposed to account for the ageing phenomena.

An active sites configuration is tentatively proposed on the basis of the main mechanistic statements.

## Structure and Reactivity of Well-Defined Pt-Cu Alloy Particles Hosted in Zeolites

E.S.Shpiro\*, O.P.Tkachenko\*, N.I.Jaeger\*\*\*, R.W.Joyner\*\*  
and G.Schulz-Ekloff\*\*\*

\* *Zelinsky Institute of Organic Chemistry, Moscow 117913, Russia.*

E-mail: es@ioc.ac.ru

\*\* *Catalyst Research Laboratory, Nottingham Trent University, Nottingham, UK*

\*\*\* *Institut für Angewandte und Physikalische Chemie, Bremen Universität, Bremen, Germany*

The elucidation of local surface structure of supported alloy particles is very essential for understanding the structure-function relationship in catalysis e.g. by alloys.

This work is addressed to the study of the local surface arrangements of Pt-Cu alloys prepared in the zeolite cages by a number of techniques: XPS X-AES, FTIR of CO chemisorbed, EXAFS, XANES and HRTEM. Pt-Cu loaded ZSM-5 materials have a considerable importance for hydrocracking and novel reaction of  $\text{NO}_x$  abatement in excess oxygen.

Pt-Cu/ZSM-5 samples with Cu/Pt ratios 6:1, 2:1 and 1:1 have been studied at progressively increased reduction temperatures (473, 493, 523, 623 and 753 K), after reoxidation and rereduction, and after the reactions with oxygen and NO.

In accordance with previous data [1], Cu Auger parameter suggests the location of  $\text{Cu}^{2+}$  and  $\text{Cu}^{1+}$  cations in the Pt-Cu calcined samples and  $\text{Cu}^0$  containing clusters in mildly reduced catalysts (473-493 K) within zeolite structure. Small  $\text{Cu}^0$  clusters which are likely to be bounded to Pt show very anomalous polarization properties resembling those of  $\text{Cu}^+$  ionic species while at higher temperatures Cu Auger parameter of the reduced copper is very close to the bulk metal.

The formation of platinum-copper alloys at all reduction temperatures was confirmed by the analysis of Pt  $L_{2,3}$  and Cu K EXAFS, the average Cu/Pt ratio in alloy being varied in rather narrow range (from 2/1 to 1/1). Progressively larger coordination numbers  $N_{\text{Pt-Pt}} + N_{\text{Pt-Cu}}$  (Pt edge) and  $N_{\text{Cu-Cu}} + N_{\text{Cu-Pt}}$  (Cu edge) evaluated from EXAFS and taken together with HRTEM indicate the increase of particle size from 1 nm to ~3-5 nm upon the increase of reduction temperature and Cu concentration. Individual Cu particles were also identified in Cu-rich catalysts.

## OP-7

The variety of the structure data and very characteristic shifts of the Pt-CO stretching bands in FTIR spectra suggest a series of local surface structures for different Pt-Cu alloy in ZSM-5:

(a) for a Pt Cu ratio 1:1, uniform Pt-Cu alloy particles (1-3 nm) mostly located within zeolite matrix show dilution effect of Pt by Cu confirmed by a small dipole-dipole shift ( $8 \text{ cm}^{-1}$ ) and the normal "singleton" frequency for linear CO -Pt obtained in thermal desorption spectra ( $2055 \text{ cm}^{-1}$ ).

(b) Reoxidation of this sample at 523 K results in Cu oxidation to  $\text{Cu}^{2+}$  and fully separated Pt microcrystallites ( $\text{O}_2$ , 523 K). This is confirmed by the dramatic decrease of Cu-CO band and the identical behaviour of Pt-CO bands in Pt-Cu H-ZSM-5 and Pt-H-ZSM-5.

(c) Rereduction of the sample ( $\text{O}_2$ , 523K- $\text{H}_2$ , 623 K) leads to the restoration of the Pt-Cu alloy. A lower singleton frequency for CO observed in thermal desorption ( $2038 \text{ cm}^{-1}$ ) indicates that platinum can be electronically modified by copper.

(d) bigger Pt-Cu particles (>5-10 nm) clearly demonstrating an inductive effect of electron donation through the metal [2] which is manifested by the increase of Pt-linear CO frequency upon evacuation at 298 K due to CO desorption from Cu atoms (Cu:Pt=6:1,  $\text{H}_2$ , 523K). (e) In the case of a Cu:Pt ratio, 6 and reduction at 623 K a copper surface phase to be assumed decorated by platinum patches which occupy low coordination sites in the alloy particle. This can explain the anomalous downward shift of Pt-CO frequency to  $1988 \text{ cm}^{-1}$  and high intensity of bridge CO band. Platinum-copper interaction is confirmed by an inductive effect observed via CO desorption from the copper sites.

Easy alternations of Pt-Cu surface structures correlate with small heat of the formation of Pt-Cu alloy. Therefore Pt-Cu alloy particles are subject to reconstruction in a redox cycle and their performance will greatly depend upon reaction temperature and atmosphere. This has been demonstrated for CO thermal desorption and selective catalytic reduction of  $\text{NO}_x$ .

I.W.Grunert, N.W.Hayes, R.W.Joyner, E.S.Shapiro, M.R.H.Siddiqui, G.N.Baeva.  
J.Phys.Chem., 98 (1994) 10832

2. F.J.C.M. Toolenaar, F.Stoop, V.Ponec, J.Catal., 82 (1983) 1

Financial support of INTAS (94-1402) is gratefully acknowledged.

**ORAL PRESENTATION**

**SECTION KINETICS**

ORTHOPHOSPHORIC AND BORIC ACID INTERACTIONS IN  
GAMMA-ALUMINA:ENDOR AND ESEEM STUDIES

M.K.Bowman\*, R.I.Samoilova, S.A.Dikanov , Yu.D.Tsvetkov

*\*Pacific Northwest Laboratory, Richland WA USA*

*Institute of Chemical Kinetics and Combustion, SB RAS, Novosibirsk , Russia*

The influence of acid modification (phosphoric and boric acids) on electron acceptor sites of aluminum oxide was studied by solid-state, high-resolution pulsed EPR methods (ENDOR and ESEEM). Paramagnetic complexes with the coordinatively-unsaturated aluminum were formed by adsorption of probe molecules such as anthraquinone and o-chloranil. The ESEEM spectra show interactions with P-31 and B-11 nuclei located in the first and second shell of paramagnetic complexes. According to our ENDOR data, complexes of the probe molecules with the coordinatively-unsaturated octahedral and tetrahedral Al atoms are formed on the aluminum oxide surfaces modified by orthophosphoric acid. The fraction of octahedral Al increases with increasing acid concentration. In the samples modified by boric acid, the probe molecules form complexes with a pair of tetrahedral Al on the surface of aluminum oxide.

Pacific Northwest Laboratory is a national laboratory operated by Battelle Memorial Institute for the U.S. Department of Energy under contract DE-AC06-76RLO 1830. This research was supported Associated Western Universities, Inc. Northwest Division (AWU NW) under grant DE-FG06-89ER-75522 or DEFG92RL-12451 with the U.S. Department of ENERGY.

## THE VERY-HIGH-FREQUENCY ELECTRON RESONANCE APPLICATIONS TO STUDY TRIPLET-STATE ENTITIES

Ya.S.Lebedev

*N.N.Semenov Institute of Chemical Physics RAS 117334 Moscow, Russian Federation*

Electron Magnetic Resonance of disordered solids and solutions does not allow discrimination between electron-nuclear and electron-electron interactions causing the splitting and broadening of ESR spectra. We had proved/1/ this kind of information become available from the ESR spectra of polarized spins as detected at very high frequency/magnetic induction (140GHz/50KGs in our case) and very low temperature (1.2-10K).

The spin polarization phenomenon does not affect single electron ( $S=1/2$ ) spectra while it produces a strong asymmetric distortion of  $S>1/2$  spectra if the spin-spin splitting is dominant in the lineshape origin. In addition, the sign of the spin-spin splitting can be determined in a straightforward way/2,3/.

The developed approach had been used to investigate the triplet-state radical pairs (RP) and higher spin entities generated in the course of mechano-activation of the donor-acceptor mixtures such as di-*t*-butyl-o-quinones plus corresponding dihydroquinones or the same quinones plus metals (Al,Cd,Ga,Zn,etc.). It was discovered that triplet or quartet species are generated not only by grinding (stirring) of the powdered mixtures but as well by the action of the pulses of elastic waves/4,5/. The triplet-state RP's were earlier obtained by the photo-excitation of the mixed crystals or frozen solutions. Still the mechano-generated RP's appeared to be much more stable and their spin-spin interaction was unexpectedly found to be positive unlike to negative interaction found for the photo-generated pairs. Therefore mechano-activation produces triplet species of the completely different nature which may be considered as specific intermediates of the solid state mechano-chemical reactions.

## OP-9

The triplet- and quartet-complexes generated by the mechanolysis of metal-quinone mixtures were proved to be identical with those synthesized by the known liquid phase procedure. In some cases the mechano-chemical synthesis was found to be extremely efficient giving about 100% yield of magnetic complexes.

In conclusion, the spin-polarized ESR was developed and successfully applied to study solid state triplet- and quartet-entities. Some new features of solid state reaction intermediates were explored by experiments with grinding and elastic wave treatment of donor-acceptor mixtures.

## REFERENCES.

1. Ya.S.Lebedev. Appl.Magn.Res. 1994,v.7,p.p.339-362
2. S.D.Chemerisov et al. Chem.Phys.Letts.1994,v.218,p.p.353-361
3. G.D.Perehodtsev et al. Russ.J.Phys.Chem.1994,v.68,p.p.1253-1256
4. A.I.Aleksandrov et.al. Ibid.,1995,v.69,p.p.743-745
5. A.I.Aleksandrov et al. Ibid.,1995,v.69 (in press).

## THE EFFECT OF SALT SOLUTIONS ON THE RATE AND EQUILIBRIUM OF CYCLOADDITION REACTIONS

Yurij G. Shtyrĭn, Gul'nara Iskhakova, Vladimir D. Kiselev

and Alexandr I. Konovalov.

*Butlerov Chemical Research Institute, Kazan State University.*

*420008, Kazan, Russia. Fax: 8482-887049*

In coordination stoichiometric catalysis by Lewis acids a powerful rate acceleration is a consequence of the decrease of LUMO energy of dienophiles in  $n,\nu$ -complexes with Lewis acids. These LUMO energy changes equal 0.7-1.1 eV for maleimides in complexes with gallium chloride and 0.9-1.25 eV with aluminum chloride.<sup>1</sup> With these new values of electron affinity energy for activated maleimides the rate constants have the same function as found for different noncatalyzed Diels-Alder reactions and the equilibrium parameters remain unchanged.<sup>1</sup>

Marked acceleration of the reactions in lithium perchlorate-diethyl ether (LPDE) medium has been suggested in the context of enhanced "internal pressure"<sup>2</sup> or catalysis by  $\text{Li}^+$  cation as Lewis acid.<sup>3</sup> At present there is no clear reason for the Diels-Alder reaction rate acceleration in LP-solutions. Three concepts of the salt solution effect in cycloaddition reactions merit consideration:

1. Specific interaction of  $n$ -donor atoms of activating groups (usually in a dienophiles) with salt as a Lewis acid. This type of rate acceleration by  $\text{MX}_3$  in cycloaddition reactions is well known and has been considered in terms of HOMO-LUMO stabilization energy.<sup>1</sup>
2. The interactions of salt ion pairs with polar ground or transition states. Two major types are commonly recognized: interactions between polar states and salt ion-pairs with a "normal" rate constant salt effect:  $k = k_0(1+B_S C_S)$  (1), or as function (2)  $\log k = \log k_0 + K_S C_S$  (2).
3. The salt induced effect of medium results in "salting out" or "salting in" consequences for nonpolar reagents and/or transition state. This behaviors of salt solution can be due to the change of the free energy solvation of particles.

The rate constant of the Diels-Alder reaction 9,10-dimethylantracene with acrylonitrile ( $1.6 \cdot 10^{-6}$ ,  $\text{dm}^3 \text{mol}^{-1} \text{s}^{-1}$ , acrylonitrile, 25 °C) is increased to  $3.2 \cdot 10^{-2}$   $\text{dm}^3 \text{mol}^{-1} \text{s}^{-1}$  in the presence of  $\text{GaCl}_3$  - typical Lewis acid.

Gallium chloride on addition diethyl ether will be distributed between two n-donors - acrylonitrile and diethyl ether. The rate acceleration of this reaction in presence of  $\text{GaCl}_3$  in acrylonitrile medium equals  $2.0 \cdot 10^4$  times and lack of in diethyl ether medium. The same behavior of  $\text{GaCl}_3$  has been observed in reaction with ethylacrylate in ethylacrylate medium (the rate acceleration  $3.1 \cdot 10^4$  times) and in diethyl ether (lack of acceleration).

If LP distribution in LPDE medium between diethyl ether and dienophile is assumed, the experimental rate constant in reaction of diene with maleic anhydride should increase with the increase of maleic anhydride concentration in the LPDE solution. But the rate constants in the reaction are decreased.

Finally, two reactions of acrylonitrile with cyclopentadiene and with 9,10-dimethylantracene were performed in LPDE and LP-acrylonitrile solutions. It is clear, that in the latter case the complex formation of LP with dienophile will be free from distribution. However the rate constants change even less for reactions in the LP-acrylonitrile medium than in LPDE. It should be noted that the rate accelerations for the reaction of 9,10-dimethylantracene with acrylonitrile in benzene solution are  $10^4$  and  $10^5$  for  $\text{GaCl}_3$  and  $\text{AlCl}_3$  correspondingly.<sup>1</sup>

The lack of the acceleration effect of LPDE in reaction of 1,3-diphenylisobenzofurane with styrene was considered<sup>3</sup> as evidence of LP catalysis as Lewis acid due to the lack of n-donor group in styrene. The measurements of the reaction rate in LPDE medium at 25 °C repeatedly performed by us resulted in near the same for this reaction, but a similar weak acceleration has been determined and for reaction with N-phenylmaleimide, in spite of there being two active n-donor centers in maleimide.

When considering the second possible cause of the salt solution effect it is useful to compare this effect on the rate constants for some dienes and dienophiles. The magnitude of speed up is seen to differ greatly in the LPDE medium. For some reactions the rates rise sharply at low concentrations of LPDE (0-0.3 M) and in the wide concentration range (0.5-5 M) there is nearly the same sensitivity for the most part of the Diels-Alder reactions in LPDE medium. The high effect of the low concentration of LPDE is observed for reactions with increased sensitivity to solvent pola-

riety. The significant effect of small LPDE concentrations is well known in solvolysis reactions, in which the "normal" kinetical salt effect (eq. 1) occurs due to electrostatic polarization and the stabilization of the dipolar transition state by salt ion-pairs. In solvolysis reactions the slopes ( $B_s$ , eq. 1) as a rule decrease with the increase of the solvent dielectric constant. Similar effects are observed in the reaction of cyclopentadiene with N-phenylmaleimide and in solvolysis reaction.

The possible source of salt effect on the Diels-Alder reaction rate can be connected with observed semilogarithm relation (eq. 2). The activity coefficient of nonpolar solute in water-salt solution had been described by equation (3):  $\ln f = V_n(V_s - V_s^0)C_s / RT \beta$  (3), where  $V_n$  is the nonpolar solute volume,  $(V_s - V_s^0)$  is the change of salt partial molar volume on dissolving in water,  $C_s$  is the molar salt concentration and  $\beta$  is the water compressibility coefficient. This means that in the electrostriction solution the activity coefficient of nonpolar solute should increase linearly with the salt concentration, with the slope proportional to the volume of solute. For the rate constant this relation assumes the form (4):

$\ln k_2 = \ln k_0 - \Delta V^\ddagger (V_s - V_s^0)C_s / RT \beta$  (4), where  $\Delta V^\ddagger$  is the activation volume. Within this method the change of free energy activation or the reaction in water salt solution connected with the volume of the process. For the Diels-Alder reactions the value  $\Delta V^\ddagger$  is about  $-25.35 \text{ cm}^3 \cdot \text{mol}^{-1}$ . The necessary parameters for some water-salt solutions are known and it is possible to calculate the  $\Delta V^\ddagger$  values. For "salting out" solutions the rate constant dependence produces the values of activation volume in reasonable agreement with the data from the external pressure effect. This reason for the water salt solution effect on the Diels-Alder reaction rate was extended in this case on the LP solutions in organic solvents. The additional term of the free energy salt effect can be written as a product  $\Delta V^\ddagger \cdot \Delta P_{\text{int}}$ , where  $\Delta P_{\text{int}}$  is the "internal pressure" change in the salt solution. With the known value of  $\Delta V^\ddagger$  it is possible to calibrate  $\Delta P_{\text{int}} / \Delta C_s$  for the LPDE medium. Thus calibration results in the parameter  $\Delta P_{\text{int}} / \Delta C_s = 560 \text{ atm} \cdot \text{M}^{-1}$ . This parameter makes it possible to calculate volumes in some other processes.

The endo/exo ratio ( $N/X$ ) of adducts in the reaction of cyclopentadiene with methylacrylate in LPDE solution reflects the rate constants ratio  $k_N/k_X$ . The difference in activation volumes  $(\Delta V_N^\ddagger - \Delta V_X^\ddagger)$  was calculated from the slope value, to be equal  $-2.1 \text{ cm}^3 \cdot \text{mol}^{-1}$  in agreement

with the data from the external pressure effect on rate constants ( $-0.5 \text{ cm}^3 \text{ mol}^{-1}$ ). With the increase of the LP concentration in LPDE the value of equilibrium constant rises a little less than the rate constant of the furane reaction. The activation volumes for (2+2)-cycloaddition reactions of TCNE with  $\alpha$ -methyl styrene ( $-49$ ) and vinyl ethyl ether ( $-46 \text{ cm}^3 \text{ mol}^{-1}$ ) from salt solution data are in agreement with those from the external pressure effect on reactions of TCNE with *p*-methoxystyrene ( $-55$ ) and vinyl ethyl ether ( $-55 \text{ cm}^3 \text{ mol}^{-1}$ ). In contrast to the Diels-Alder reaction the reaction rate for nitrones is decreased in a polar solvent.<sup>1</sup> While the solubility of dienes decreases in going from ether to LPDE medium, the nitron solubility becomes larger. Thus LPDE solution does not contribute to the "salting out" of nitron, but is "salting in" medium. The unusual LPDE effect on the nitron reaction is not connected with the nitron-LP complex formation because gallium chloride accelerates this reaction more than by 4 orders.<sup>1</sup> For the Diels-Alder reaction of cyclopentadiene with acrylonitrile a very weak reaction rate sensitivity to solvent polarity and H-bond formation was observed, so it is possible to define the magnitude of the internal pressure change in ethanol-water and dioxane-water mixtures. The effects of rate accelerations of water addition to ethanol or dioxane are similar to those of LP to ethanol. Based on the activation volume of this reaction ( $-25 \text{ cm}^3 \text{ mol}^{-1}$ ) it is possible to calculate the internal pressure changes from ethanol to water as 2500 and from dioxane to water as 3000 atm. With these internal pressure changes calculated for solutions of LP in diethyl ether, acetone, ethanol or in ethanol-water, dioxane-water binary solutions there exists the possibility of salt probing of reaction polarity as the difference between the observed reaction rate effect of these solutions and the one calculated from contribution of PV term. From our data it is evident that in going from inert organic solvent to the water or to LP solutions the contribution of PV term in the total rate acceleration effect is predominant only for a few Diels-Alder reactions.

This approach of the salt-solution effect is in accord with hydrophobic and solvophobic effects. The main part of the change of free activation energy can be controlled by the differences in the change of the free energy of interaction in the range of the low LP concentrations in LPDE (0-0.5M) and by the change of the free energy cavity formation in the range of 0.5-5M of LP.

The data obtained in this case on the internal pressure change in binary solutions dioxane-water (3000 atm.) and ethanol-water (2500 atm.) were

used for calculation of the volume of argon, using the data of the free energy change in argon solvation in these binary solutions. The values  $\Delta V_{Ar}$  thus determined equal 21 and 24  $\text{cm}^3\text{mol}^{-1}$  correspondingly and are in agreement with the magnitudes of solid (24) and hydration (27  $\text{cm}^3\text{mol}^{-1}$ ) argon. Due to near the same value of  $\Delta P_{int}$  in going from dioxane to water and from diethyl ether to 5M LPDE we should propose near the same change of the free energy in argon solvation in going from diethyl ether to 5 M LPDE.

The addition reaction between tributylphosphine and carbon disulfide with formation of zwitter-ionic product has been studied in LPDE medium. From our data the activation volume of forward reaction is -20 and for back reaction +35  $\text{cm}^3\text{mol}^{-1}$  so that reaction volume is -55  $\text{cm}^3\text{mol}^{-1}$ . If take this reaction as a model for [2+2]-cycloaddition process, which has zwitter-ionic transition state, then the reaction volume (-55  $\text{cm}^3\text{mol}^{-1}$ ) looks as quite real value.

We should emphasize that only for a few Diels-Alder reactions the change in the rate constants in a series of solvents is as consequence of the difference in the solvent internal pressure but not for all Diels-Alder reactions. It can be expected that the addition of Al, Ga and B halides will be more accelerate the rate of reactions with orbital control and  $\text{LiClO}_4$  - the rate of reactions with charge control.

### Acknowledgments

The authors gratefully acknowledge partial financial support Russian Foundation for Fundamental Research (grant no. 95-03-09070) and are thankful to Professors Jurgen Sauer (Regensburg University), Nikolay Zefirov (Moscow University), Luis Salvatella (Zaragoza University), Giovanni Desimoni (Pavia University) and Tsumotu Asano (Oita University) for useful discussions.

- 
1. V.D.Kiselev and A.I.Konovalov, *Usp.Khim.*, 1989, **58**, 383.
  2. P.A.Grieco, J.J. Nunes and M.D.Gaul, *J.Am.Chem.Soc.*, 1990, **112**, 4595.
  3. M.A.Forman and W.P.Daily, *J.Am.Chem.Soc.*, 1991, **113**, 2761

## Hot Atom and Tunneling Reactions of Recoil Tritium Atom with H<sub>2</sub> and D<sub>2</sub> in Solid Phase at Very Low Temperature

Yasuyuki Aratono and Tetuo Miyazaki

Advanced Science Research Center, Japan Atomic Energy Research Institute, Tokai-mura, Ibaraki-ken 319-11, Japan

### 1. Introduction

The reaction of hydrogen atoms (H, D, T) with hydrogen molecules is the prototype bimolecular reaction and many theoretical and experimental studies have been carried out. In the present paper, the experimental results on the reaction of recoil T atom with hydrogen molecules (n-H<sub>2</sub>, p-H<sub>2</sub>, D<sub>2</sub>) at cryogenic temperature (4.2 and 77K) are briefly presented and the possibility of tunneling abstraction and reactivity difference between o- and p-H<sub>2</sub> are reported.

### 2. Experimental

The experimental conditions have been reported elsewhere<sup>1,2</sup>. Thus, the brief explanation will be given below.

The samples for reactor irradiation are the mixtures of (n-H<sub>2</sub> or p-H<sub>2</sub> + D<sub>2</sub> + Xe + <sup>6</sup>LiF) and (n-H<sub>2</sub> + D<sub>2</sub> + <sup>6</sup>LiF), where <sup>6</sup>Li serves as the tritium source through the nuclear reaction of <sup>6</sup>Li(n, α)T and Xe as a moderator for energetic tritium atom. Separation of p-H<sub>2</sub> from n-H<sub>2</sub> was carried out by a column of 13X molecular sieve at 14K. The content of p-H<sub>2</sub> was about 95%. In order to prevent p-H<sub>2</sub> from changing into o-H<sub>2</sub>, the samples of p-H<sub>2</sub> sealed into quartz cells were stored at 4.2K till neutron irradiation. The thermal neutron flux and the dose rate of γ-rays were 1.7 × 10<sup>13</sup> m<sup>-2</sup> s<sup>-1</sup> and 4.1 × 10 Gy h<sup>-1</sup>, respectively. The irradiation time was 6 h. The separation of HT and DT was carried out with radio-gas chromatograph at 77K. The isotope effect was defined as  $K_H/K_D = ([HT]/[H_2])/([DT]/[D_2])$ , where [HT] and [DT] show radioactivity of tritiated protium and -deuterium and [H<sub>2</sub>] and [D<sub>2</sub>] are concentration of H<sub>2</sub> and D<sub>2</sub> in the mixture of (H<sub>2</sub> + D<sub>2</sub> + Xe).

### 3. Results and Discussion

#### 3.1 Recoil tritium atom reaction and tunneling

Fig. 1 shows the fraction of HT yields produced by recoil T atom in

(n-H<sub>2</sub>-D<sub>2</sub>) mixture at 4.2K (●)<sup>3</sup> and (n-H<sub>2</sub>-D<sub>2</sub>-Xe) mixture (Δ: total hydrogen of 0.2mol%, ○: total hydrogen of 1 mol%) at 77K<sup>4</sup>. The isotope effect for (n-H<sub>2</sub>-D<sub>2</sub>) mixture is close to 1 (dashed line). On the other hand, in case of H atom produced by photolysis or γ-radiolysis, a very large isotope effect has been reported by Miyazaki et al.<sup>5,6</sup>. Thus, the similar isotope effect is also expected for T atom. Though the reason is still unsolved, the difference of reaction site associated with the initial recoil energy, 2.7MeV for T atom and few eV for H atom, may cause such a large difference in reaction behavior between H and T atoms.

When 99.0 and 99.8 mol% of Xe is added, the isotope effect increases and is very close to the calculated value of 7 (solid line)<sup>4</sup>. Therefore it is concluded, that thermalized T atom also reacts through tunneling reaction similar to H atoms reported by Miyazaki et al.<sup>5,6</sup>.

### 3.2 Effect of rotational quantum states (J=0,1) on the tunneling reaction of H<sub>2</sub> + T → H + HT

As was described in 3.1, the tunneling reaction of T atom in n-H<sub>2</sub> system was observed in well-moderated reaction system such as Xe concentration of more than 99.0 mol%. As is well known, n-H<sub>2</sub> has two spin isomers, o-H<sub>2</sub> (75%) and p-H<sub>2</sub> (25%). Thus, the reactivity difference between these nuclear spin isomers in the tunneling reaction was expected. Fig. 2 shows [HT]/[DT] ratio against [H<sub>2</sub>]/[D<sub>2</sub>] ratio in solid (p-H<sub>2</sub>-D<sub>2</sub>-Xe) (closed circles) and (n-H<sub>2</sub>-D<sub>2</sub>-Xe) (open circles) mixtures at 77K, where the total concentration of H<sub>2</sub> and D<sub>2</sub> was fixed at 1 mol%<sup>2</sup>. The dotted line indicates the results in the n-H<sub>2</sub>-D<sub>2</sub> mixtures without xenon at 4.2K showing the isotope effect of 1. Though the experimental results are rather scattered, the [HT]/[DT] ratio increases linearly with an increase in the [H<sub>2</sub>]/[D<sub>2</sub>]

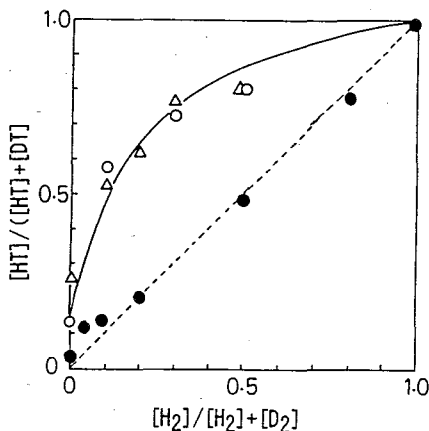
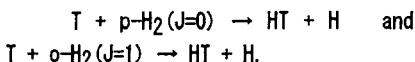


Fig. 1 Fraction of HT yield produced by recoil T atom reaction  
 (●) n-H<sub>2</sub>-D<sub>2</sub>  
 (Δ) n-H<sub>2</sub>-D<sub>2</sub>-Xe (99.8 mol%)  
 (○) n-H<sub>2</sub>-D<sub>2</sub>-Xe (99.0 mol%)

ratio and the slopes for (p-H<sub>2</sub>-D<sub>2</sub>-Xe) and (n-H<sub>2</sub>-D<sub>2</sub>-Xe) are obviously larger than that for H<sub>2</sub>-D<sub>2</sub> mixtures without xenon.

The reactivity ratio of p-H<sub>2</sub> to o-H<sub>2</sub> against thermalized T atom,  $k(\text{H}_2(J=0)+\text{T})/k(\text{H}_2(J=1)+\text{T})$ , was estimated as  $4 \pm 2$  from the isotope effects derived from the slopes by taking into consideration of spin isomer ratio in n-H<sub>2</sub>. Since H<sub>2</sub> molecules in solid Kr<sup>7)</sup>, water ice<sup>8)</sup>, and crystalline ethanol<sup>9)</sup> are reported to rotate in quantized state, it was assumed here that H<sub>2</sub> molecules are rotating in a xenon matrix. Thus, the ratio described above represents the effect of initial rotational quantum states of H<sub>2</sub> on the following reactions:



The effect of rotational quantum states on a tunneling reaction of H atom with p-H<sub>2</sub> and o-H<sub>2</sub>,  $k(\text{H}_2(J=0)+\text{H})/k(\text{H}_2(J=1)+\text{H})$ , was reported to be 3.6<sup>10)</sup>.

Therefore, it is concluded that both T and H atom react more effectively with H<sub>2</sub> molecules at J=0 than that at J=1.

#### 4. Conclusion

It was shown in the present study, that the thermalized T atom diffuses into reaction matrix and reacts with H<sub>2</sub> and D<sub>2</sub> through quantum mechanical tunneling process at 77K and that the nuclear spin isomers of hydrogen, p-H<sub>2</sub> and o-H<sub>2</sub>, have different reactivity against the thermalized T atom; the former has higher reactivity than the latter by a factor of about 4.

The present experimentally obtained isotope effect through tunneling process seems to be much smaller than theoretical prediction<sup>1)</sup>. The difference may be attributed mainly to the incomplete thermalization of recoil T atom even at the present concentration of Xe. Though the radiolysis effect due to in-pile radiation was minimized<sup>4)</sup>, it may partially contribute to a decrease of the selectivity.

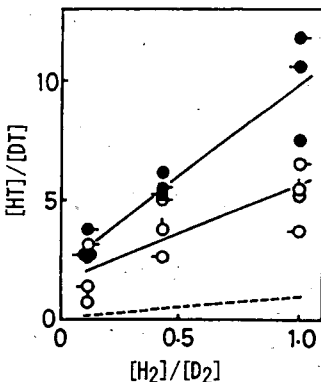


Fig. 2 The ratio of HT yields,  $[\text{HT}]/[\text{DT}]$ , against hydrogen isotope ratio,  $[\text{H}_2]/[\text{D}_2]$ .  
 (● ● ●) p-H<sub>2</sub>-D<sub>2</sub>-Xe (99.0 mol%)  
 (○ ○ ○) n-H<sub>2</sub>-D<sub>2</sub>-Xe (99.0 mol%)  
 (-----) n-H<sub>2</sub>-D<sub>2</sub>

Theoretical approaches were also proposed to elucidate the difference of the reactivity between  $p\text{-H}_2$  and  $o\text{-H}_2$  by some groups but is still controversial<sup>11,12</sup>. Thus, further experimental and theoretical investigation are necessary for more detailed discussion.

### References

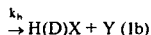
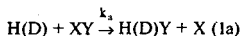
- 1) Y. Fujitani, T. Miyazaki, N. M. Masaki, Y. Aratono, M. Saeki, and E. Tachikawa, *Bull. Chem. Soc. Jpn.* **63**(1990)520.
- 2) Y. Fujitani, T. Miyazaki, N. M. Masaki, Y. Aratono, and E. Tachikawa, *Chem. Phys. Letters*, **214**(1993)301.
- 3) Y. Fujitani, T. Miyazaki, K. Fueki, N. M. Masaki, Y. Aratono, M. Saeki, and E. Tachikawa, *J. Phys. Chem.*, **95**(1991)1651.
- 4) T. Miyazaki, Y. Fujitani, M. Shibata, K. Fueki, N. M. Masaki, Y. Aratono, M. Saeki, and E. Tachikawa, *Bull. Chem. Soc. Japan*, **65**(1992)735.
- 5) H. Turuta, T. Miyazaki, K. Fueki, N. Azuma, *J. Phys. Chem.*,
- 6) T. Miyazaki, *Bull. Chem. Soc. Japan*, **58**(1985)2413.
- 7) D. G. Taylor III and H. L. Strauss, *J. Chem. Phys.*, **96**(1992)3367.
- 8) H. J. Jodl, *Vib. Spectra Struct.* **13**(1984)285.
- 9) H. Hase, K. Ishioka, and M. Miyatake, *Bull. Chem. Soc. Japan*, **65**(1992)2526.
- 10) T. Miyazaki, T. Hiraku, K. Fueki and Y. Tsuchihashi, *J. Phys. Chem.*, **95**(1991)26.
- 10) T. Miyazaki, S. Kitamura, H. Morikita, and K. Fueki, *J. Phys. Chem.*, **96**(1992)10331, and references therein.
- 11) J. M. Bowman, *J. Phys. Chem.*, **95**(1991)4921.
- 12) T. Takayanagi and N. M. Masaki, *J. Chem. Phys.*, **95**(1991)4154.

## Isotopic effect in branching ratios and kinetics of two-channel hydrogen and deuterium atom reactions with interhalogen molecules: an ESR study

*I.B. Bykhalo, V.V. Filatov, E.B. Gordon, A.P. Perminov*

*Institute of Energy Problems of Chemical Physics (Branch), Russia Academy of sciences,  
Chernogolovka, Moscow region, 142432, Russia*

For the two-channel hydrogen and deuterium atoms reactions



where XY = FCl, BrF, and ICl molecules, the rate constants and the two available reaction channel rates ratios  $\Gamma = k_a/k_b$  (branching ratios) were measured using a fast-flow reactor with RF discharge as source of atoms and with superheterodyne ESR spectrometer as detector [1]. For the reaction with FCl a substantial difference in branching ratios when substituting hydrogen atoms for deuterium ones:  $\Gamma_{\text{D+FCl}}/\Gamma_{\text{H+FCl}} = 3.3 \pm 0.2$  was found for the first time.

Data obtained along with results known for us is shown in Table 1.

**Table 1.** H(D)+XY reaction branching ratios and rate constants. L denotes light atom (H or D).

L+XY	$\Gamma$	Ref.	$k_{\text{L+XY}}, \text{cm}^3\text{s}^{-1}$	Ref.
H+FCl	6.7±0.8	2		
	5.2±0.5	3	4.1 · 10 <sup>-11</sup>	3
	6.1	4	(3.7±0.4) · 10 <sup>-11</sup>	**
	<b>2.5±0.2</b>	*	<b>(4.04±0.25) · 10<sup>-11</sup></b>	*
D+FCl	<b>8.5±0.5</b>	*	<b>(3.14±0.20) · 10<sup>-11</sup></b>	*
H+FBr	≥(5-24)	5		
	<b>0.38±0.06</b>	*	<b>(2.9±0.7) · 10<sup>-11</sup></b>	*
D+FBr	<b>0.38</b>	*	<b>(1.9±0.4) · 10<sup>-11</sup></b>	*
H+ClI	<0.5	6	4.9 · 10 <sup>-11</sup>	3
			(5±2) · 10 <sup>-11</sup>	7
	<b>0.65±0.10</b>	*	<b>(1.21±0.09) · 10<sup>-10</sup></b>	*
D+ClI	<b>0.65</b>	*	<b>(9.69±0.12) · 10<sup>-11</sup></b>	*

\*This work; \*\*Rate constant for the HCl + F channel, see Ref.[8].

The results obtained are compared with the known experimental data and theoretical calculations; in particular, possible influence of light atom (H or D) migration in collision complex on reaction mechanism is discussed.

*References*

1. I.B.Bykhalo, E.B.Gordon, A.P.Perminov, and V.V.Filatov, *Khim.Fizika*, 1985, **4**, 770; *ibid.* 1985, **4**, 1096; *ibid.* 1986, **5**, 1025 (in Russian).
2. D.Brandt, J.C.Polanyi, *Chem.Phys.*, 1979, **35**, 23.
3. J.P.Sung, R.J.Malins, D.W.Setser, *J.Phys.Chem.*, 1979, **83**, 1000, 1007.
4. G.P.Zhitneva, S.Ya.Pshezhetski, *Kinetika i Katalis*, 1978, **19**, 296 (in Russian).
5. D.Brandt, J.C.Polanyi, *Chem.Phys.*, 1980, **45**, 65, and references therein.
6. D.W.Setser, *Faraday Disc.Chem.Soc.*, 1979, **67**, 126.
7. L.M.Loewenstein, J.G.Anderson, *J.Phys.Chem.*, 1985, **89**, 5371.
8. N.F.Chebotaryov, L.I.Trakhtenberg, S.Ya.Pshezhetski, *Kvantovaya Elektronika*, 1976, **3**, 2552 (in Russian).

**KINETIC NON-UNIFORMITY IN RADICAL POLYMERIZATION  
PROCESSES**

S.S. Ivanchev, V.A. Pavlyuchenko

*Plastpolimer Co, S.Petersburg, 198108, Russia*

Conditions and reasons originating kinetic non-uniform zones at a radical polymerization both in bulk and in heterogeneous systems (emulsion polymerization and polymerization in the presence of solid dispersed phase) are discussed in the report.

Kinetic non-uniformity at bulk polymerization appears at the definite critical conversion for each system and is caused by the change of reaction system properties at process run, i.e., by the change of elementary reaction rate. The classification of polymerization systems regarding their particular kinetic non-uniformity is suggested.

Another important factor governing kinetic non-uniformity since process start is the concentration heterogeneity of polymerization system components.

The authors show the feasibility to control the formation of kinetic non-uniform zones in polymerization systems as well as the structure and properties of polymers produced.

## Electron-Transfer Properties of Mixed-Valence Molecules

R.D. Cannon

School of Chemical Sciences  
University of East Anglia  
Norwich, NR4 7TJ, UK

The internal electron transfer behaviour of mixed-valence polynuclear metal cluster complex compounds is now well understood in a general way. Using various structural and spectroscopic criteria, the molecules can be graded on a scale from fully localised to fully delocalised electron configurations, in consistent with the original Robin-Day classification scheme [1, 2]. But much remains to be done to understand the situations that arise when magnetic interactions have to be considered as well, and even more to understand and predict kinetic behaviour in electrochemical and homogeneous bimolecular reactions.

The lecture will review these two problems and describe recent results [3].

1. M.B. Robin and P. Day, *Adv. Inorg. Chem. Radiochem.*, **1967**, *10*, 247.
2. R.D. Cannon, *Electron Transfer Reactions*, London, 1980.
3. INTAS 94-2496.

**Anomalous strong magnetic effects during photochemical reactions in polymer systems with high molecular organisation**

Ivanov V.B., Efremkin A.F., Selikhov V.V.

Semenov Institute of Chemical Physics, Russian Academy of Science, Kosygin St. 4, Moscow, 117977, Russia

The character of anomalous strong (up to 30,000%) magnetic effects (AME) during the photolysis of aromatic ketones in polymer systems based on mixtures of amphiphilic polymers and ionogenic surfactants or polyelectrolyte complexes of polymethacrylic acids and surfactants is discussed. AMEs are displayed as a sharp rise in the rate of optical property variation (light scattering) under the action of the external magnetic field at a strength up to 0.5 T.

The primary magnetic-spin effects were evaluated in the systems under consideration by using of laser photolysis and spectrophotometry. It was shown that these effects measured by decrease in geminate decay rate and by increase in escape yield of radical produced in photochemical transformation of the triplet photoinitiator do not exceed the effects in micellar solutions.

The absence of the stringent and unambiguous connection between the primary processes such as ketyl radical decay or LAT formation and total values of AMEs is an evidence that AMEs are attributed to a general set of chemical reactions and physical processes in systems.

An external magnetic field has an faint effect on the change of polymer molecular mass and hence this process can not be an immediate reason of the AMEs.

By direct experiments it was established that AMEs are caused by secondary processes which proceed in microemulsion particles with a size of the order of 1  $\mu\text{m}$ . Apparently these particles have an extended anisotropic structure like the liquid-crystal one.

Depending on polymer character, the variation in the

particle structure during irradiation mainly consists in the increase of particle size (in PVA) or the increase of the refraction index (in agarose gel). The size of particles at the different stages of the process, their refraction indices and composition are evaluated.

The dependencies of AME on the concentration and structure of photoinitiators, polymers and surfactants, intensity and wavelength of light as well as magnetic intensity were studied. The effect of other chemical reagents (H-donors,  $O_2$  and electrolytes) on the rise in light scattering was analysed.

Two critical concentrations of surfactants beyond which the AMEs disappeared were determined. The low critical concentration corresponds to critical concentration of the micelle formation, and the high critical concentration corresponds to the range of microemulsion particle disintegration. The extra factor determining the critical concentrations in solutions of polyelectrolyte complexes is their stability which depends on substitution fraction of polyacides.

Oxygen and electrolytes practically arrest an increase of the light scattering even in the presence of external magnetic field although these substances slightly decrease (twice as large for  $O_2$ ) or practically do not effect (NaCl) on the product yield of cage recombination reaction of ketone photochemical transformation. Phenols and aromatic amines depress both formation of the cage recombination products and light scattering increase.

At the present time the AMEs are observed for dispersions of benzophenone and its derivatives (3-methyl-, 4-methyl- and 4-methoxybenzophenone) and are not discovered for 4',4-dimethylbenzophenone and derivatives of anthraquinone containing the group  $(CH_3)_3C$ ,  $CH_3C(=O)$  or  $SO_3Na$  in position 2.

These experimental data as well as the other results which are given in report corroborate the developed mechanism of AMEs.

#### Acknowledgement

The research described in this publication was made possible in part by grant No M9W000 from the International Science Foundation.

**IR laser induced selective isomerisation of the vibrationally highly excited perfluorodimethylketene molecules**

Laptev V.B., Tumanova L.M., Ryabov E.A.

Institute of Spectroscopy, Russian Academy of Sciences

Troitsk, Moscow region, 142092,

**RUSSIA**

The experimental results for the isomerisation of the vibrationally highly excited perfluorodimethylketene  $(CF_3)_2C=C=O$  (FDMK) molecules to perfluoromethacrylic acid anhydride molecules  $F_2C=C(CF_3)COF$  (FMAA) are presented.

FDMK molecules were prepared in high-lying vibrational states by means of IR multiple photon excitation. For this purpose the first or second harmonics of the  $CO_2$  laser pulsed ( $\tau=80$  ns) radiation were used. In the first case laser radiation with frequency  $\Omega_{las}=983.25$   $cm^{-1}$  was in resonance with IR absorption band of  $\nu_{16}=991$   $cm^{-1}$  mode assigned to the antisymmetric C-C stretch. The FDMK molecules excitation by the second harmonic ( $2143.8+2169.3$   $cm^{-1}$ ) was carried out on the "red" wing of IR band  $\nu_1=2192$   $cm^{-1}$  assigned to the antisymmetric C=C=O stretch.

The isomerisation process was studied by means of measurements of the FDMK IR- and mass- spectra before and after irradiation. The dependences of the isomerisation conversion on number of laser shots, fluence, FDMK pressure and etc. were studied.

It was shown under our experimental conditions - FDMK pressure  $0.22\div 0.75$  mm Hg ( $30\div 100$  Pa) and the fluence of the first as well as the second harmonic radiation being  $0.5\div 4$   $J/cm^2$  - the main channel of photochemical reaction was the isomerisation of FDMK to FMAA. To detect the dissociation channel the appearance of the primary product CO was recorded. However, the dissociation was found insignificant in spite of rather high level of vibrational excitation of the FDMK molecules (up to 250 kcal/mole).

The isomerisation predominance over the dissociation we explain by considerable difference between their reaction rates because of different reaction barriers. It was pointed that photochemical reactions during vibrational excitation of the FDMK molecules in ground electronic state were essential differ from ones in case of UV photolysis of the ordinary (unfluorinated) dimethylketene.

For the first time the oxygen isotope selectivity was recorded in the isomerisation FDMK process due to the second harmonic of the CO<sub>2</sub> laser radiation. The changes in isotope composition of the FDMK and isomer were measured after irradiation by mass-spectrometer. The highest in our experimental conditions <sup>18</sup>O-selectivity value was 3.9 under frequency of excitation radiation 2143.8 cm<sup>-1</sup>.

The improvement of the <sup>18</sup>O-selectivity is limited due to influence of weak IR absorption band at 2136 cm<sup>-1</sup> connected with combined vibration of the <sup>16</sup>O-contained molecules.

PECULIARITIES OF CHAIN REACTIONS OF HYDROCARBON OXIDATION  
IN "WALL-LESS" REACTOR WITH LASER HEATING

A.A.Mantashyan

Institute of Chemical Physics of Armenian Academy  
of Sciences

The chain reactions of oxidation of different hydrocarbons in "wall-less" reactor, allowing to avoid the influence of heterogeneous factors, have been studied. The process was carried out in thermal regime under the effect of laser IR-radiation in the presence of  $SF_6$  as a sensitizer.

It is known that thermal oxidation of propane begins at  $T = 320-350^\circ C$ . But, in "wall-less" reactor propane-oxygen mixture conversion starts only at temperatures above  $T = 500^\circ C$ . At this, oxygen is not consumed and oxidation does not proceed. Oxidation products are not more than 1%. Selective formation of propylene, methane, ethylene, hydrogen is observed e.g. cracking of propane takes place. However in the absence of oxygen the process does not proceed at all. The regularities observed could be connected with the absence of influence of heterogeneous factors. Experiments show that reactor wall is at room temperature and the conversion proceeds inside a laser beam and heterogeneous reactions are avoided. Among the possible homogeneous initiation reactions the interaction of hydrocarbon with oxygen can proceed with the lowest activation energy:  $RH + O_2 \rightarrow R + HO_2$  (1). For propane this reaction is  $C_3H_8 + O_2 \rightarrow C_3H_7 + HO_2$ , which cannot provide effective radical generation at low ( $300-400^\circ C$ ) temperatures, and therefore, in "wall-less" reactor propane conversion begins from temperatures above  $500^\circ C$ . At this temperatures the concentration of  $RO_2$  radicals decreases because of equilibrium shift in the reaction  $R + O_2 \rightarrow RO_2$  to  $RO_2$  destruction. As peroxy radicals react with each other:  $RO_2 + RO_2 \rightarrow RO + RO + O_2$  (2), the rate of oxidative route of the process depends on those concentration squared. Therefore  $RO_2$  radicals concentration decrease will lead to an abrupt decrease of oxidation rate. Naturally, in this

case, reactions of R radicals become major:  $R \rightarrow \text{propylene} + H$  (3);  $R \rightarrow \text{ethylene} + CH_3$  (4);  $RH + H \rightarrow R + H_2$  (5);  $RH + CH_3 \rightarrow R + CH_4$  (6).

So, from obtained results the conclusion that usually chain initiation in hydrocarbon oxidation proceeds heterogeneously on reactor wall can be done. If the wall does not take part in the initiation, then oxidative route is negligible. In "wall-less" reactor, when secondary heterogeneous reactions are avoided, it becomes possible to realize selective processes. For instance, the selectivity of propane conversion into olefins exceeds 95%.

Distinguished results were obtained for methane and butane. In the case of methane initiation reaction starts at higher temperature ( $T > 500^\circ C$ ) and therefore different oxidation reactions of methyl radicals take place. For example, at  $T > 500^\circ C$  the reaction  $CH_3 + O_2 \longrightarrow CH_3O + O$  become more intensive. It leads to the different reactions responsible for further oxidation.

Due to weak C-H bond in butane, initiation reaction occurs at low temperature and peroxy radicals concentration has to be higher than in the case of propane. As a result oxidative route increases.

The kinetic analysis of possible channels of conversion for mentioned hydrocarbons has been done by numerical simulation. The conclusion that a competition of oxidative and cracking routes is determined by reversible reaction  $R + O_2 \rightleftharpoons RO_2$  was made. The course of the process depends on alkyl and peroxy radicals concentrations ratio. At low temperatures, when concentration of peroxy radicals exceeds that of alkyl radicals to a great extent, the increase of initiation rate leads to a preponderance of oxidative route. In conventional reactors high initiation rate can be provided by the heterogeneous reactions. The calculations show that homogeneous initiation is too low and cannot start the process at low temperature.

A part of the results included in this report was obtained in work supported by International Science Foundation (ISF) under Grant # BYFC00.

## PICOSECOND TIME RESOLVED HARD X-RAY DIFFRACTION

Chen, I. V. Tomov and P. M. Rentzepis

Department of Chemistry, University of California, Irvine CA 92717

We report the development of a novel hard x-ray diffraction system which generates picosecond x-ray pulses by excitation of an x-ray diode with picosecond ultraviolet light pulses at a repetition rate of 300 Hz. The x-ray pulses are synchronized to the optical pulses with picosecond accuracy and have been used for obtaining, for the first time, picosecond time resolved x-ray diffraction data. The technique which we have developed to generate synchronizable picosecond x-ray pulses is based on the utilization of picosecond ultraviolet (UV) pulses to excite an x-ray diode. The x-rays are generated in a conventional diode except that the thermoionic cathode is replaced by a photocathode. The photo effect electron ejection has subpicosecond response time and therefore the duration of the electron pulse in the vicinity of the photocathode should be equal to that of the exciting light pulse. In such diode when the applied voltage is 75 kV the maximum available charge per pulse is 66 pC/mm<sup>2</sup>. This charge produces  $5 \times 10^5$  Cu K $\alpha$  photons/pulse/Sr. A high power ArF amplifier has been developed that generates <1 ps, 2.5 mJ, 300 Hz repetition pulses at 193 nm, fig.1. The radiation from the ArF excimer amplifier was used to operate the x-ray diode. The x-ray radiation was measured by a streak camera for its width, which was found to be <10 ps, and a CCD for its energy and profile. In our studies we have used the standard pump probe experimental technique using a ps laser as the pump and the ps x-ray pulses as the probe, fig. 2. Temperature changes in the crystal affect the scattered x-rays in two ways: (1) Thermal ionic motion which will decrease the height of the Bragg peak intensity (Debye-Waller effect), and (2) The thermal expansion which will result in the increase of the lattice spacing and thus change the Bragg angle for coherent scattering, resulting in "shift" of the Bragg diffracted band.

We will report the results from several samples including Au (111) and Pt (111) single crystals. The Au (111) single crystal used in the experiment was 150 nm thick with  $9 \times 15$  mm<sup>2</sup> surface area grown on a 100  $\mu$ m thick mica crystal. The penetration depth of Cu K $\alpha$  radiation (defined as attenuation of the input x-ray intensity to 0.5 level) in gold is about 550 nm and therefore the whole thickness of the crystal was probed by the incoming x-ray pulses. The calculated rocking curve width of our crystal is 1 mrad and a 100°C temperature increase of the crystal will shift the Bragg angle by about 1 mrad. In the experiment the incoming x-ray beam divergence of 4 mrad was large enough to cover those changes. The diffracted x-rays were displayed by the CCD detection system. Typically, two consecutive picosecond x-ray exposures were made, one with UV radiation heating the selected part of the crystal and another without UV heating. Then a comparison of both exposures was made.

The spatial distribution of the intensity in the cross section of the 193 nm beam was a flat top with uniform intensity of about 80%. Rough estimates show that a pulse

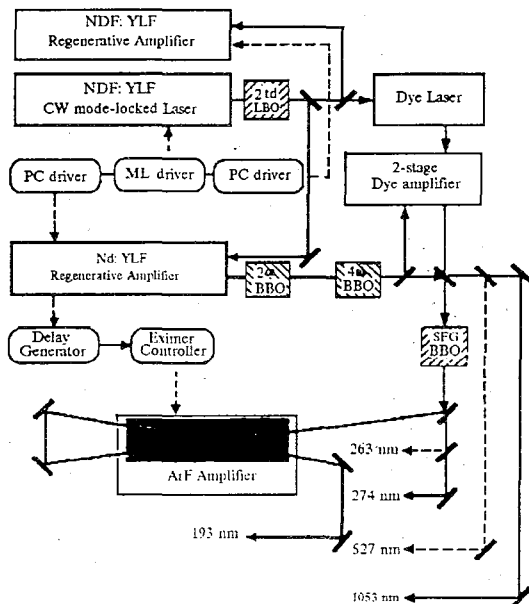


Fig. 1

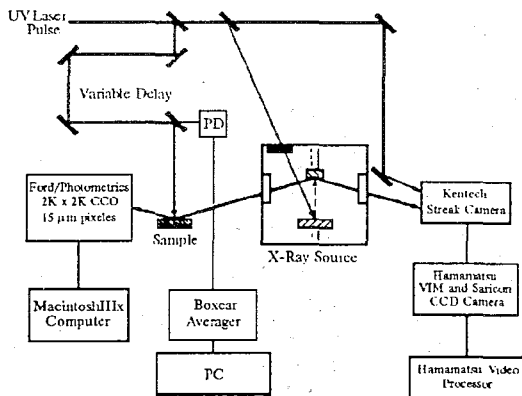


Fig. 2

energy of 0.1 mJ will increase the temperature of the heated area of the gold crystal by about 90°C. After about 100 ps, according to heat diffusion theory, the absorbed energy will be distributed in the crystal volume of 3 mm diameter and 150 nm thickness. Using the Debye-Waller factor data for gold crystal we find that for a uniform lattice temperature increase of 100°C, above room temperature, the decrease in the scattered x-ray intensity of the Bragg peak will be about 2%, correspondingly, for a temperature change of 200°C the intensity will decrease by 5%. The ratio of the scattered x-ray intensities for cold and heated crystal samples were measured. For negative delays, that means the x-ray probe pulse reaches the crystal before the UV pulse, the ratio is 1. When the x-ray probe pulse arrives after the UV heating pulse the ratio drops to about 0.90 and stays on that level for the maximum delay, 1.8 ns, used in our experiments. Assuming one-dimensionality of the strain normal to the heated surface, we calculate that 100°C in the crystal temperature will change the Bragg angle by about 1 mrad. This value in our experimental set up, translates to a shift of 3 pixels on the CCD, which is exactly the value that we observed in our experiments. Both effects, the decrease in the scattered x-ray intensity and the shift in Bragg angle were clearly detected. Their time evolution is shown in fig.3. We have also performed experiments on powder diffraction from polycrystalline materials including Ta, Pb, Au, TaC and CsI using ps x-ray pulses. Other experiments on time resolved dissociation and isomerization will be presented.

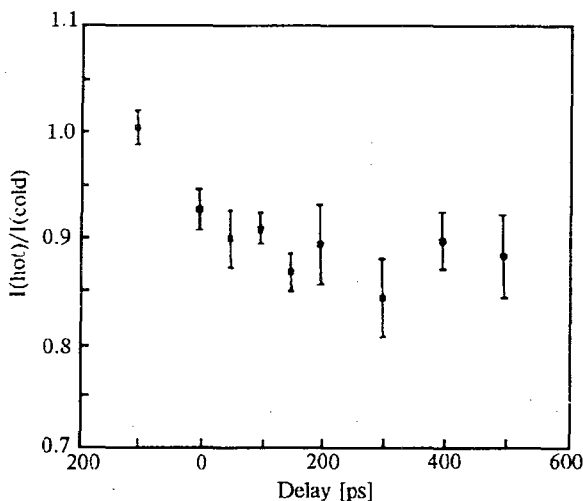


Fig.3

This work was funded in part by the W. M. Keck Foundation and NSF #CHE-95-01388.

## CONTENT

### PART 1

#### PLENARY LECTURES

PL-1	K.I. ZAMARAEV CATALYSIS BY MOLECULAR DESIGN.....	7
PL-2	A.S. DVORNIKOV and P.M. RENTZEPIS PHOTOCHEMISTRY OF 3D OPTICAL STORAGE MEMORY.....	8
PL-3	V.I.GOLDANSKII NON-TRADITIONAL MECHANISMS OF SOLID PHASE ASTROCHEMICAL REACTIONS.....	13
PL-4	Yu.N.MOLIN, B.M.TADJIKOV, V.M.GRIGORYANTS, D.V.STASS and O.M.USOV SPIN COHERENCE PHENOMENA IN RADICAL PAIRS RECOMBINATION.....	15
PL-5	A.L. BUCHACHENKO and V.L.BERDINSKY SPIN CATALYSIS.....	19
PL-6	C.BLAETTLER and H. PAUL ESR STUDIES OF RADICAL KINETICS IN SOLUTION AND ZEOLITES.....	22
PL-7	T.V.LESHINA ELECTRON TRANSFER PROCESSES IN COMPLEX ORGANIC REACTIONS STUDIED BY SPIN EFFECTS.....	24
PL-8	V.B.KAZANSKY ON THE REAL MECHANISM OF CARBENIUM ION REACTIONS IN SULFURIC ACID.....	28
PL-9	W. KEIM NEUTRAL OR IONIC ORGANOMETALLIC COMPLEXES IN HOMOGENEOUS CATALYSIS.....	32
PL-10	A.E.SHILOV FIVE-COORDINATE CARBON IN OXIDATION REACTIONS.....	38
PL-11	I.I. MOISEEV ACTIVATION OF H <sub>2</sub> O <sub>2</sub> AND ALKYLHYDROPEROXYDES WITH METAL COMPLEXES: ACHIEVEMENTS AND PROBLEMS.....	40
PL-12	G.A. TOLSTIKOV and S.S. SHAVANOV PHASE TRANSFER CATALYSIS IN THE SYNTHESIS OF ORGANIC CHLORINE COMPOUNDS. SOME FUNDAMENTAL ASPECTS AND INDUSTRIAL USE.....	44

PL-13	B.C. GATES CATALYSIS BY SUPPORTED TRANSITION METAL CLUSTERS.....	47
PL-14	V.V. LUNIN THE ROLE OF SOLID-PHASE INTERACTION IN FORMATION OF OXIDE CATALYST SURFACE ON SUPPORTS.....	50
PL-15	V.A. LIKHOLOBOV THE ROLE OF SUPPORT IN FORMATION AND STABILIZATION OF CLUSTER METAL COMPOUNDS.....	52
PL-16	E.B.GORDON, V.S.PAVLENKO and O.S.RZHEVSKY PHOTOASSOCIATION - THE PHOTON ASSISTED TWO-BODY RECOMBINATION OF ATOMS, IONS AND FREE RADICALS.....	55
PL-17	O.M.NEFEDOV, M.P.EGOROV, V.A.KUZMIN, M.B.TARABAN, T.V.LESHINA, V.F.PLUSNIN and R.WALSH NEW TRENDS IN THE STUDY OF CARBENE ANALOGS BY MODERN PHYSICO-CHEMICAL TECHNIQUES.....	59
PL-18	R.J.HULSEBOSCH, J.S. VAN DEN BRINK, P. GAST, T.N.KROPACHEVA, R.I.SAMOILOVA, J.RAAP, J.LUGTENBURG, Yu.D.TSVETKOV and A.J. HOFF MULTIFREQUENCY EPR OF SITE-SELECTIVELY <sup>13</sup> C- LABELLED QUINONE AND TYROSINE ELECTRON TRANSPORT COMPOUNDS <i>IN VIVO</i> AND <i>IN VITRO</i> .....	62
PL-19	S.A. DZUBA ELECTRON SPIN ECHO SPECTROSCOPY APPLIED TO INTERMEDIATE STATES OF PHOTOSYNTHETIC REACTION CENTERS.....	63
PL-20	V.P.ZHDANOV and P.R.NORTON SURFACE RECONSTRUCTION AND RATE PROCESSES IN ADSORBED OVERLAYERS.....	67
PL-21	N.ROESCH CLUSTER AND SLAB MODEL STUDIES OF CATALYSIS-RELEVANT ADSORPTION PHENOMENA ON METAL AND METAL OXIDE SURFACES.....	71
PL-22	V.V.GORODETSKII*, W.DRACHSEL and J.H.BLOCK MECHANISM OF CHEMICAL WAVES PROPAGATION DURING THE CO AND H <sub>2</sub> - OXIDATION ON PLATINUM SURFACE.....	72
PL-23	TETSUO MIYAZAKI TUNNELING REACTION AND HIGH RESOLUTION ESR SPECTROSCOPY IN QUANTUM SOLID PARAHYDROGEN AT 4K .....	76
PL-24	V.V.BOLDYREV MECHANISM OF MECHANICAL ACTIVATION OF SOLIDS.....	80

PL-25	A. PLONKA FRACTAL-TIME DYNAMICS OF ELEMENTARY REACTIONS IN CONDENSED MEDIA.....	81
PL-26	V.A.BENDERSKII and S.Yu.GREBENSHCHIKOV CHEMICAL DYNAMICS AT LOW TEMPERATURES.....	86
PL-27	N.M.BAZHIN and V.V.KOROLEV DIFFUSION MOBILITY IN QUENCHING REACTION OF ELECTRONIC EXCITED STATES OF ORGANIC SYSTEM AT LOW TEMPERATURES.....	90
PL-28	S.G.NEOPHYTIDES, I.V.YENTEKAKIS, S.BEBELIS, and C.G.VAYENAS <i>IN-SITU</i> CONTROLLED PROMOTION OF CATALYST SURFACES: NON-FARADAIC ELECTROCHEMICAL MODIFICATION OF CATALYTIC ACTIVITY.....	94
PL-29	J.H. MALIN REACTIVITY PATTERNS AMONG SUBSTITUTED PENTACYANOIRON(II) COMPOUNDS IN AQUEOUS SOLUTION.....	98
PL-30	V.N.PARMON and K.I. ZAMARAEV PHOTOCATALYSIS AND GLOBAL CHEMISTRY OF ATMOSPHERE.....	101

## ORAL PRESENTATIONS

### SECTION CATALYSIS:

OP-1	M.M.SLIN'KO DIFFERENT TYPES OF OSCILLATORY BEHAVIOUR IN HETEROGENEOUS CATALYTIC SYSTEMS.....	107
OP-2	G.S. YABLONSKII and A.V.MYSHLYAVTSEV* THEORY OF COMPLEX KINETIC BEHAVIOUR OF CATALYTIC REACTIONS.....	108
OP-3	V.I.SAVCHENKO, E.A.IVANOV, S.I.FADEEV, N.I.EFREMOVA, A.V.KALINKIN, A.N.SALANOV, A.V.PASHIS, S.N.PAVLOVA and V.A.SADYKOV MULTI-CENTER CATALYSIS - THE WAY TO GOVERN CATALYTIC ACTIVITY.....	111
OP-4	M.C. BONNET, L. CARMONA, B. CHAUDRET, I. GUIBERT, D.NEIBECKER, X.D. HE AND I. TKATCHENKO CATALYTIC DIMERISATION OF FUNCTIONALIZED ALKENES.....	114
OP-6	V.C.H.KROLL, H.M. SWAAN, S.LACOMBE and C. MIRODATOS A MECHANISTIC STUDY OF THE METHANE REFORMING REACTION WITH CARBON DIOXIDE OVER Ni/SiO <sub>2</sub> CATALYST.....	116

OP-7	<b>E.S.SHPIRO</b> , O.P.TKACHENKO, N.I.JAEGER, R.W. JOYNER and G.SCHULTZ-EKLOFF STRUCTURE AND REACTIVITY OF WELL-DEFINED Pt-Cu ALLOY PARTICLES HOSTED IN ZEOLITES.....	117
------	---	-----

## SECTION KINETICS

OP-8	M.K.BOWMAN, R.I.SAMOILOVA, S.A.DIKANOV and Yu.D.TSVETKOV ORTHOPHOSPHORIC AND BORIC ACID INTERACTIONS IN GAMMA-ALUMINA: ENDOR AND ESEEM STUDIES.....	120
OP-9	Ya.S.LEBEDEV THE VERY-HIGH-FREQUENCY ELECTRON RESONANCE: APPLICATIONS TO STUDY TRIPLET-STATE ENTITIES.....	121
OP-10	Yu.G.SHTYRLIN, G.ISKHAKOVA, V.D.KISELEV and A.I.KONOVALOV THE EFFECT OF SALT SOLUTIONS ON THE RATE AND EQUILIBRIUM OF CYCLOADDITION REACTIONS.....	123
OP-11	YASUYUKI ARATONO, TETUO MIYAZAKI HOT ATOM AND TUNNELING REACTIONS OF RECOIL TRITIUM ATOM WITH H <sub>2</sub> AND D <sub>2</sub> IN SOLID PHASE AT VERY LOW TEMPERATURE.....	128
OP-12	I.B.BYKHALO, V.V.FILATOV, E.B.GORDON, A.P.PERMINOV ISOTOPIC EFFECT IN BRANCHING RATIOS AND KINETICS OF TWO-CHANNEL HYDROGEN AND DEUTERIUM ATOM REAC- TIONS WITH INTERHALOGEN MOLECULES: AN ESR STUDY.....	132
OP-13	S.S.IVANCHEV and V.N.PAVLYUCHENKO KINETIC NON-UNIFORMITY IN RADICAL POLYMERIZATION PROCESSES.....	134
OP-14	R.D.CANNON ELECTRON-TRANSFER PROPERTIES OF MIXED-VALENCE MOLECULES.....	135
OP-15	V.B.IVANOV, A.F.EFREMKIN and V.V.SELIKHOV ANOMALOUS STRONG MAGNETIC EFFECTS DURING PHOTOCHEMICAL REACTIONS IN POLYMER SYSTEMS WITH HIGH MOLECULAR ORGANIZATION.....	136
OP-16	V.B.LAPTEV, L.M. TUMANOVA and E.A. RYABOV IR LASER INDUCED SELECTIVE ISOMERIZATION OF THE VIBRATIONALLY HIGHLY EXCITED PERFLUORODIMETHYL- KETENE MOLECULES.....	138

OP-17	A.A.MANTASHYAN PECULIARITIES OF CHAIN REACTIONS OF HYDROCARBON OXIDATION IN "WALL-LESS" REACTOR WITH LASER HEATING.....	140
OP-18	CHEN, I.V.TOMOV and P.M. RENTZEPIS PICOSECOND TIME RESOLVED HARD X-RAY DIFFRACTION.....	142
CONTENT.....		145

The Second Conference  
**"Modern trends in chemical kinetics and catalysis"**

Editor: Professor Valentin N. Parmon

The Organizing Committee notifies that the Conference papers have been printed by direct photo offset from the camera-ready originals submitted by the authors, and declines all responsibility for possible mistakes and misprints in the texts.

Подписано в печать 20.10.95

Формат 60x80/16

Печ.л. 9,4

Заказ № 219

Тираж 400

---

Отпечатано на Полиграфическом участке издательского отдела Института катализа СО РАН  
630090, Новосибирск, пр. Академика Лаврентьева, 5